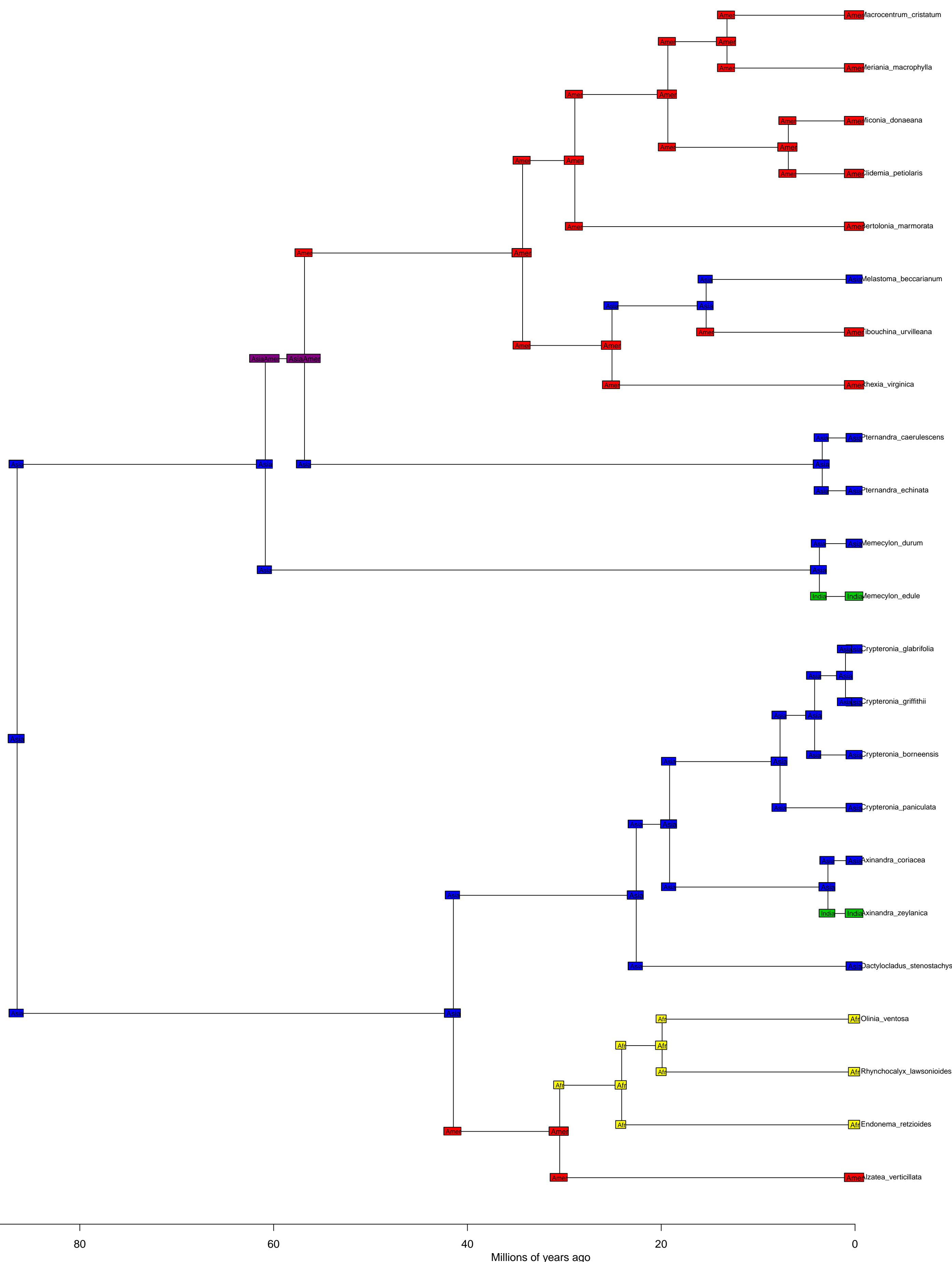
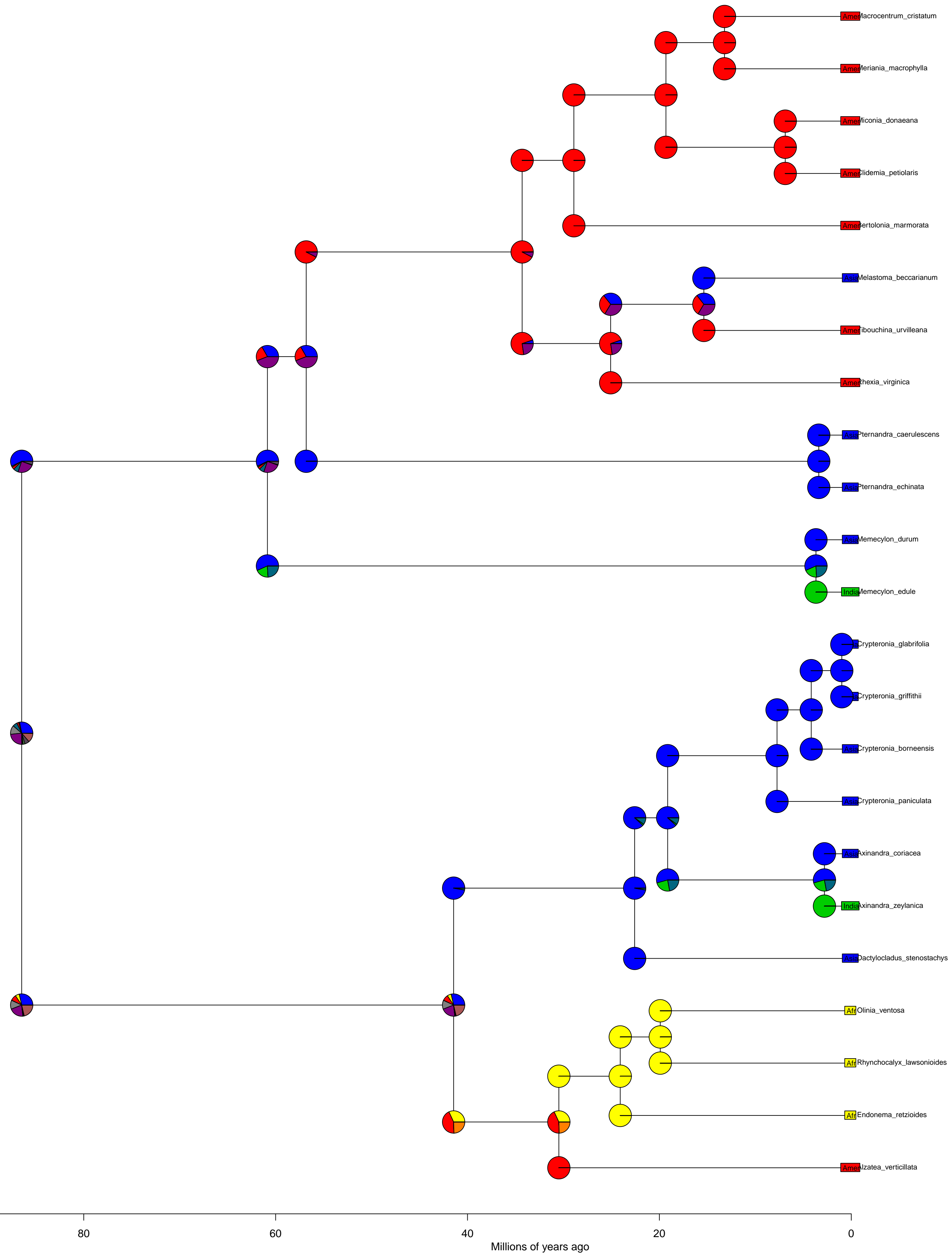
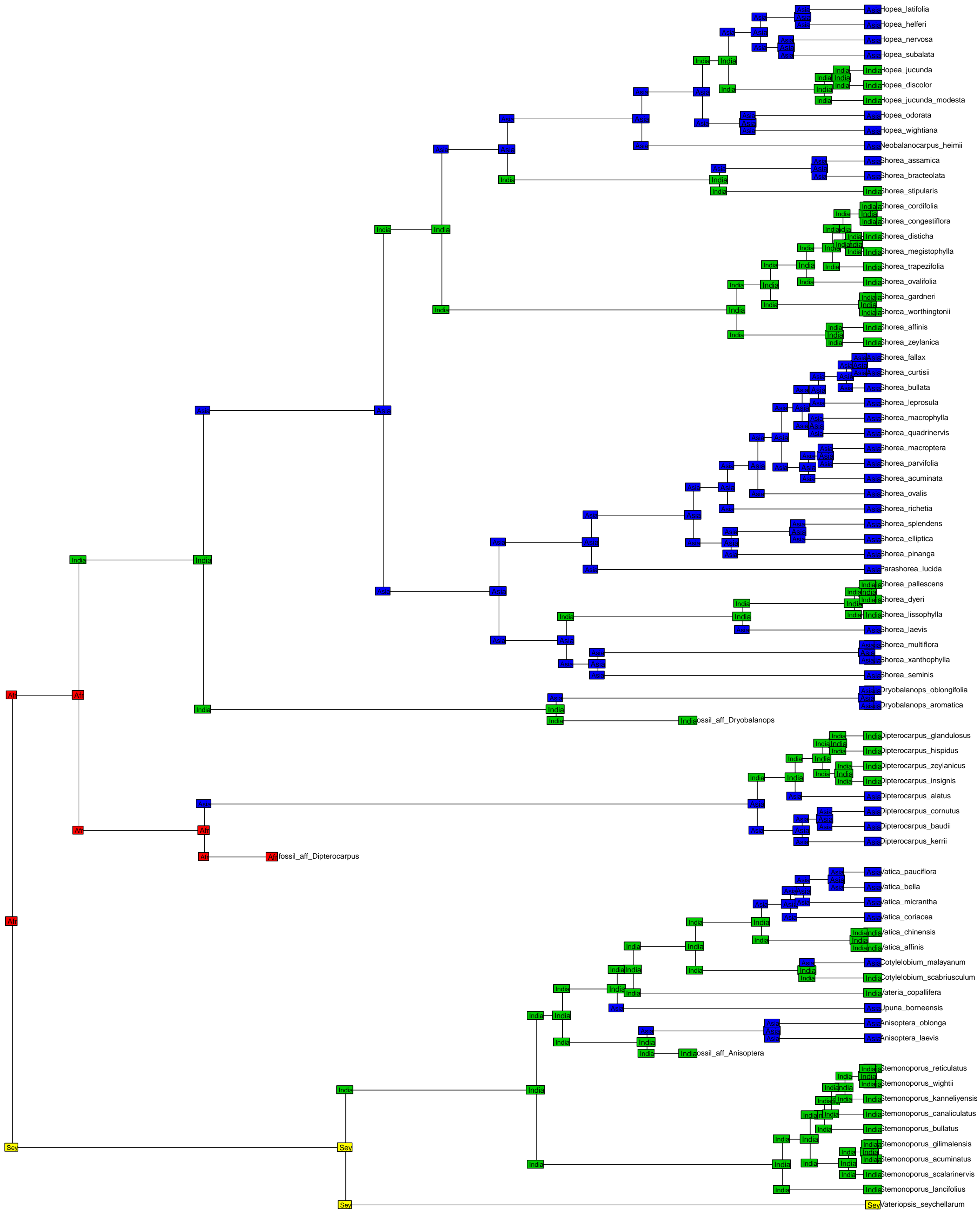


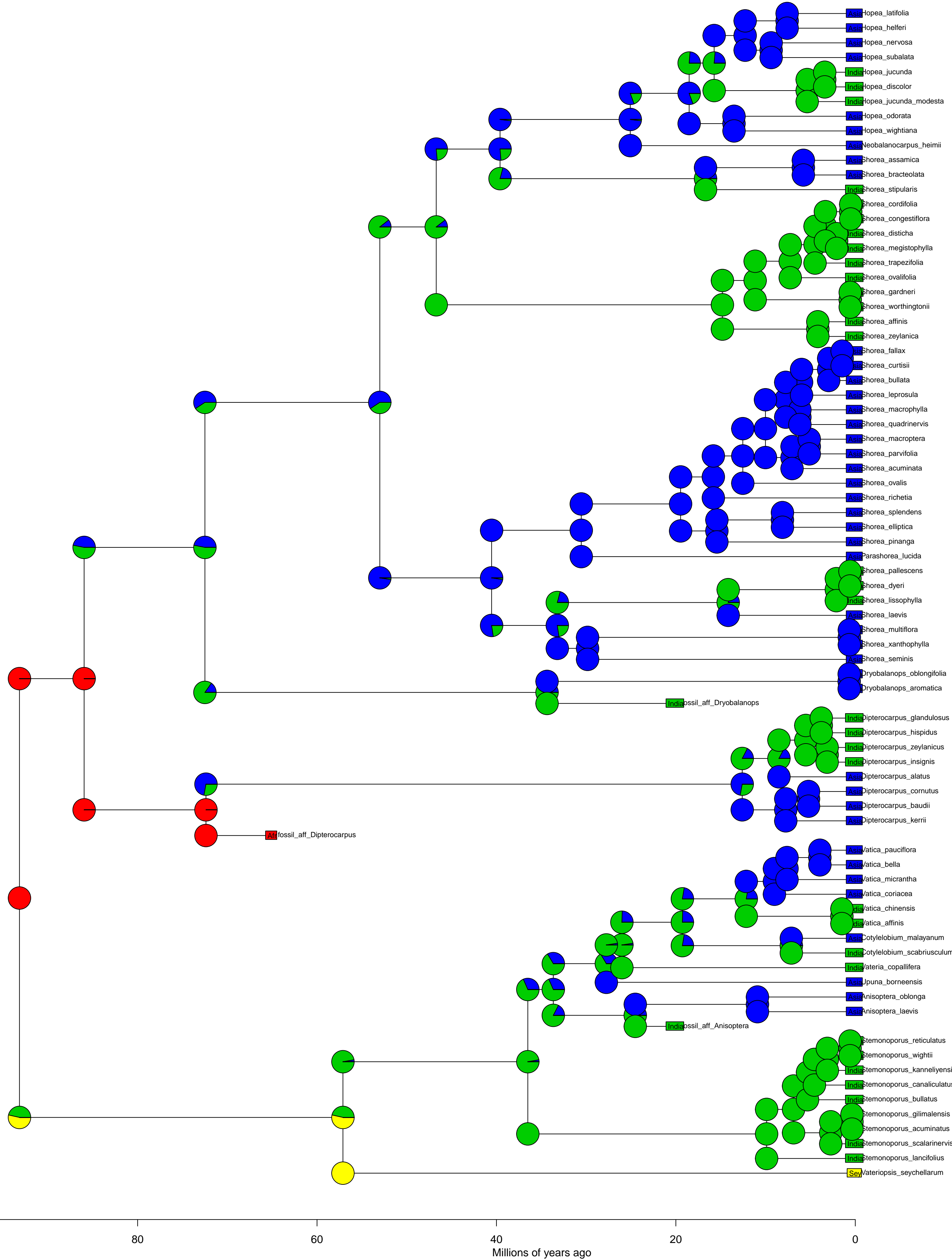
## **Supplementary Figure 1**

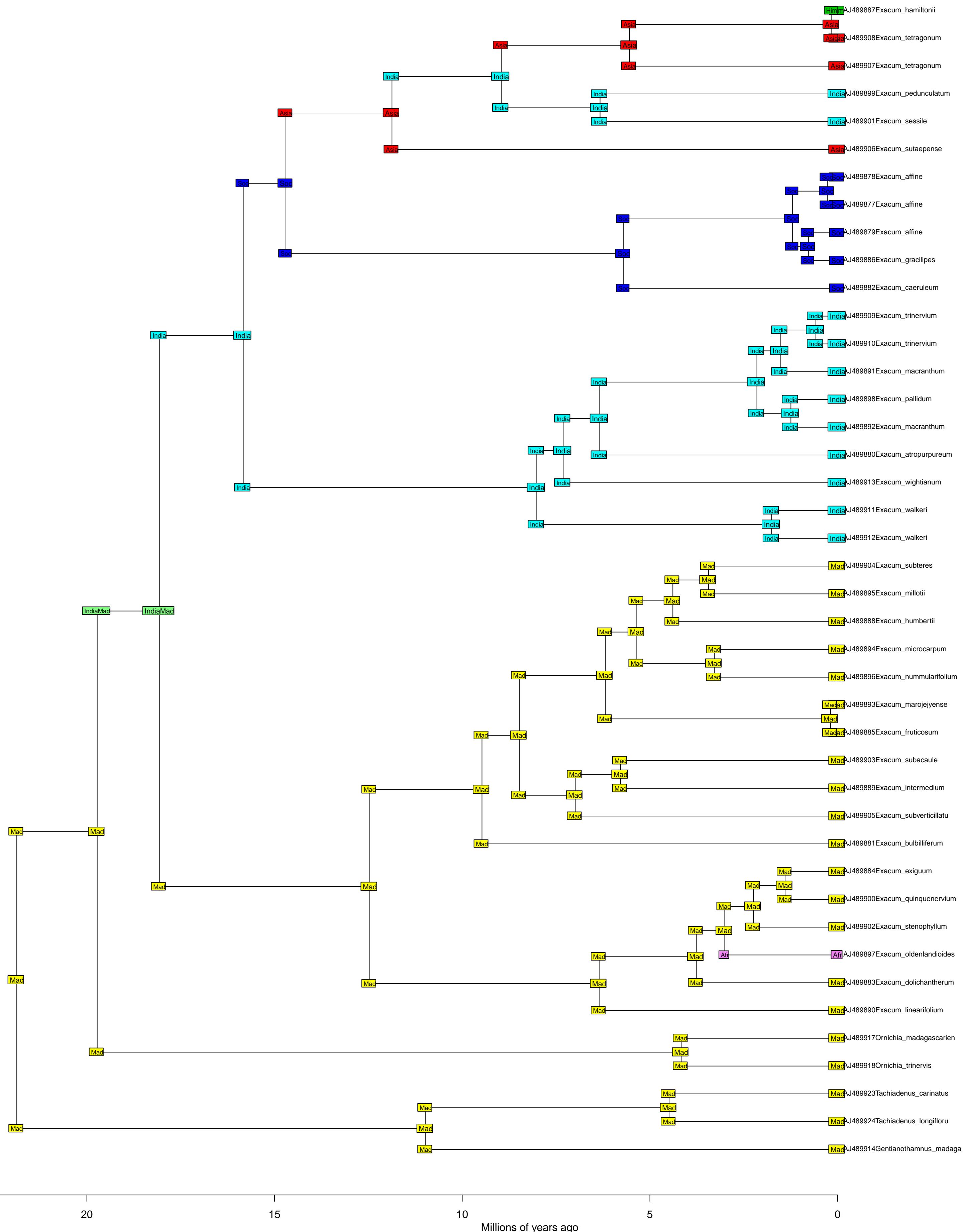
**Suppl. Fig. 1 | Time calibrated phylogenetic trees with annotated biogeographical range estimates used to infer dispersal events between the Indian subcontinent and mainland Asia.** The 37 phylogenies are shown once with the best range estimate and once with the relative probability for the respective areas/ranges; annotated with the model used (DEC or DEC+j), the maximum number of areas allowed within a range, the resulting extinction rate ( $e$ ), dispersal rate ( $d$ ), founder-event weight ( $j$ ), and the log likelihood ( $\ln L$ ).

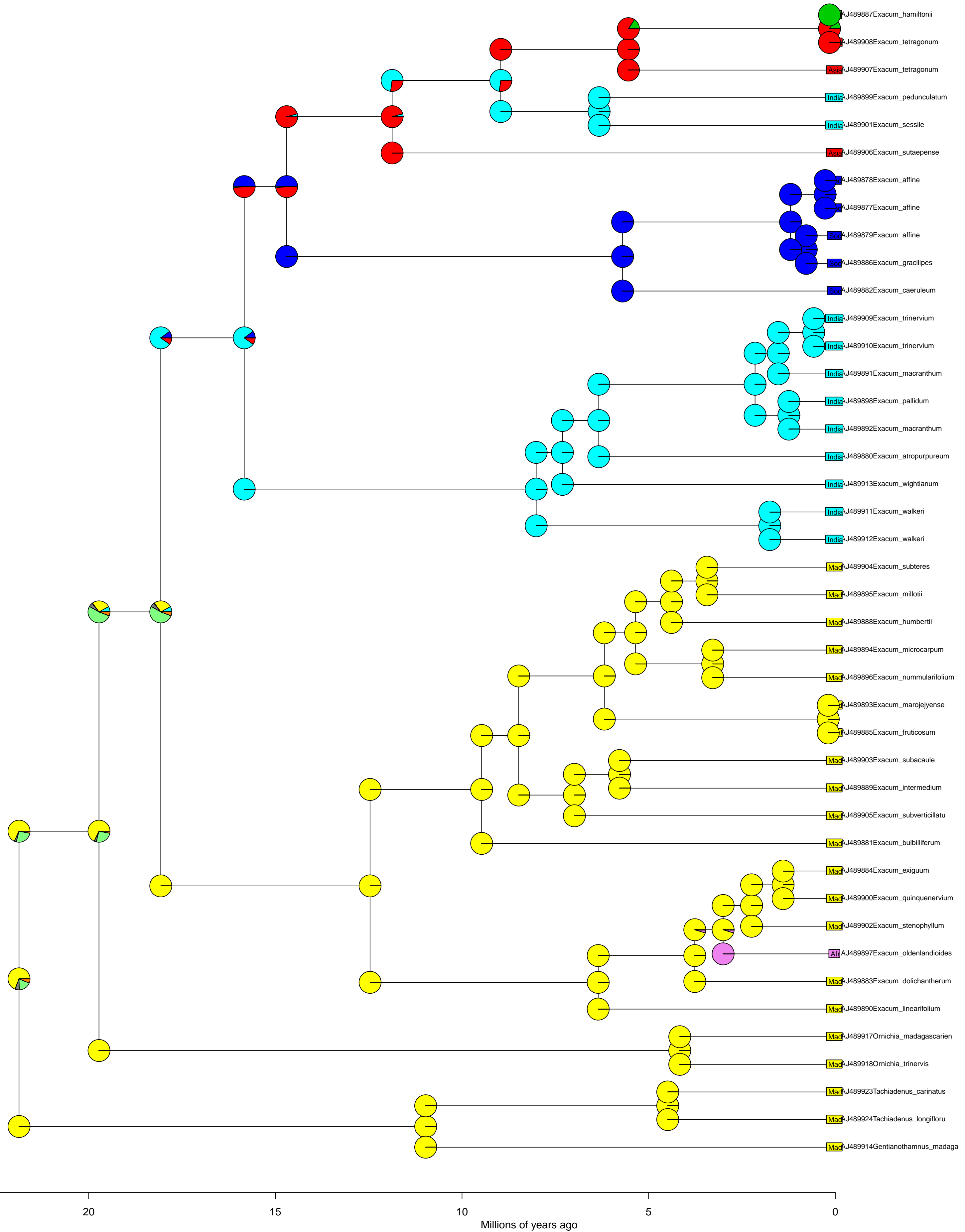




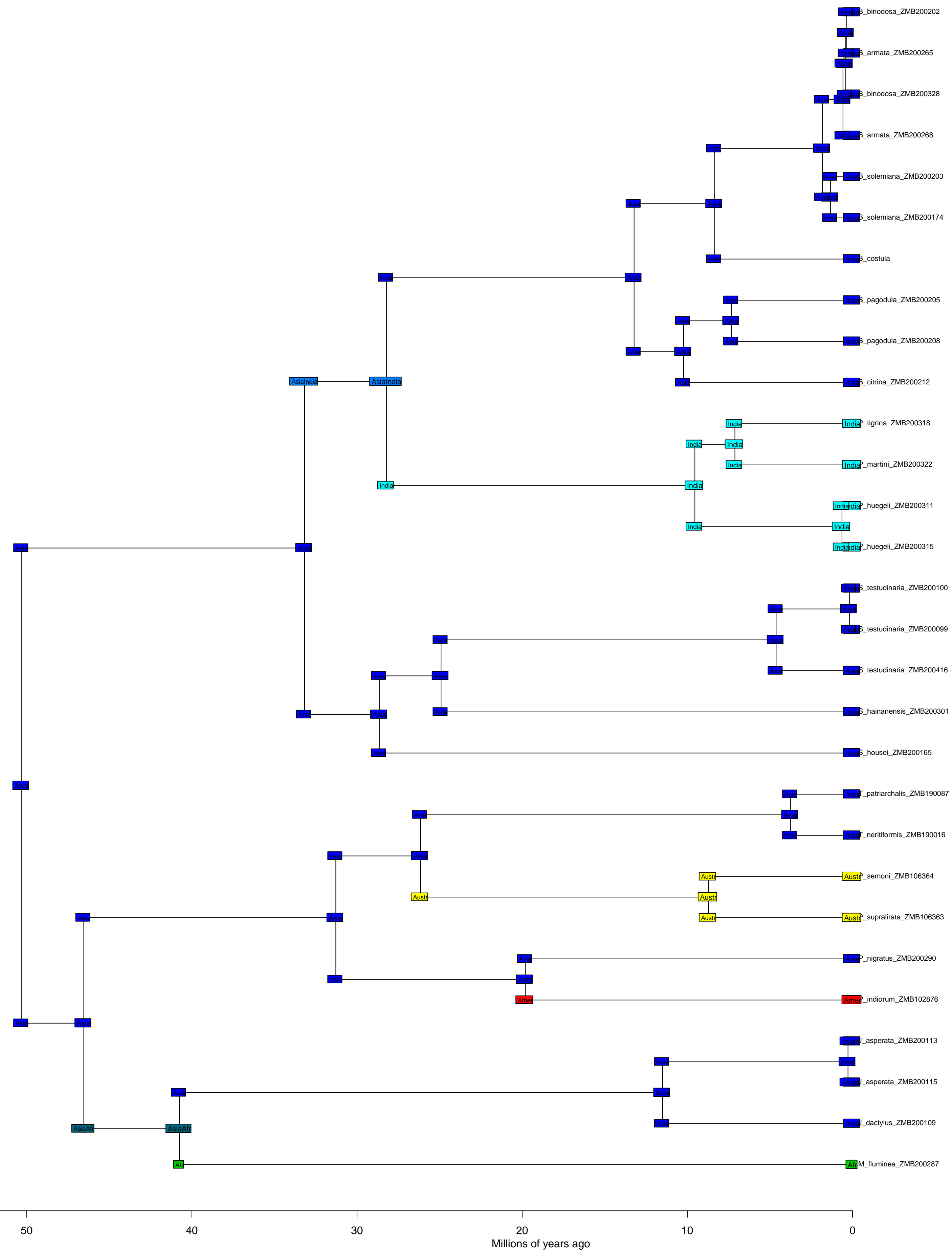


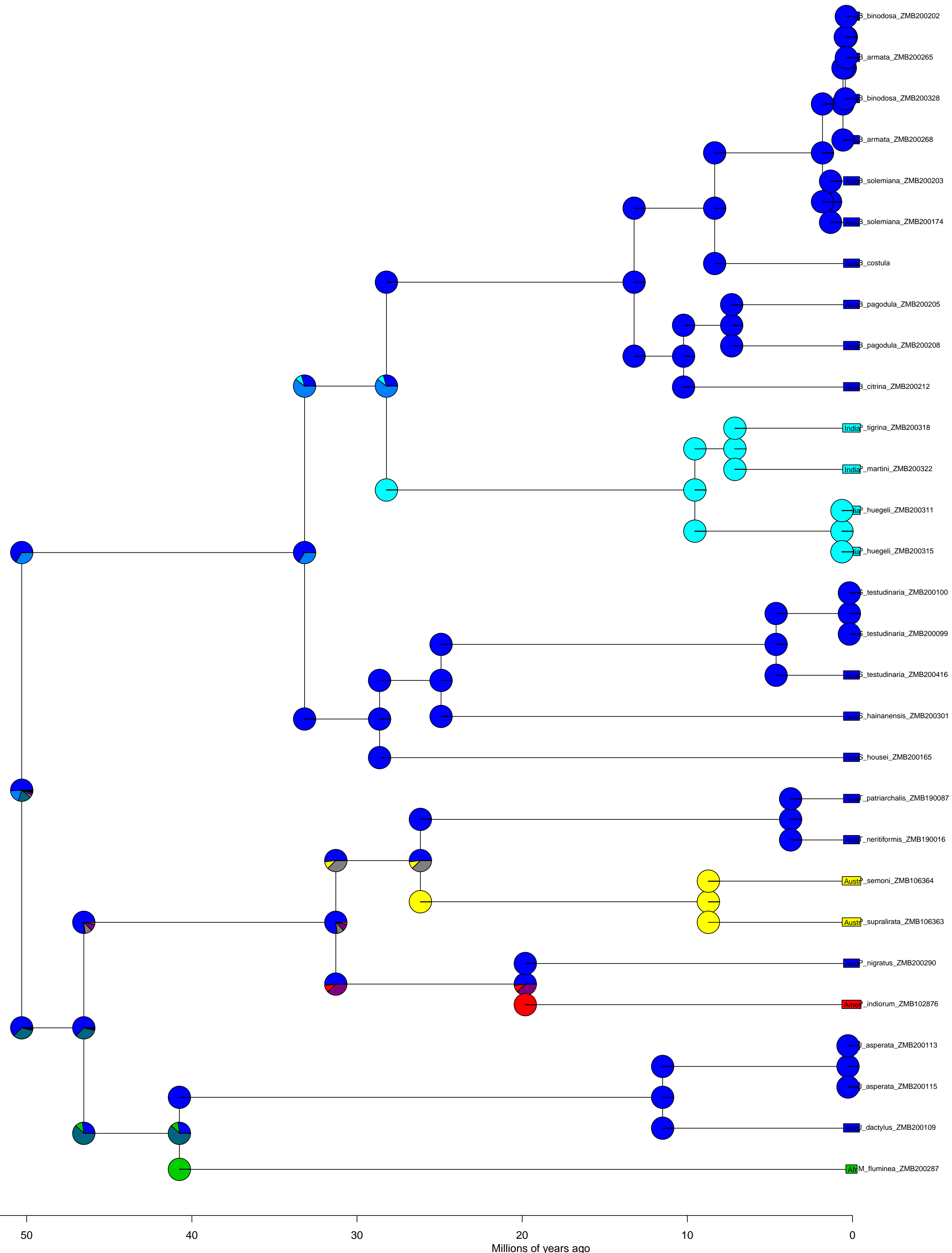


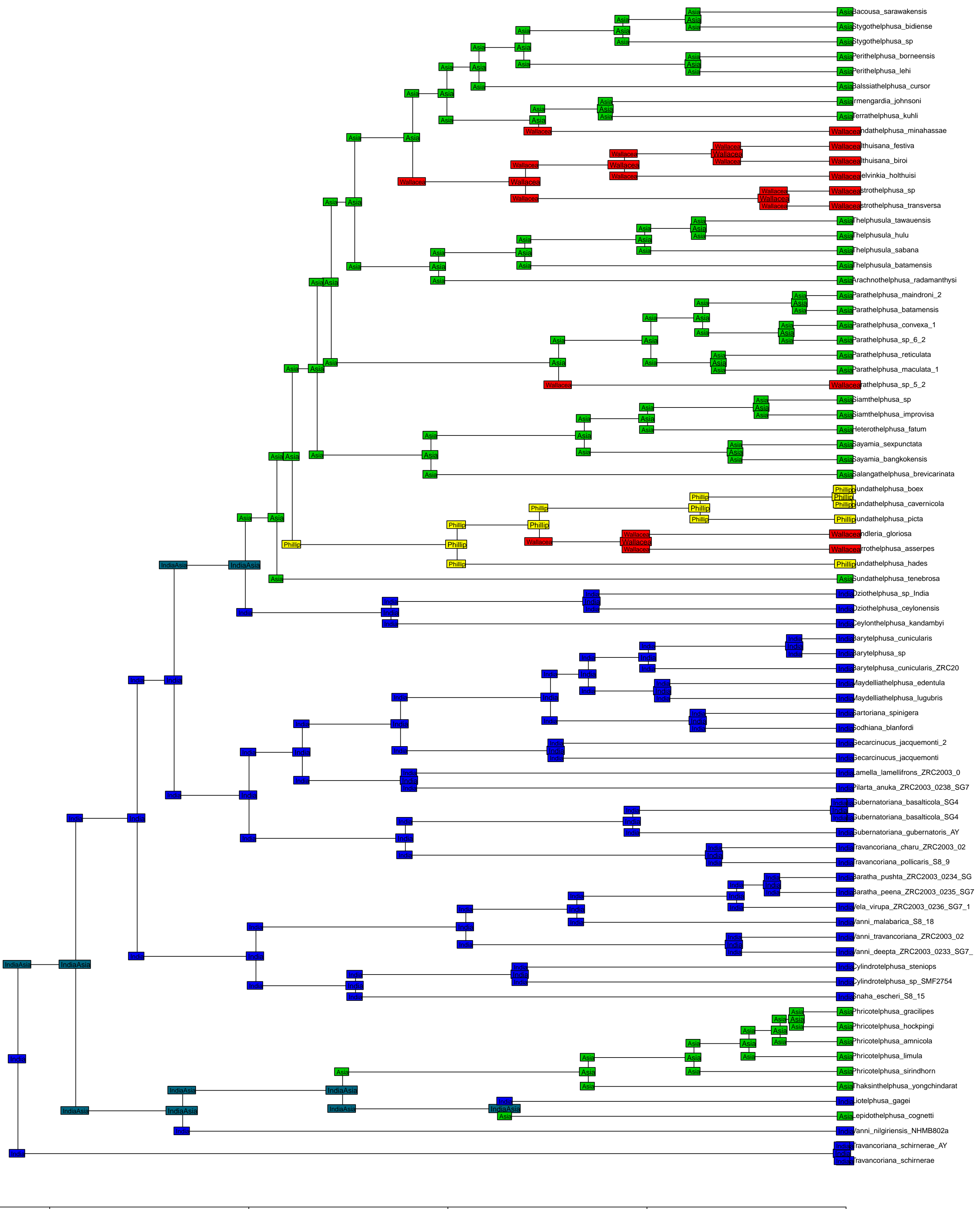


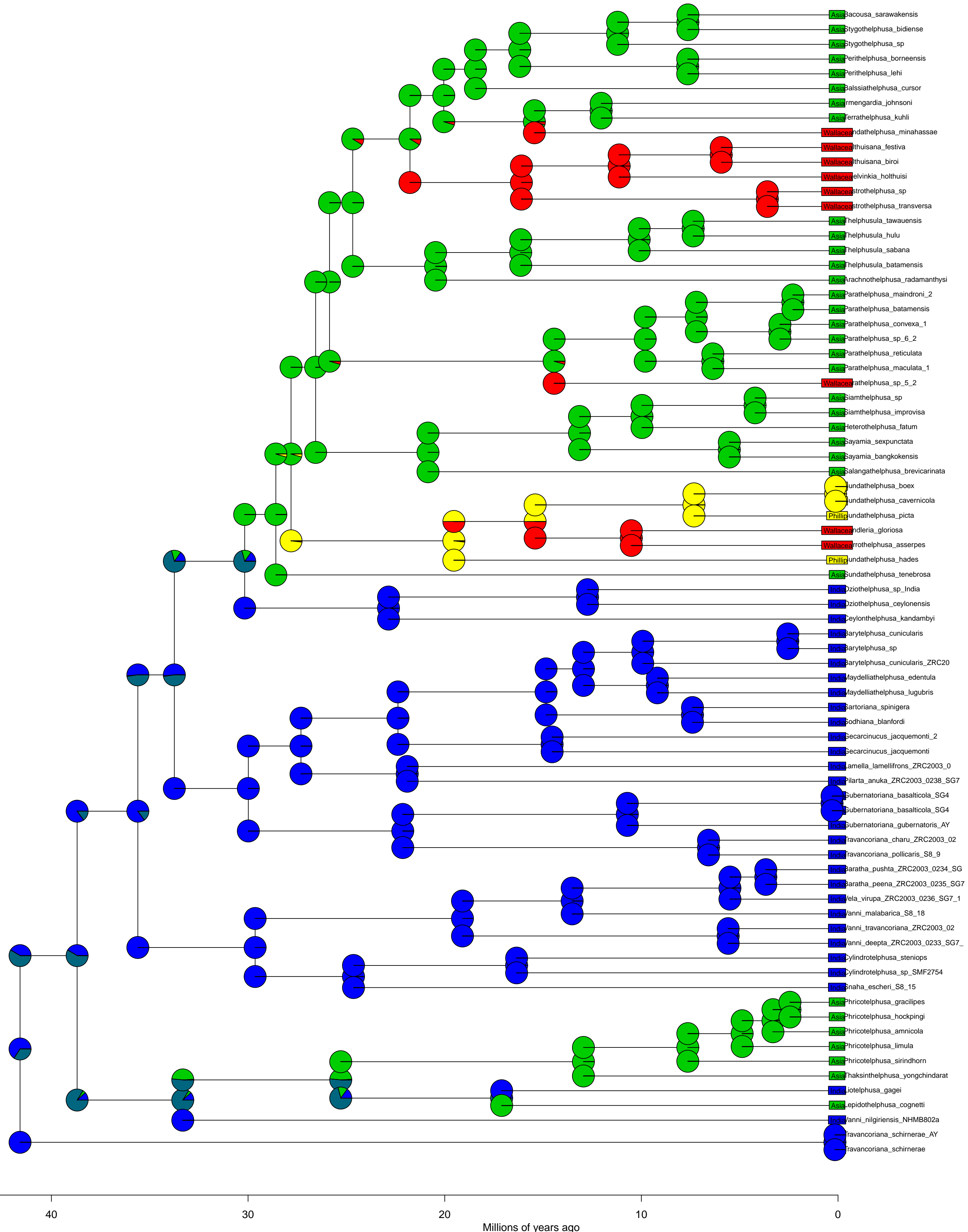


Pachychilidae BioGeoBEARS DEC+J  
 ancstates: global optim, 3 areas max. d=0; e=0; j=0.0197; LnL=-19.05

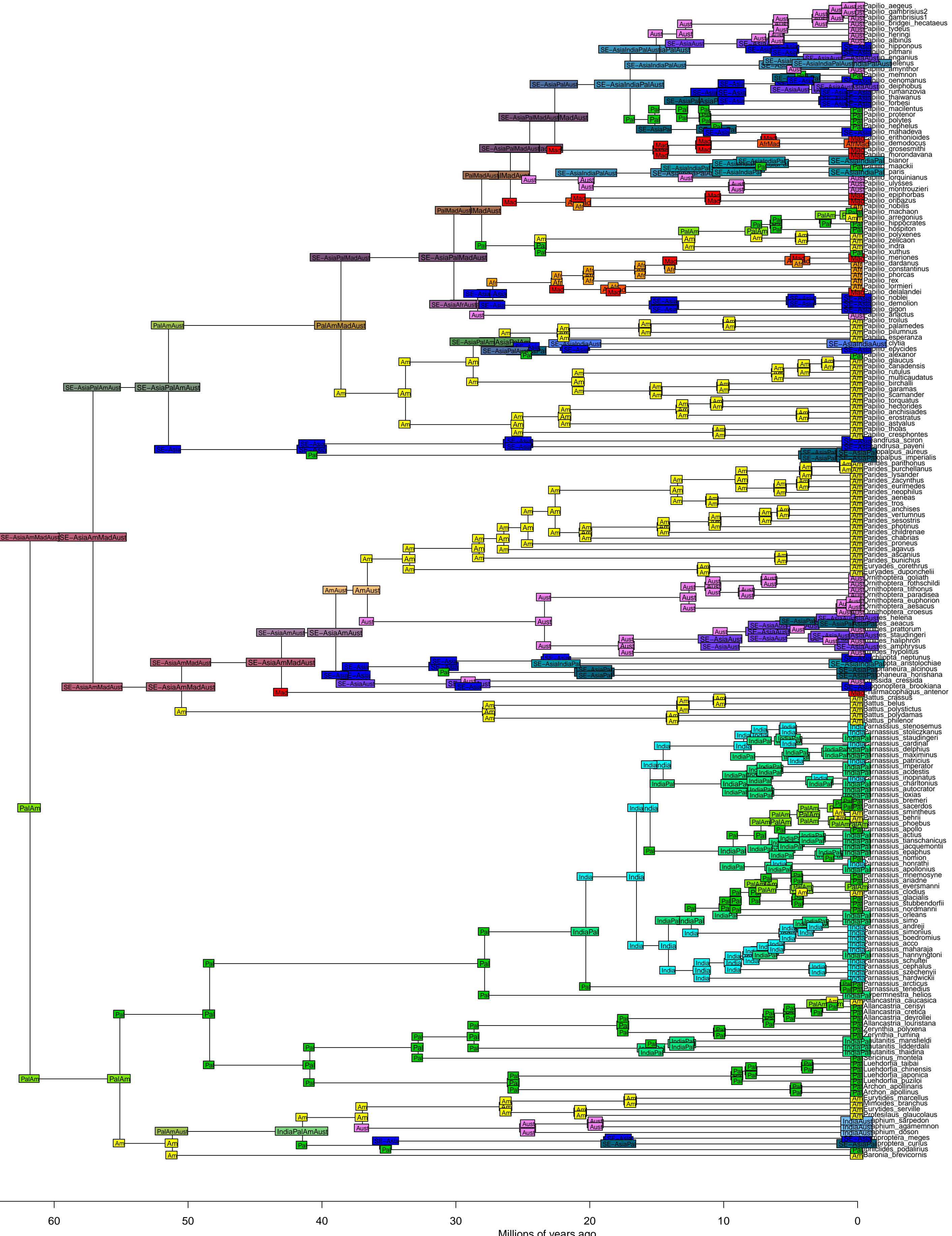




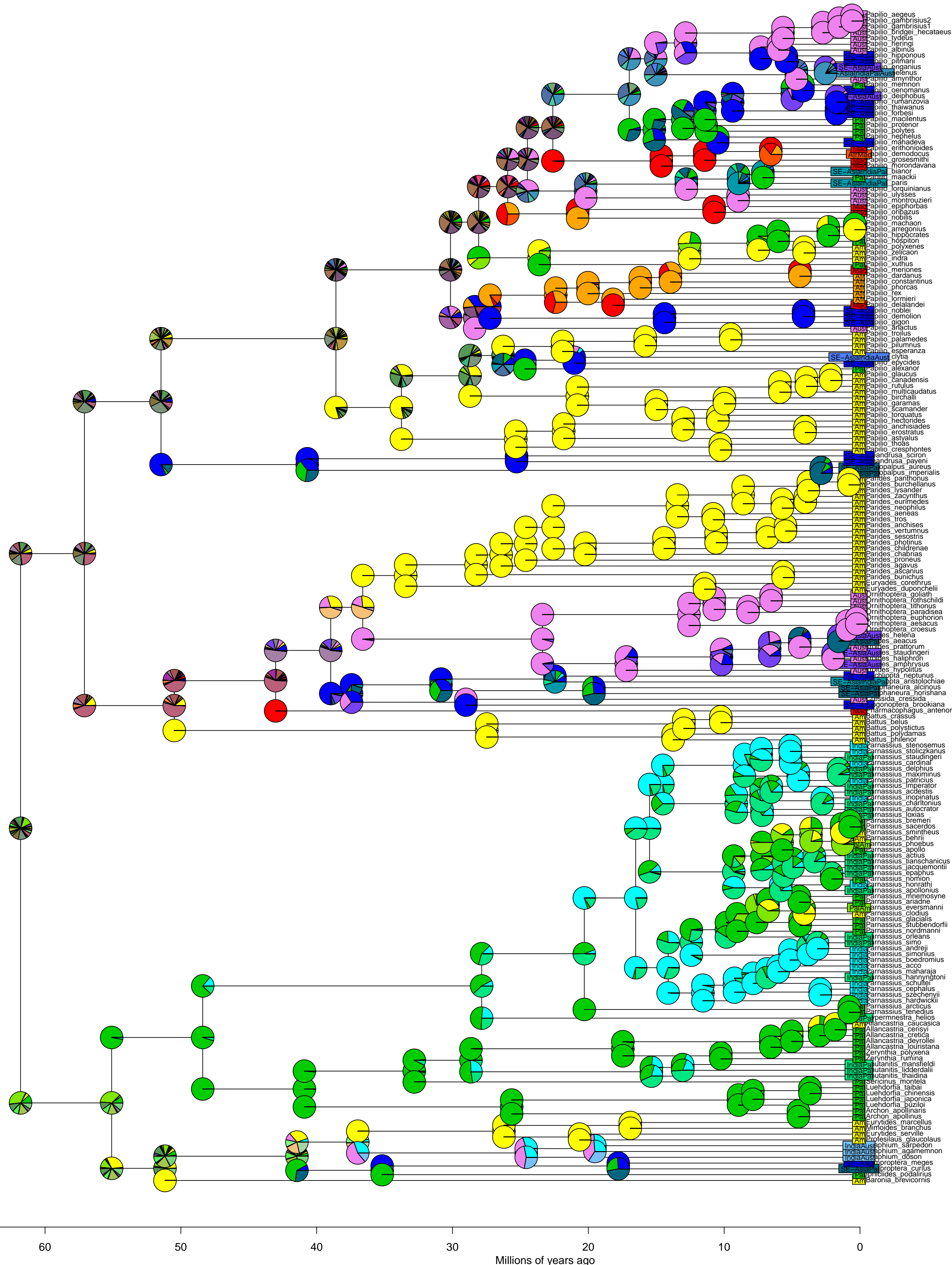


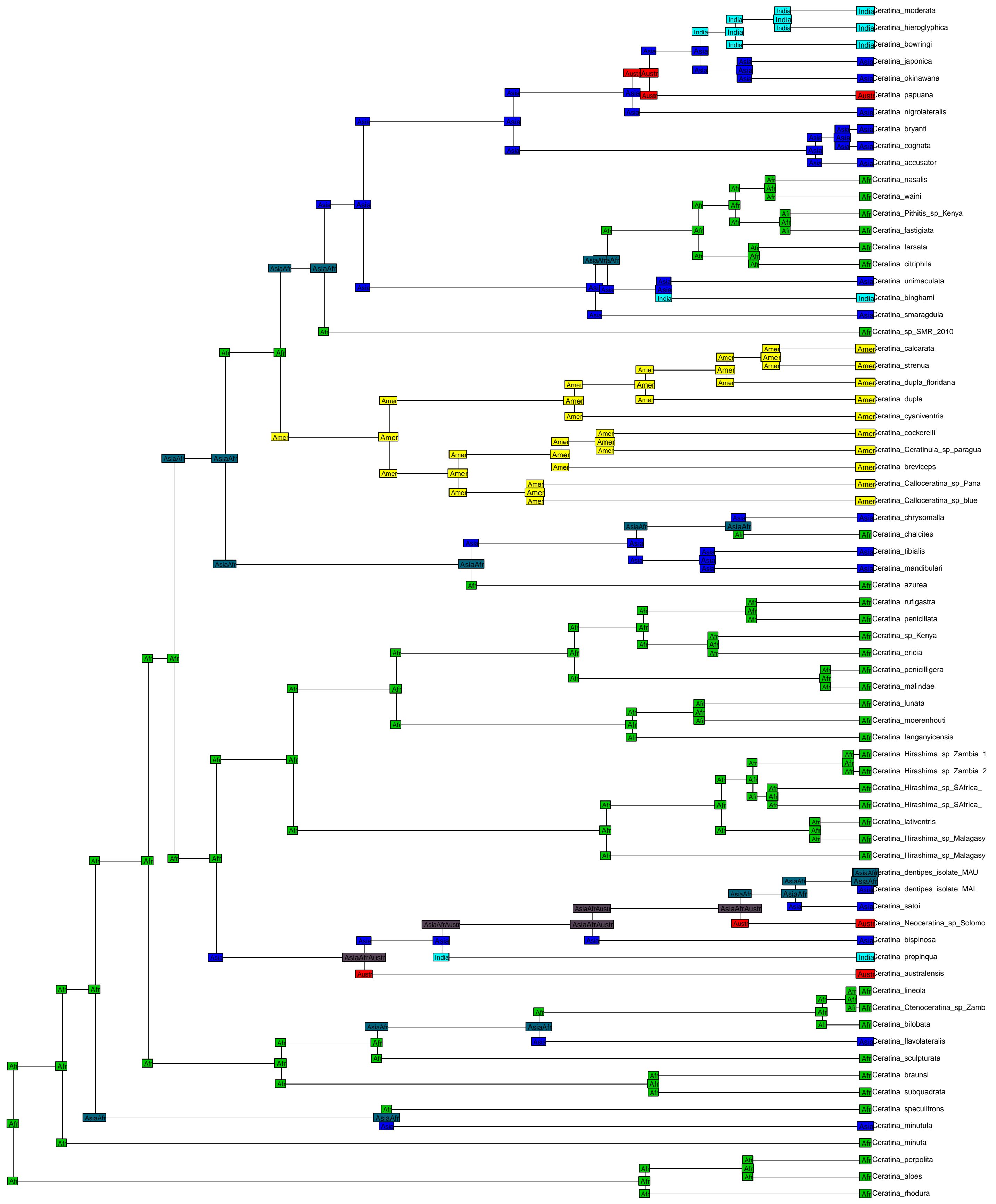


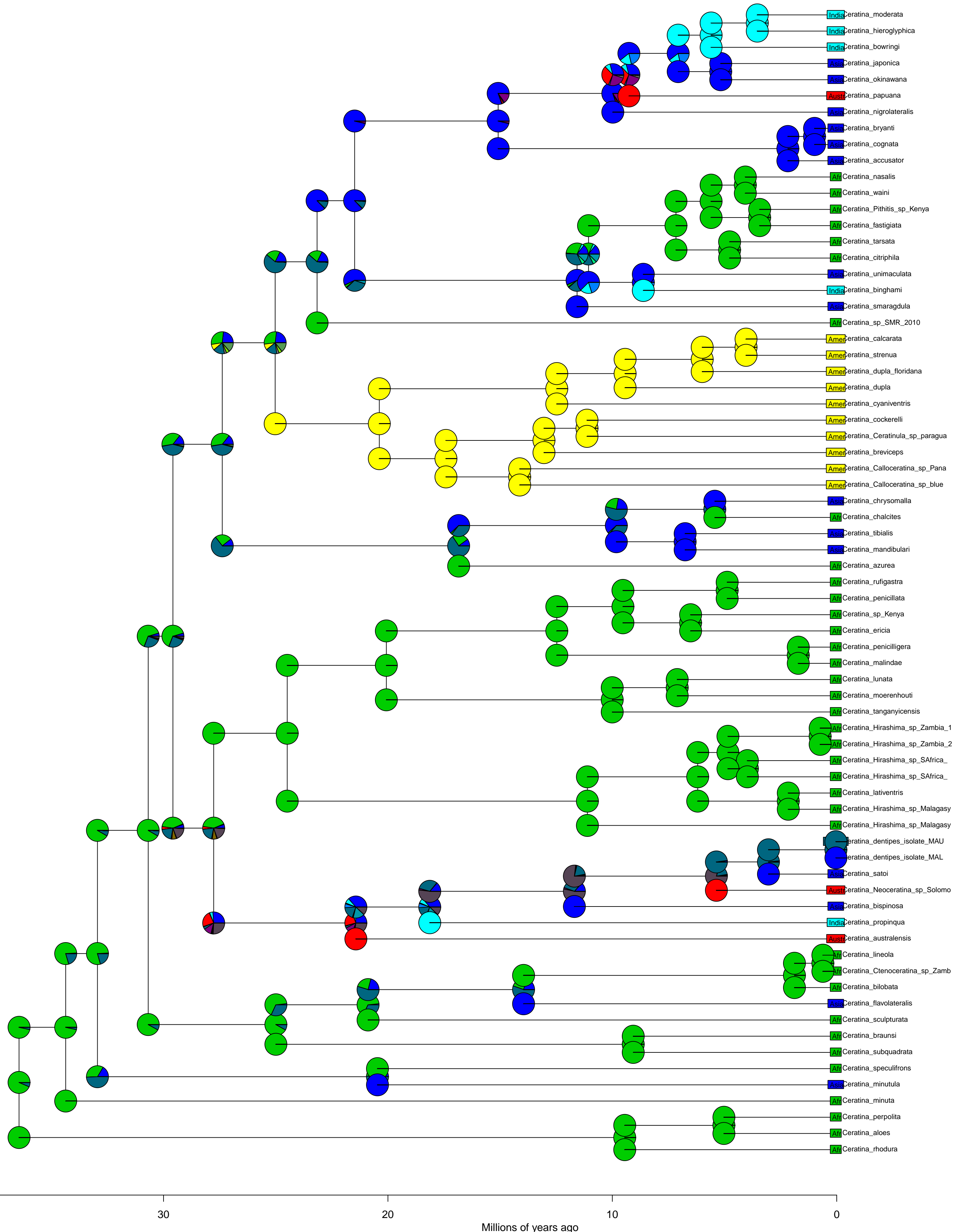
## Papilionidae BioGeoBEARS DEC+J

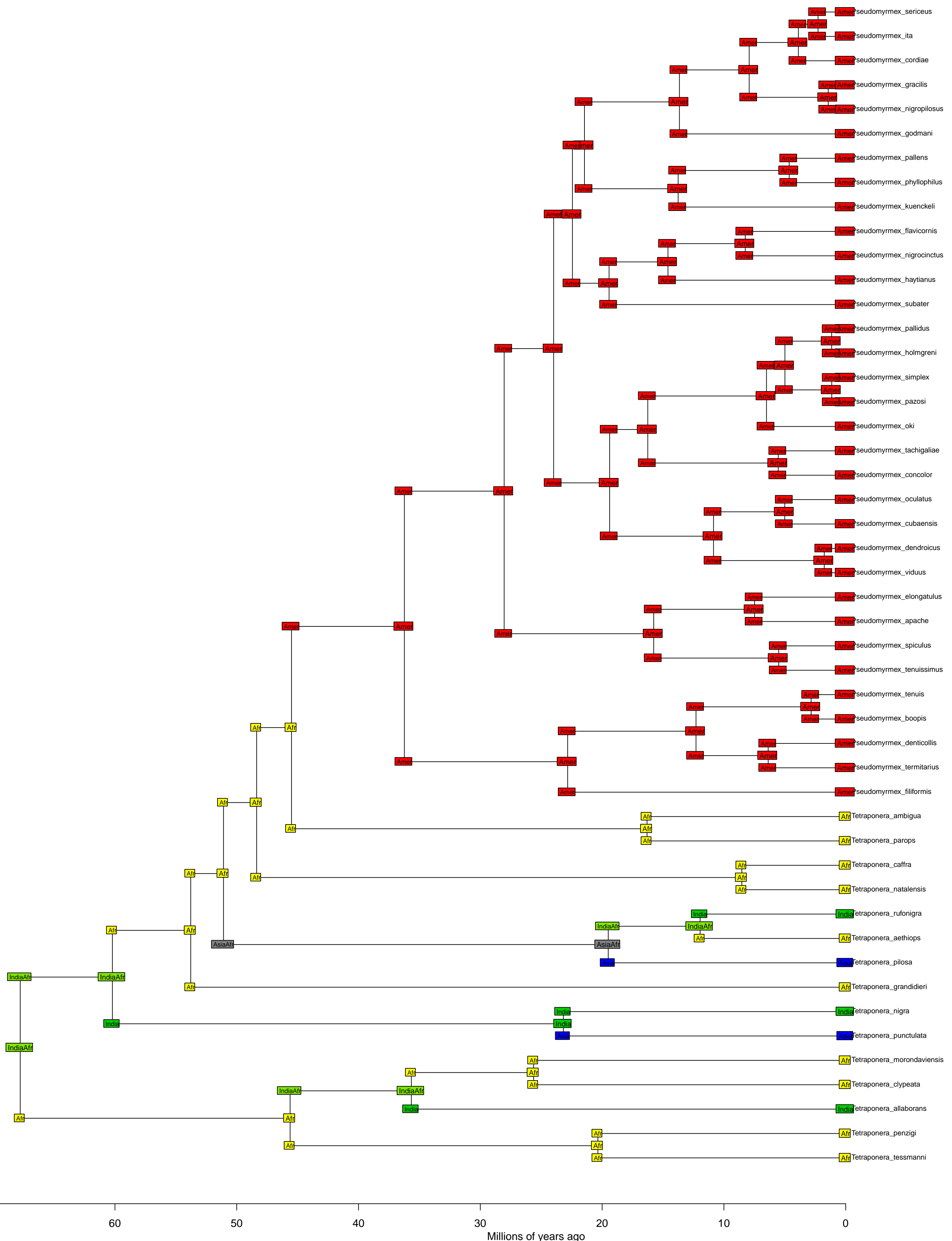


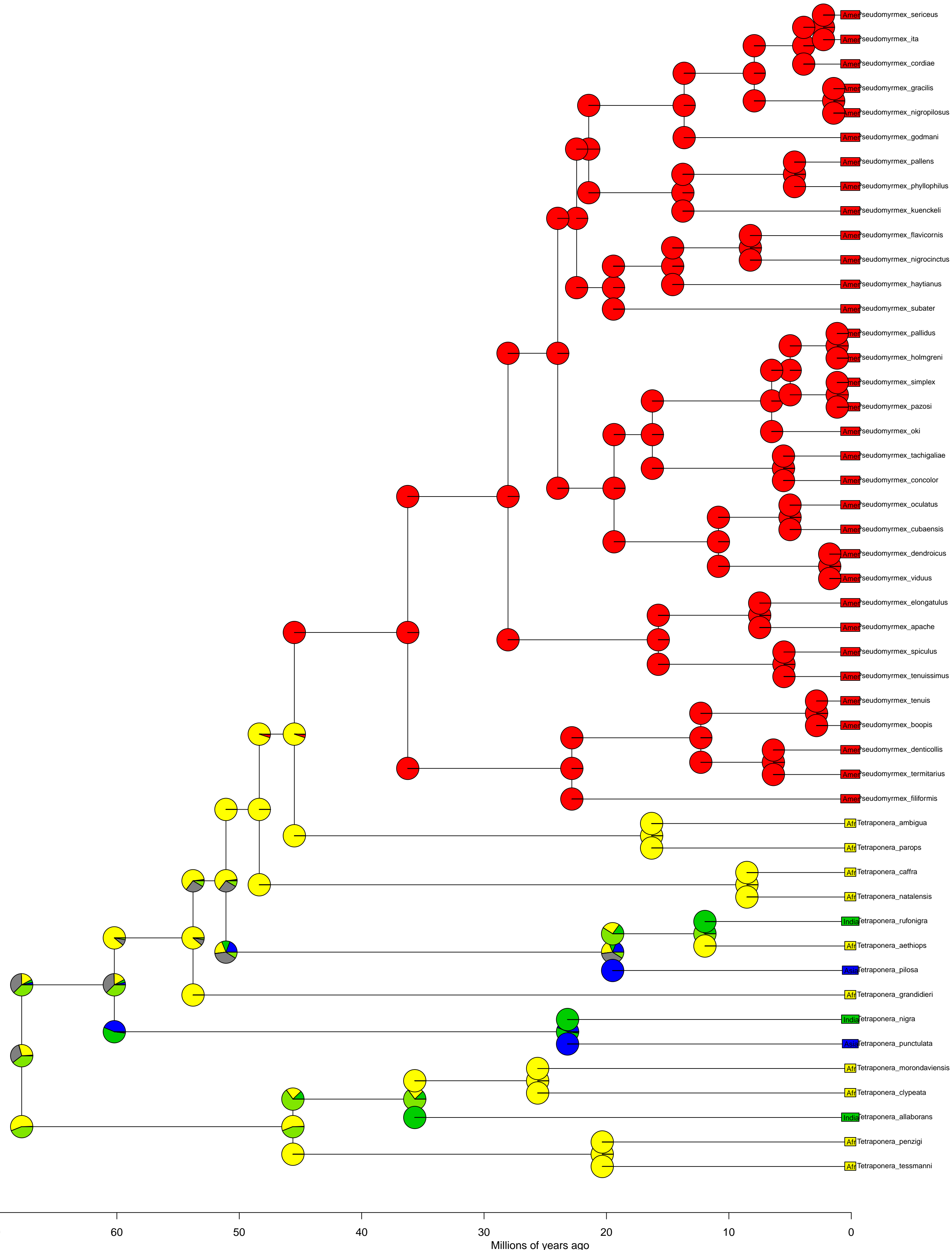
Papilionidae BioGeoBEARS DEC+J  
 ancstates: global optim, 4 areas max. d=0.0029; e=0; j=0.0105; LnL=-384.97

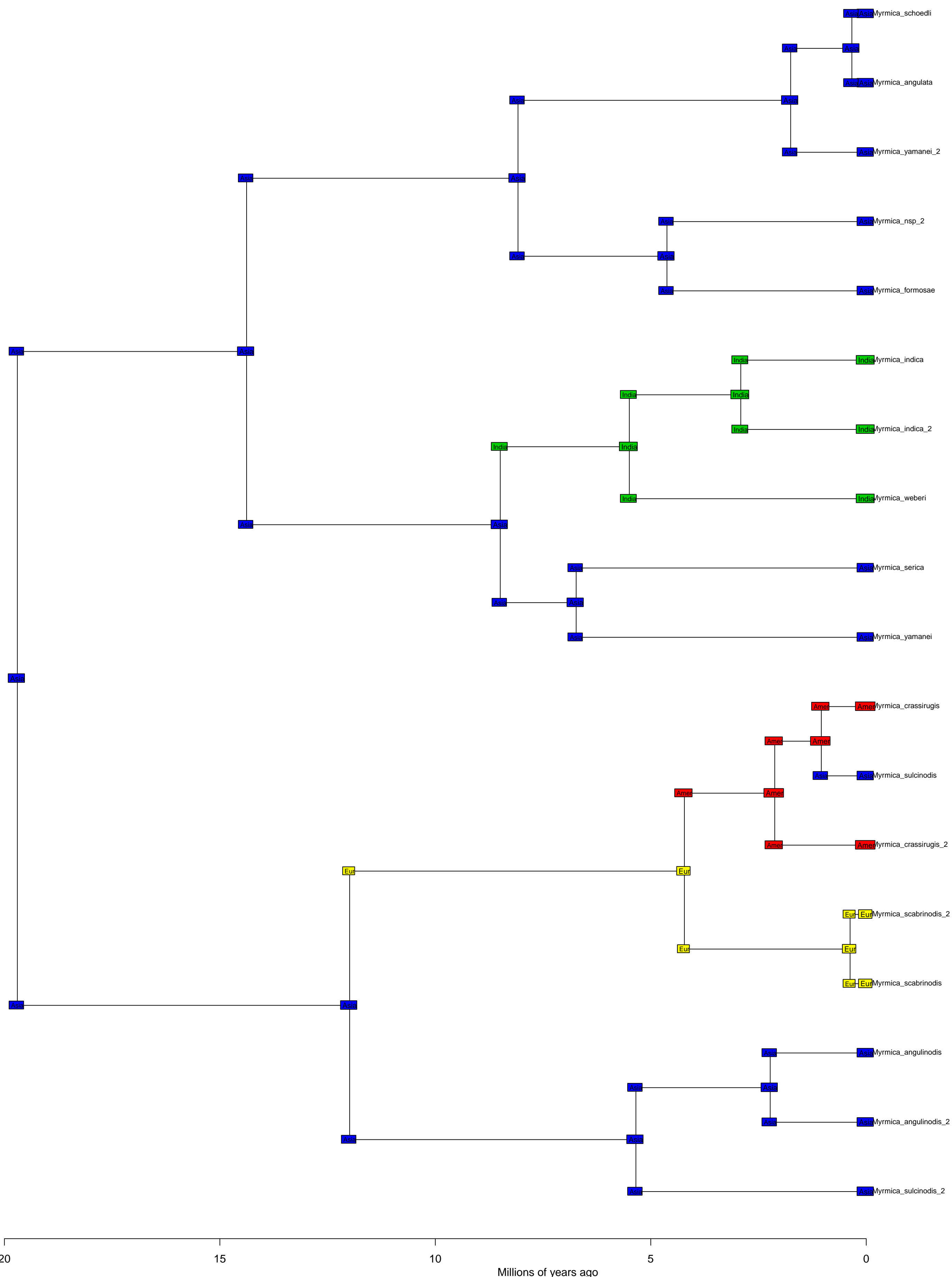


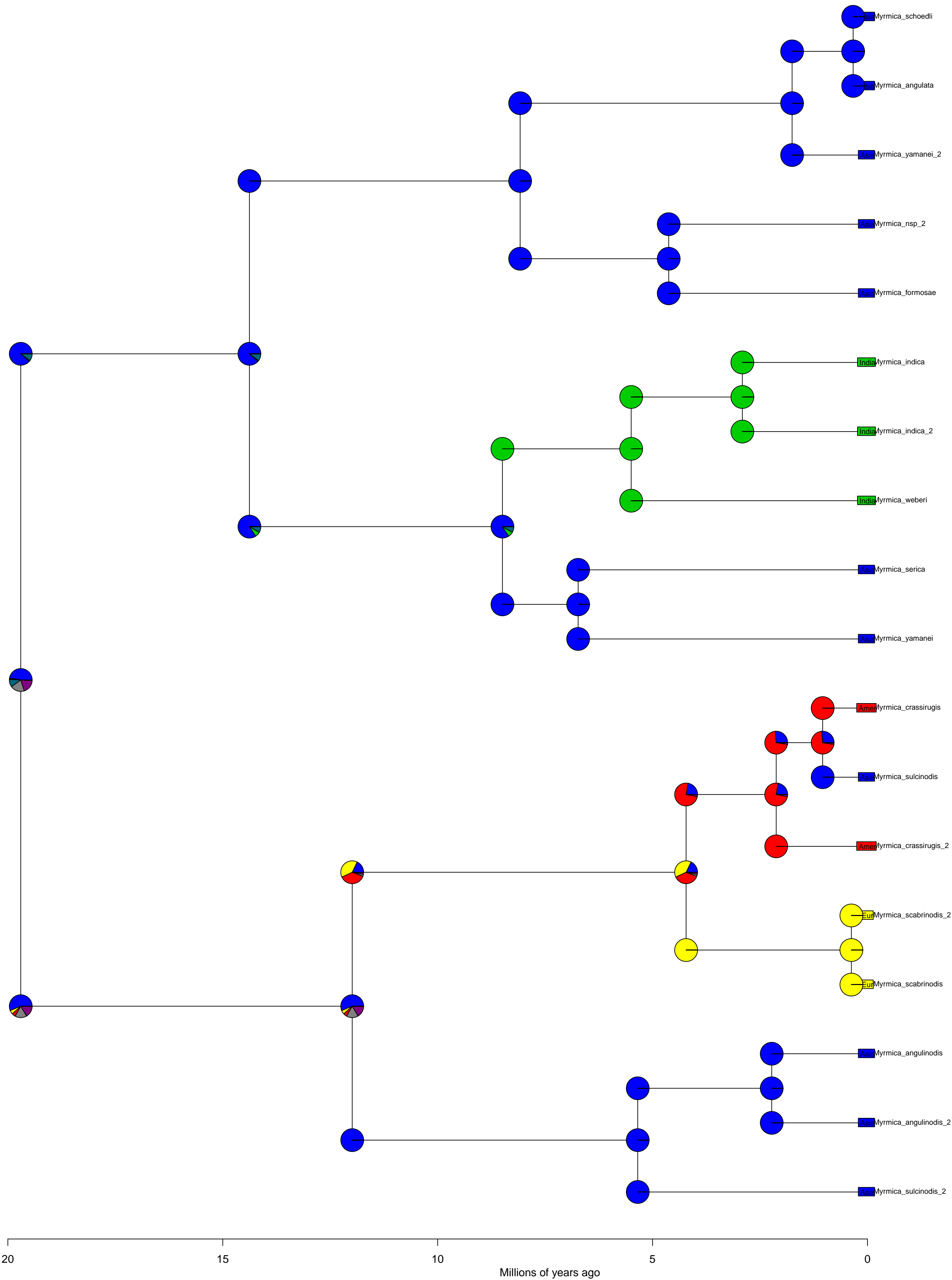


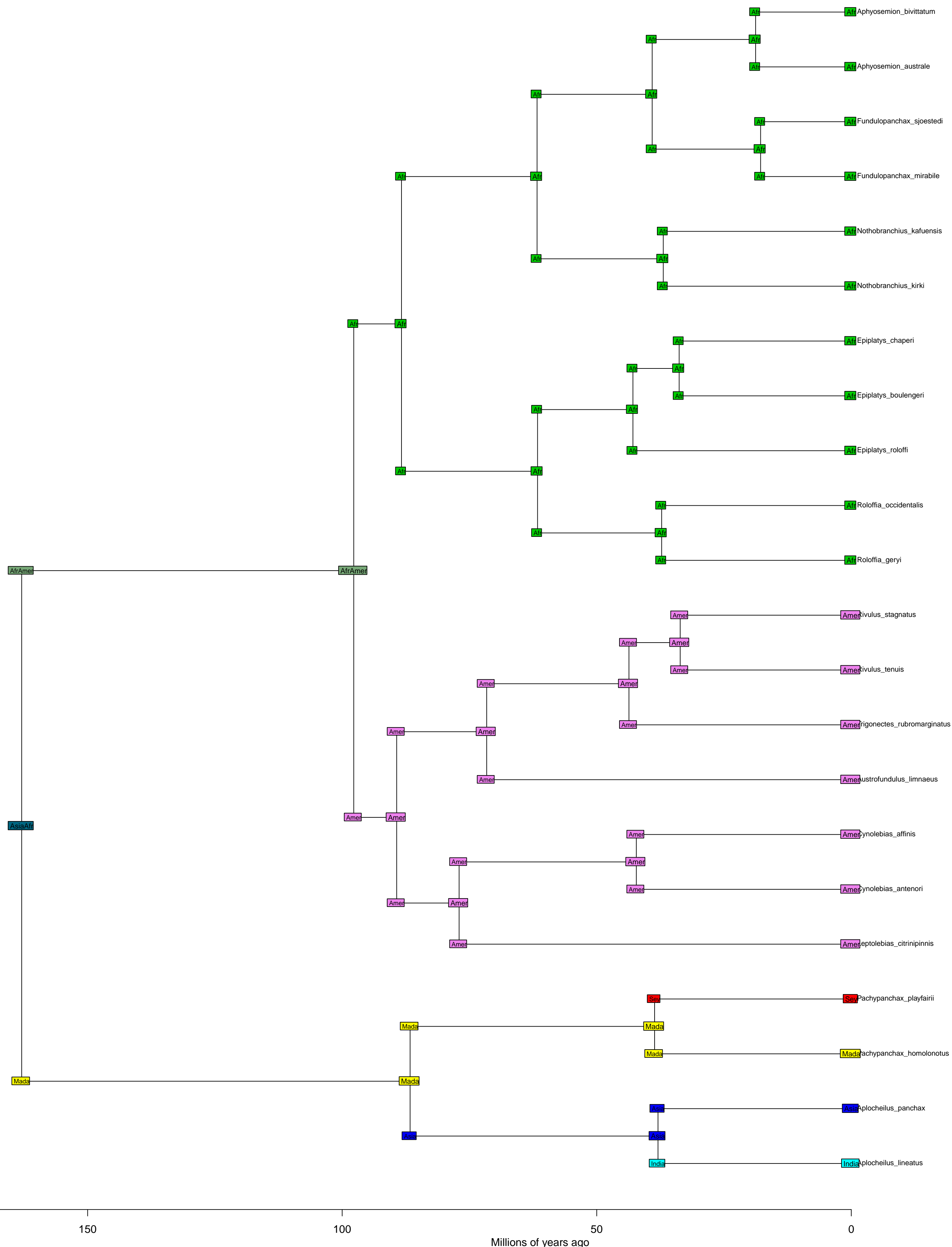


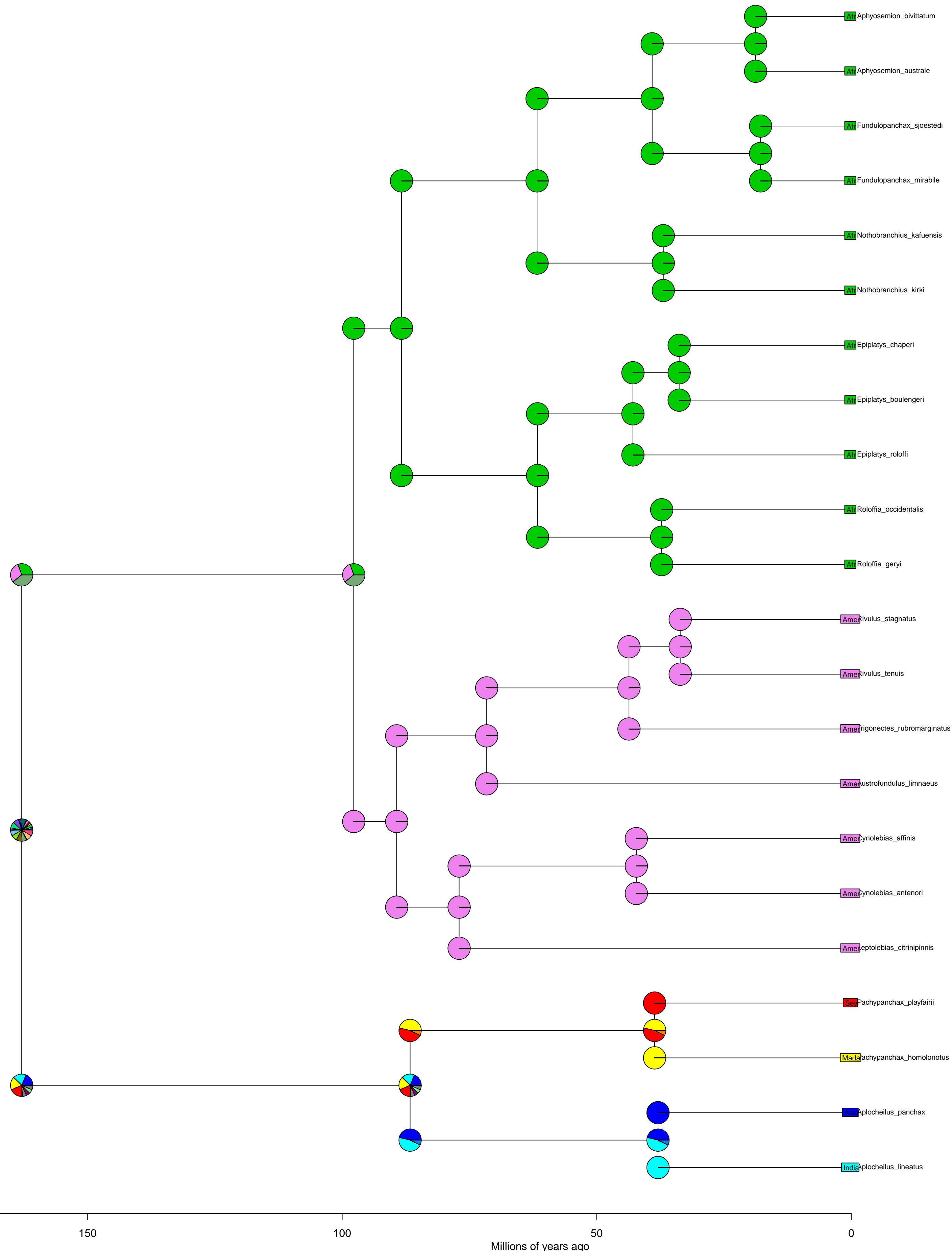


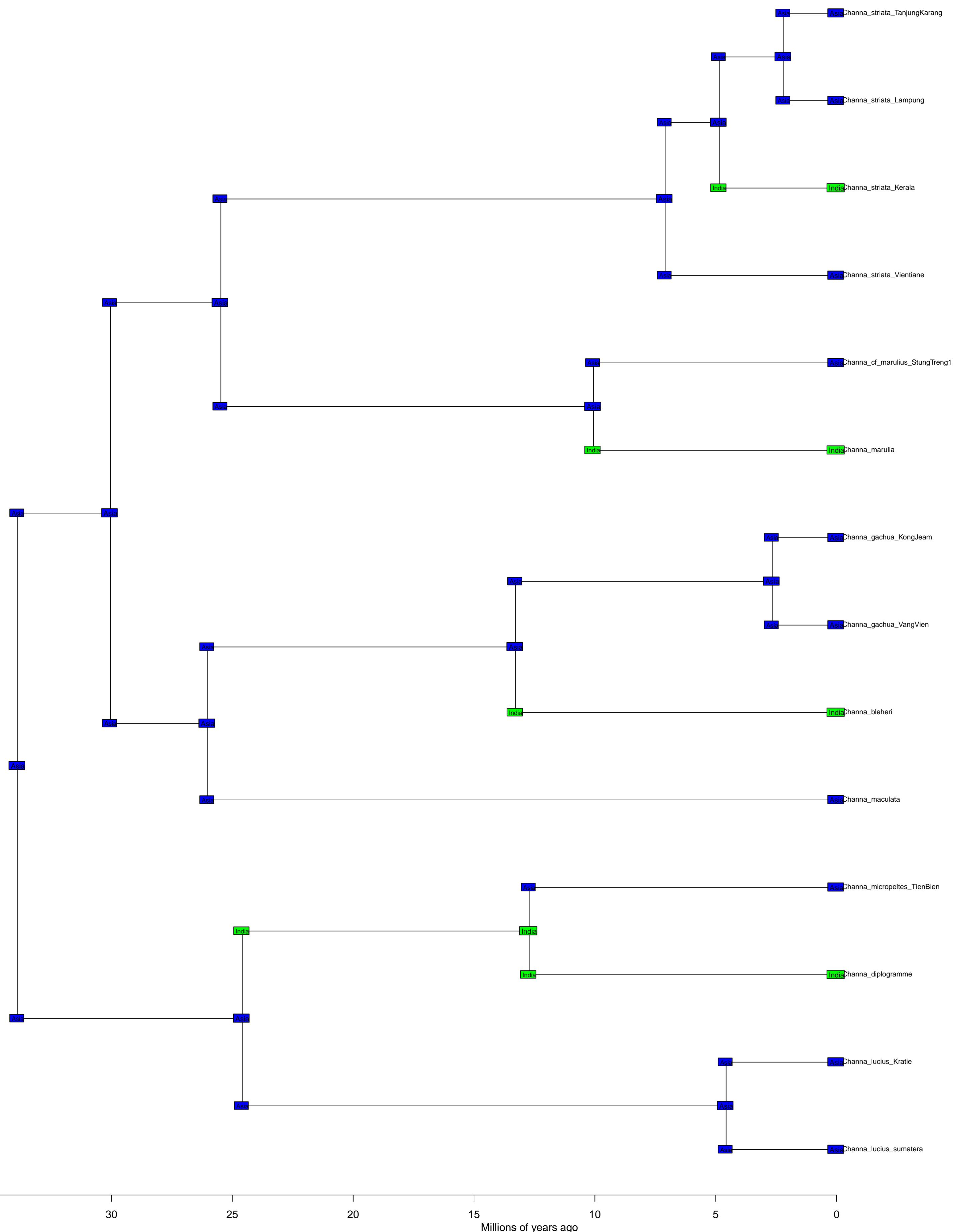


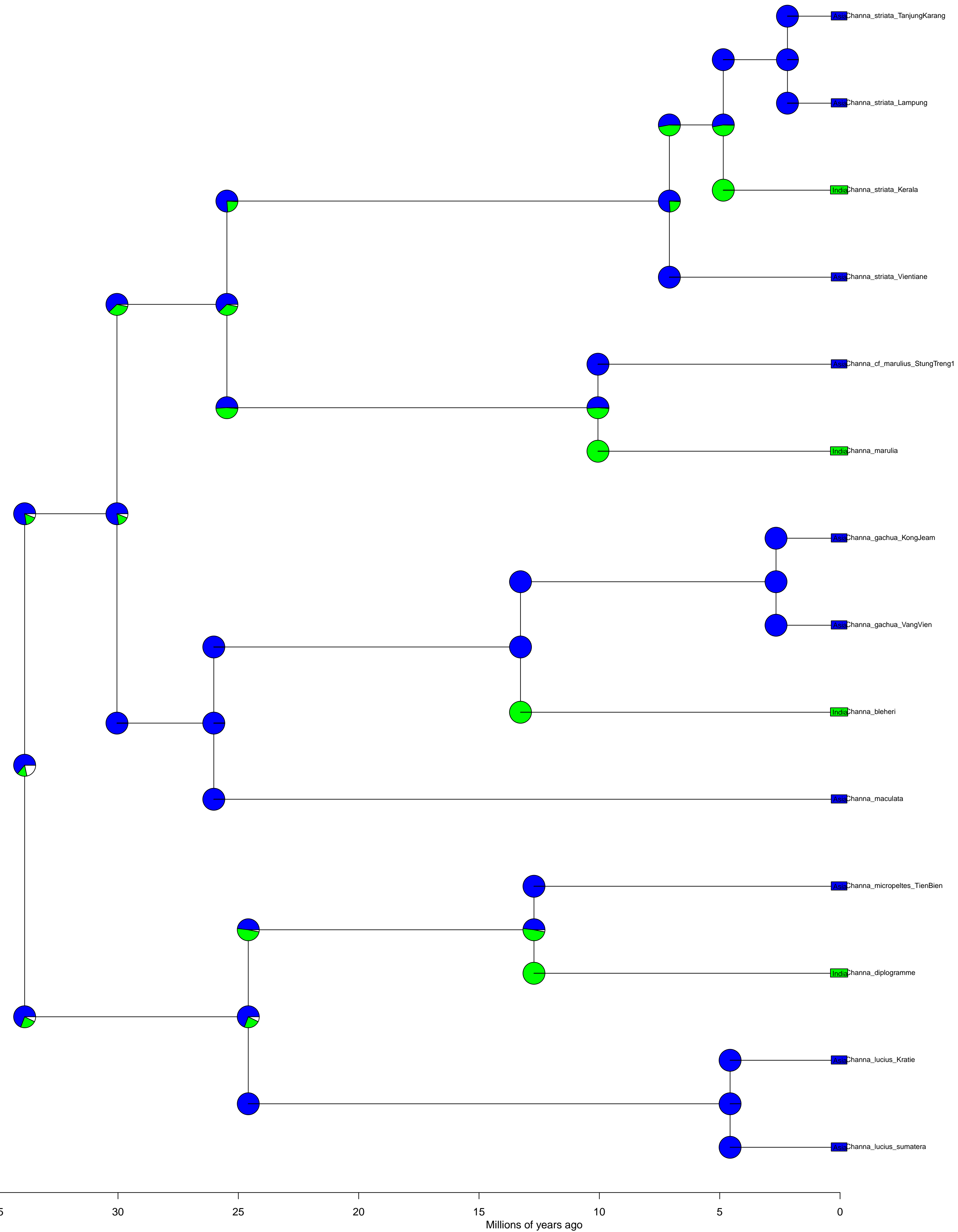




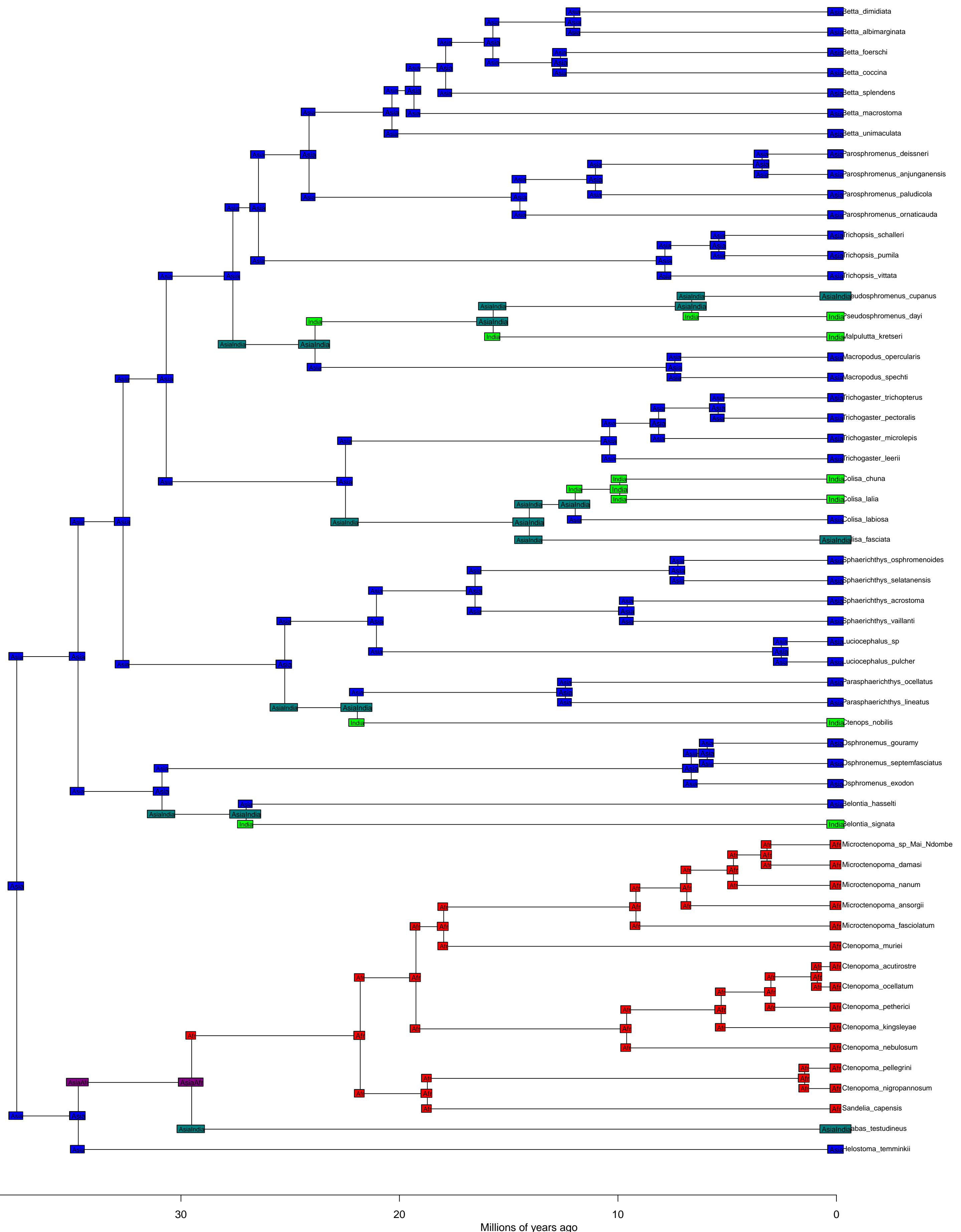


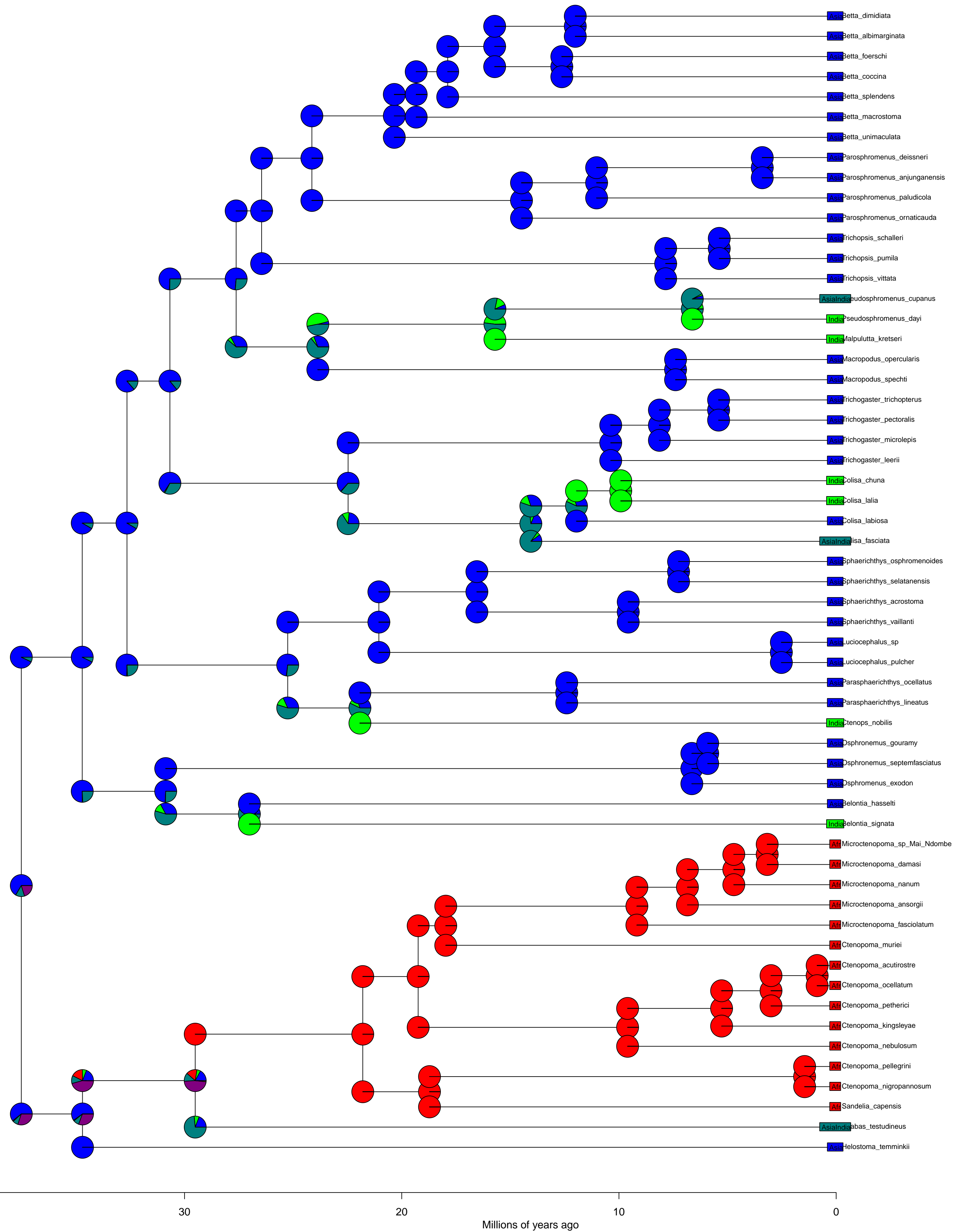


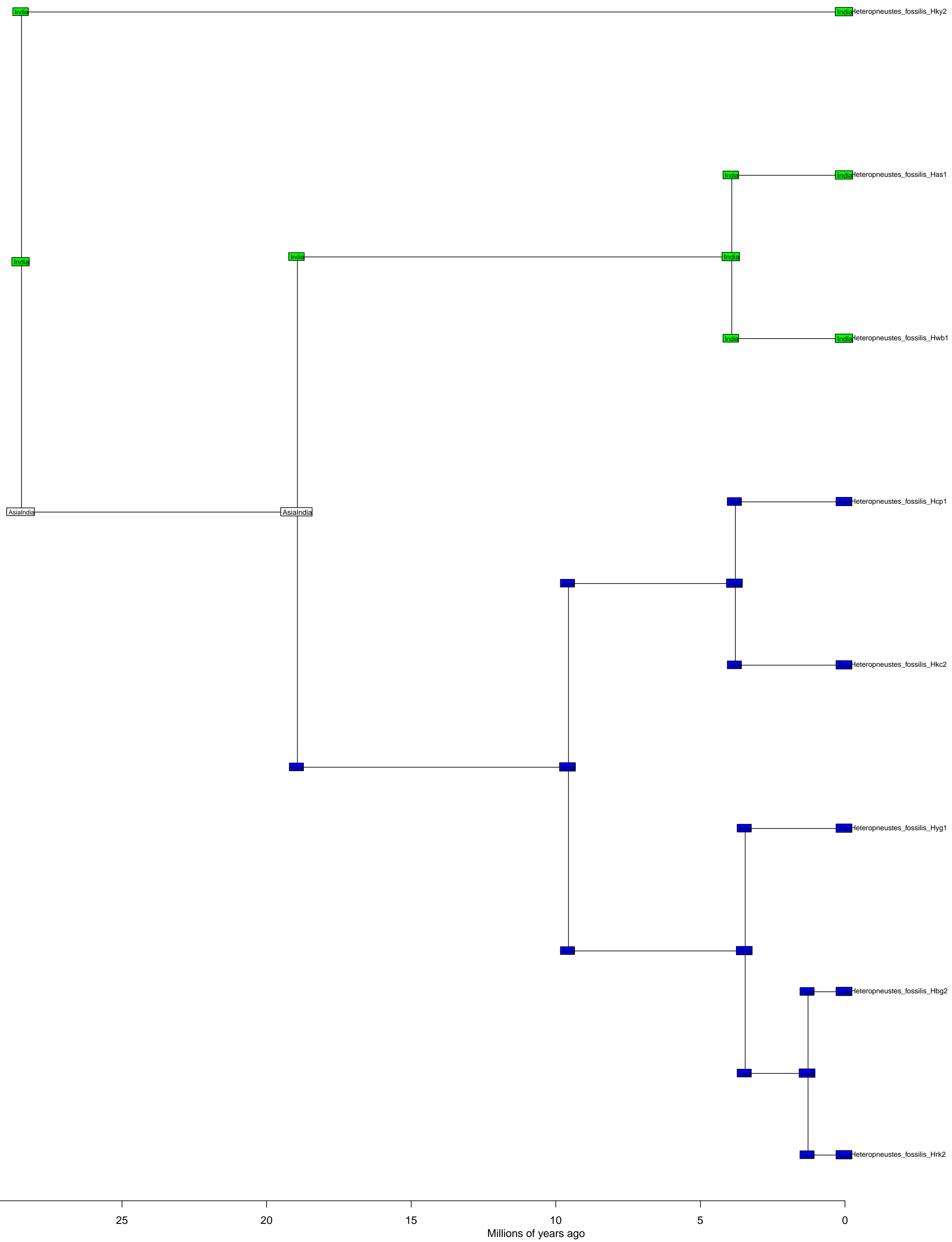


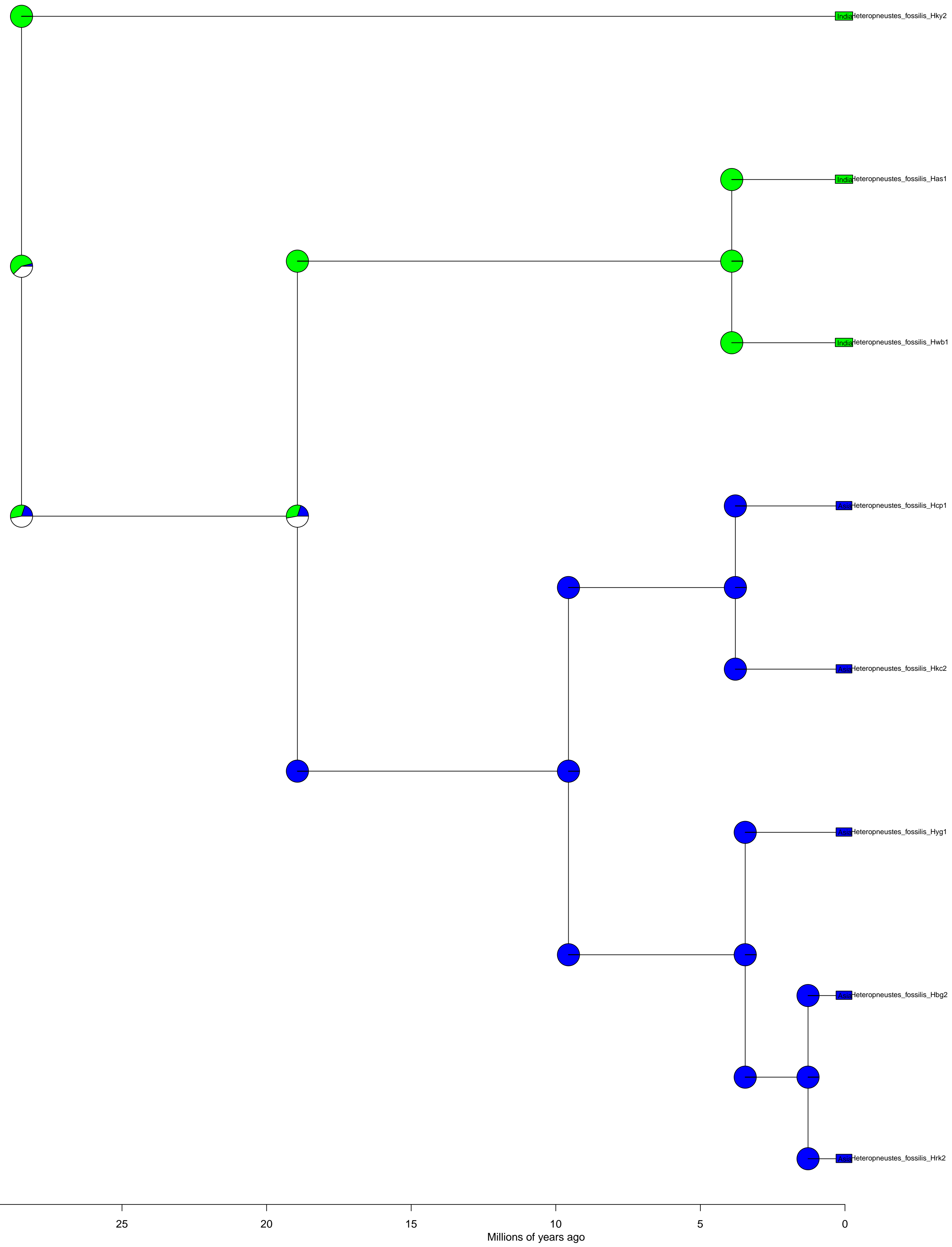


Anabantoidei, Osphronemidae BioGeoBEARS DEC+J  
ancstates: global optim, 2 areas max. d=0.0019; e=0; j=0.0207; LnL=-35.48

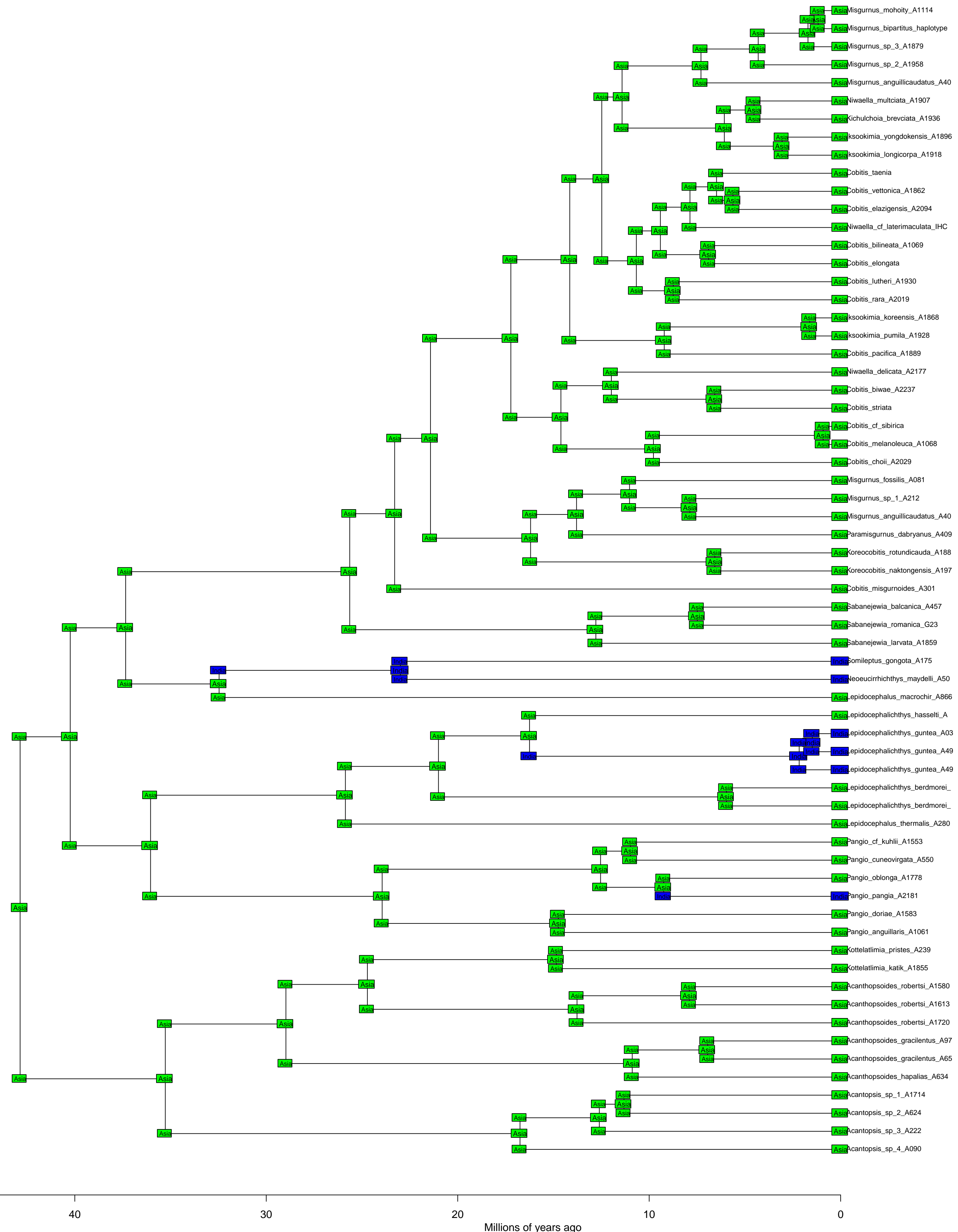


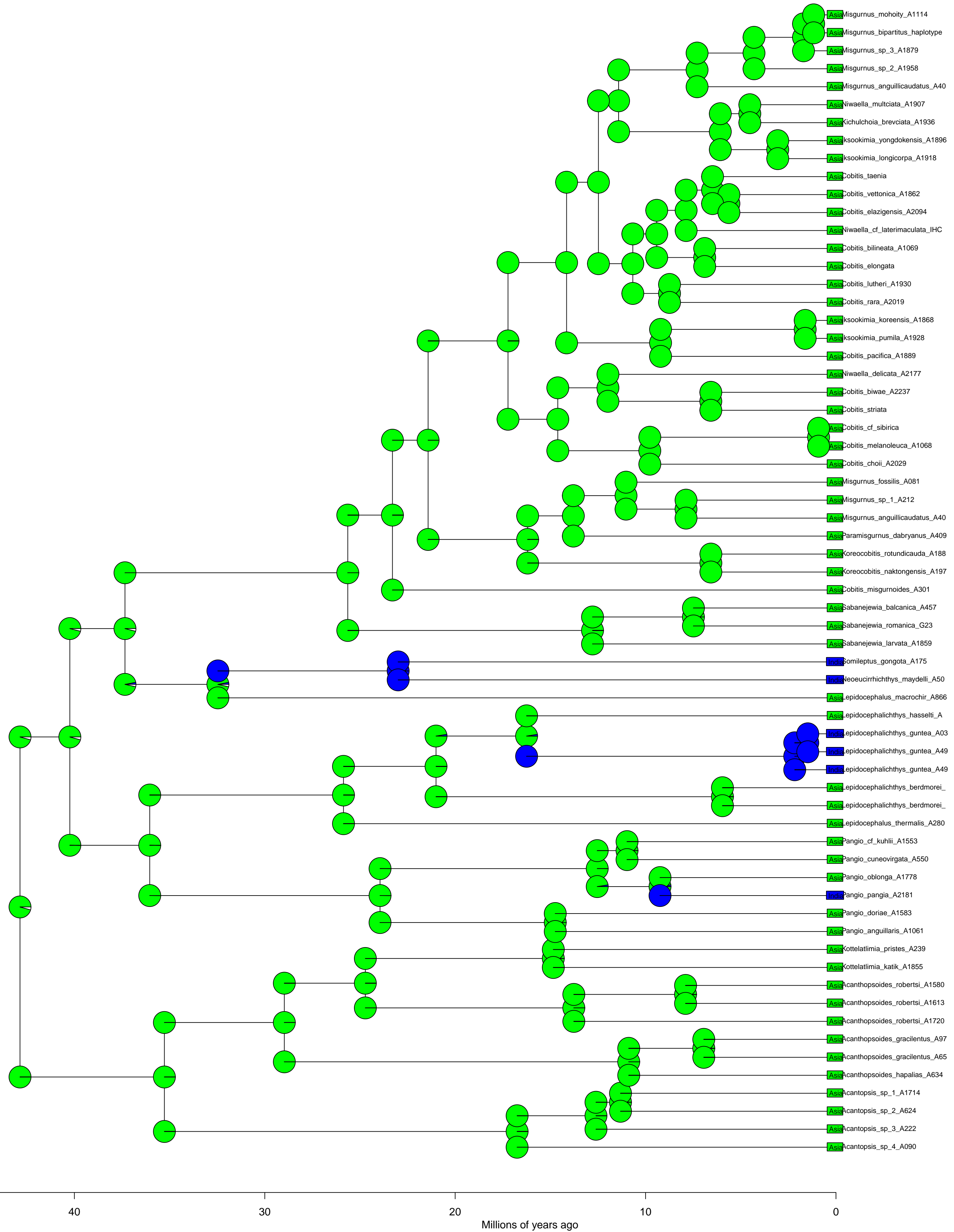


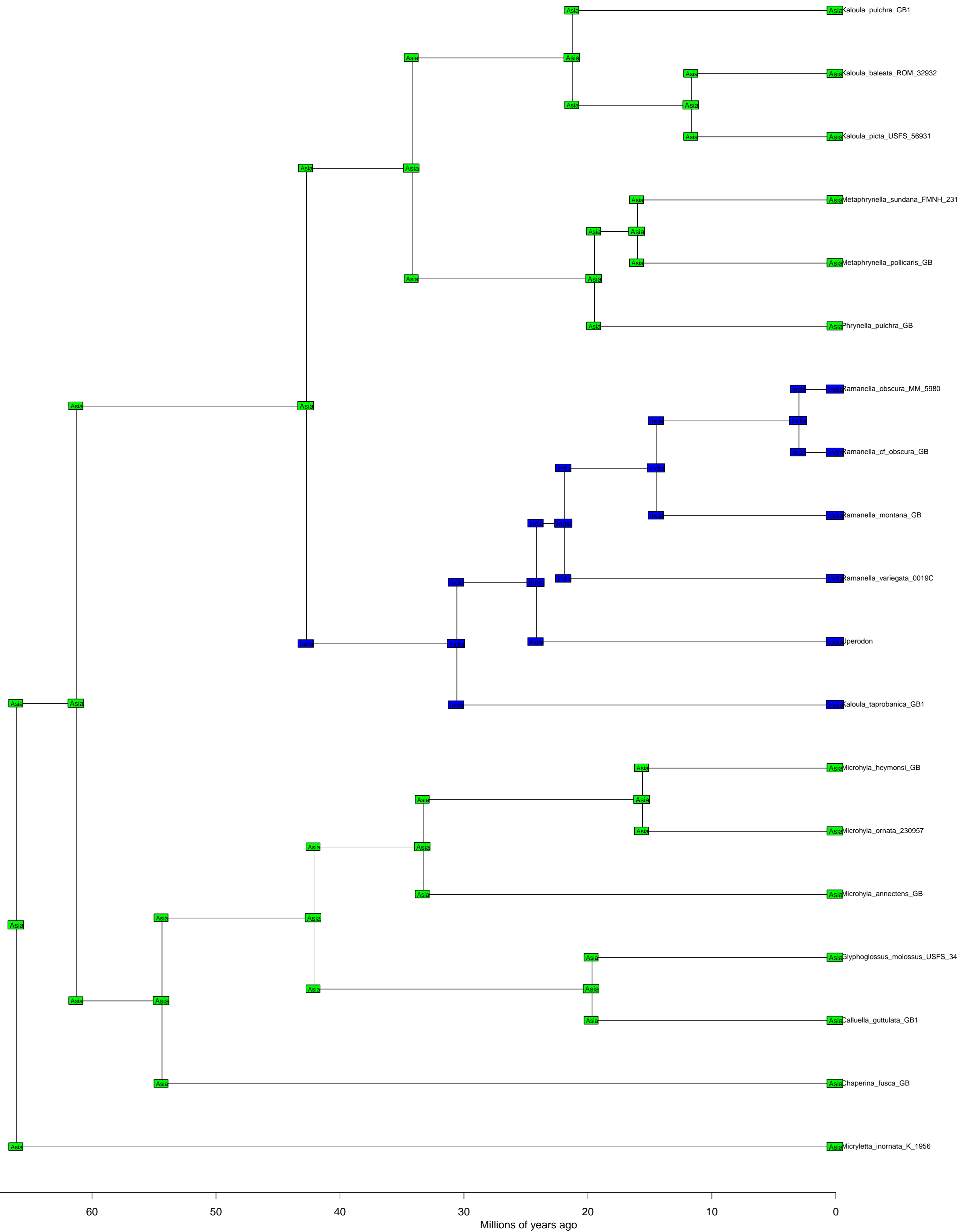


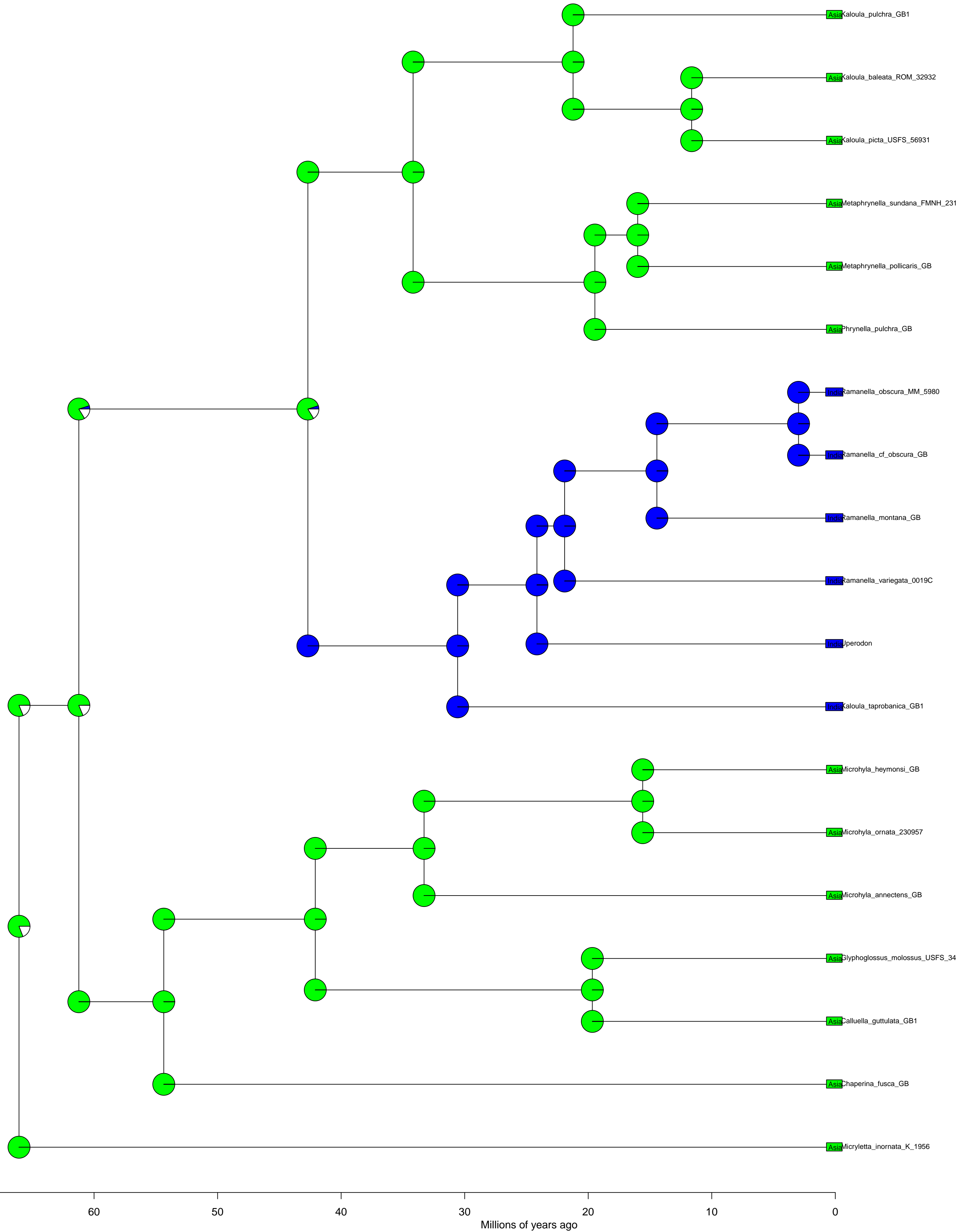


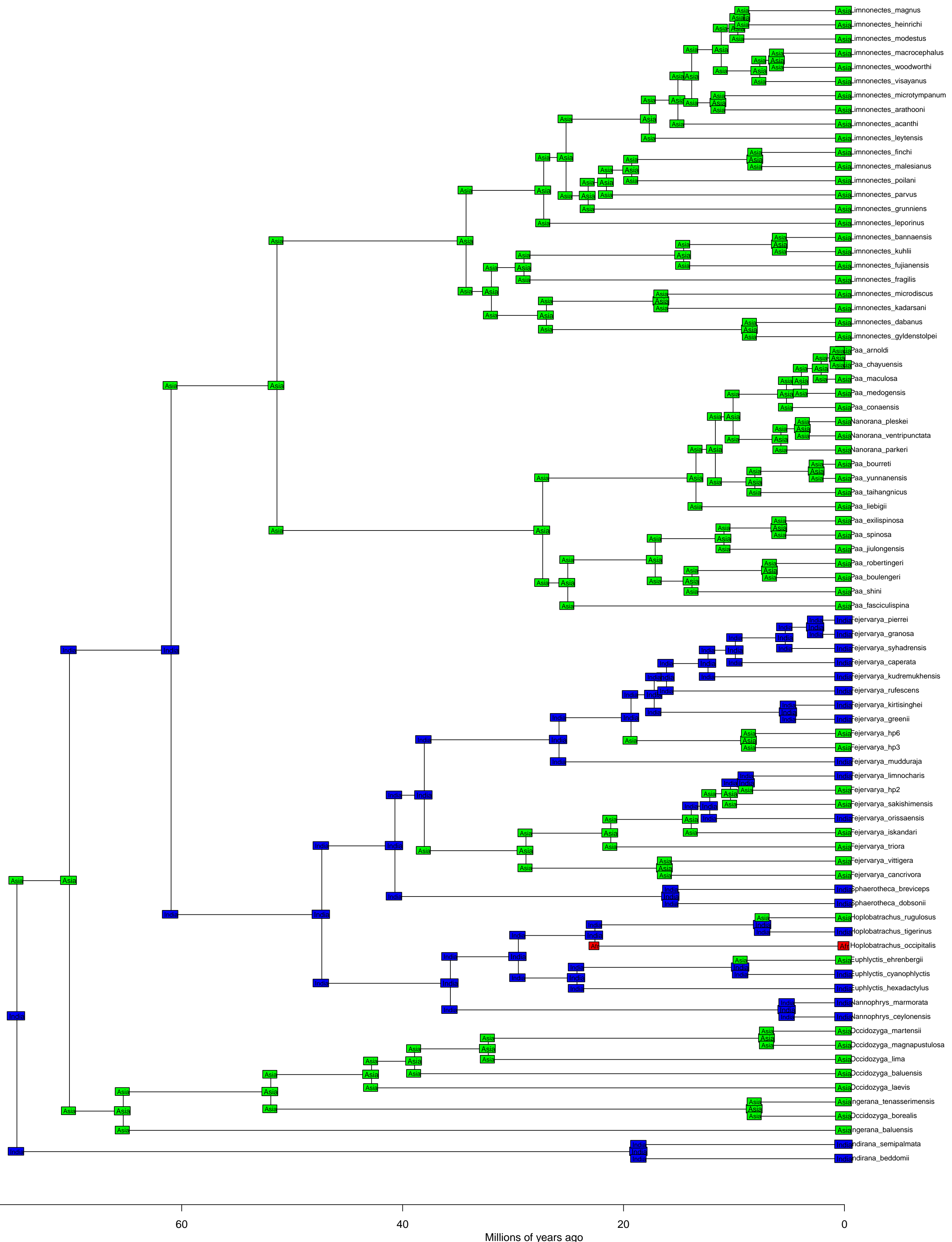
**Cobitidae BioGeoBEARS DEC+J**  
ancstates: global optim, 2 areas max. d=0; e=0; j=0.0252; LnL=-14.02

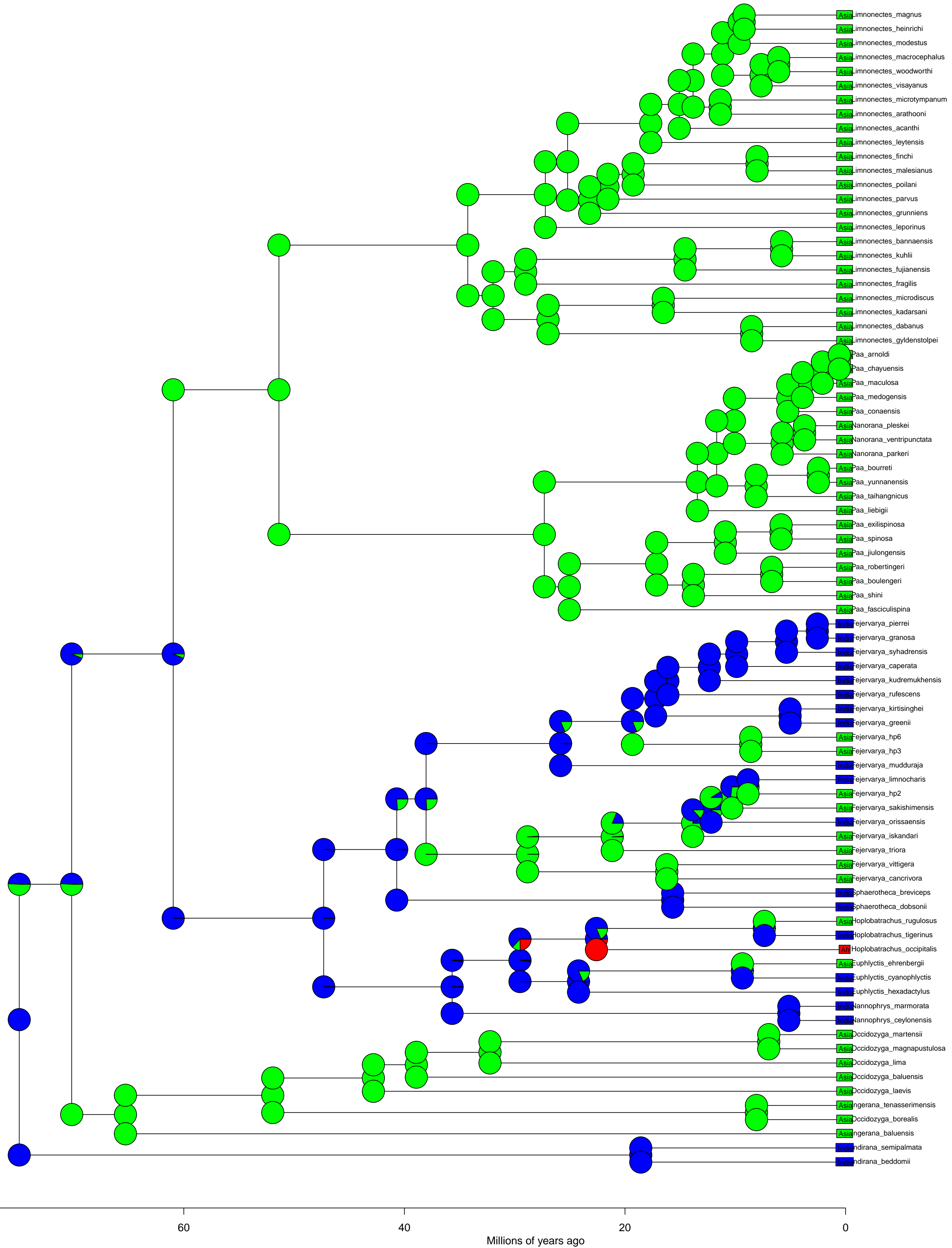




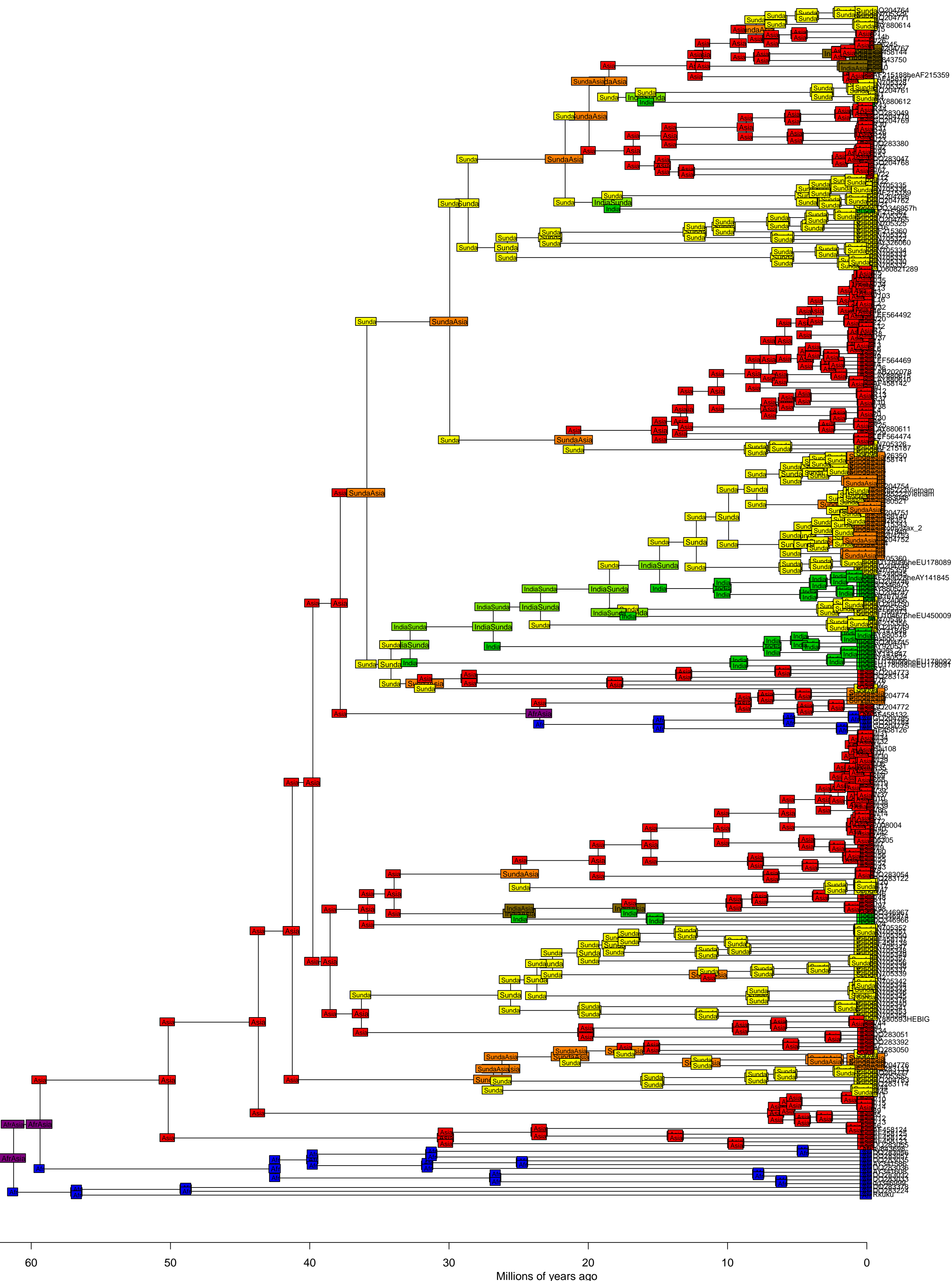


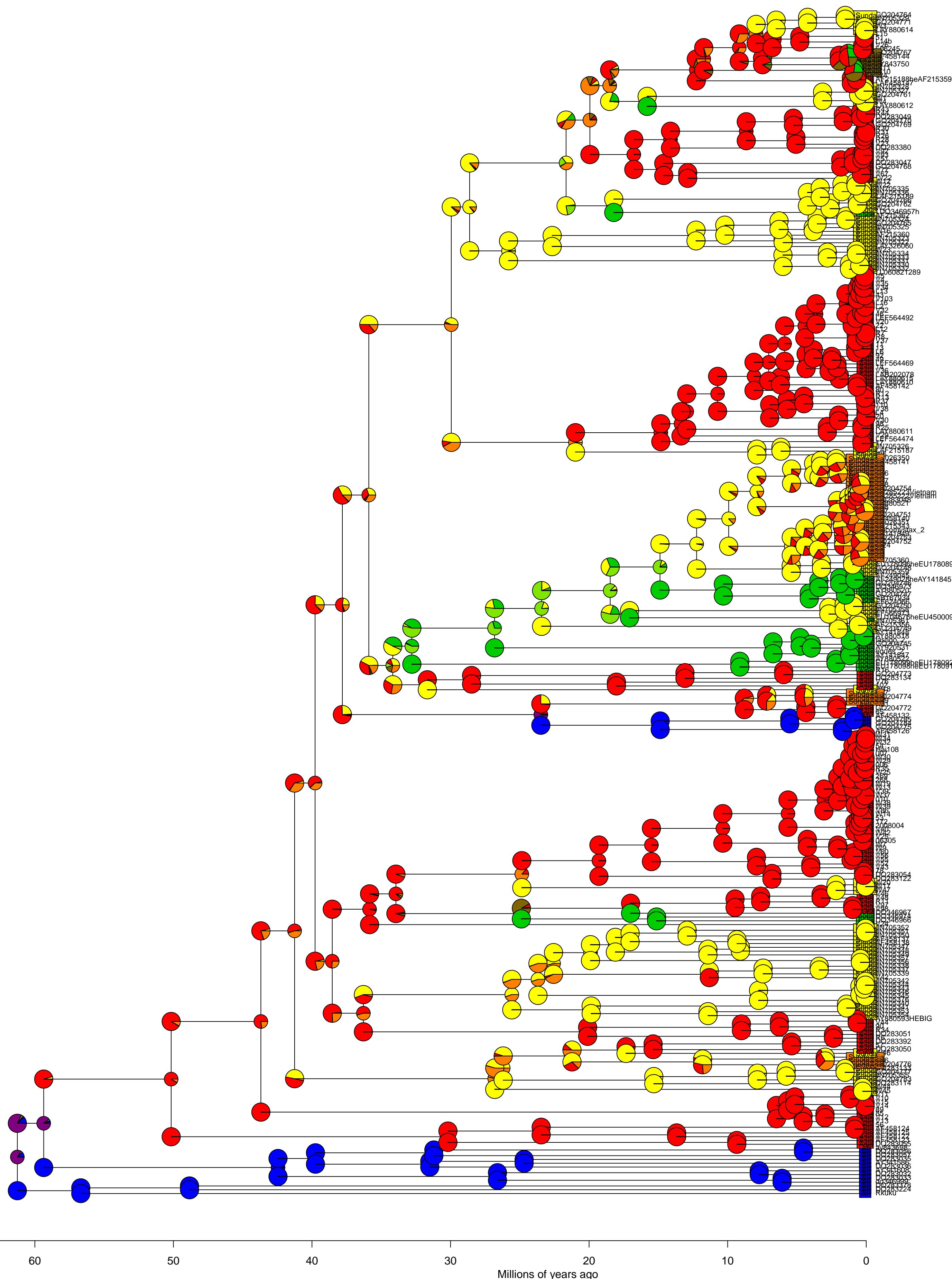


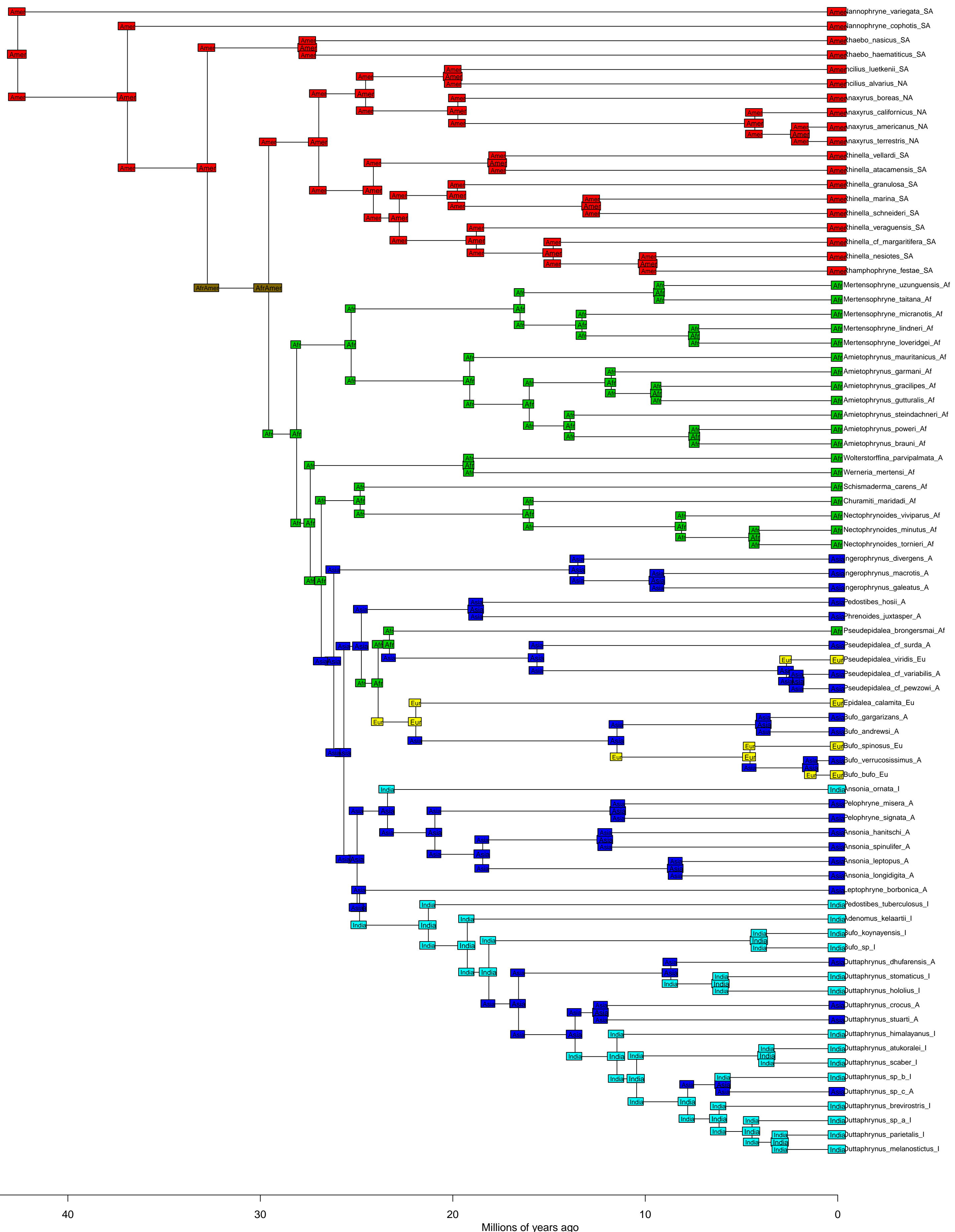


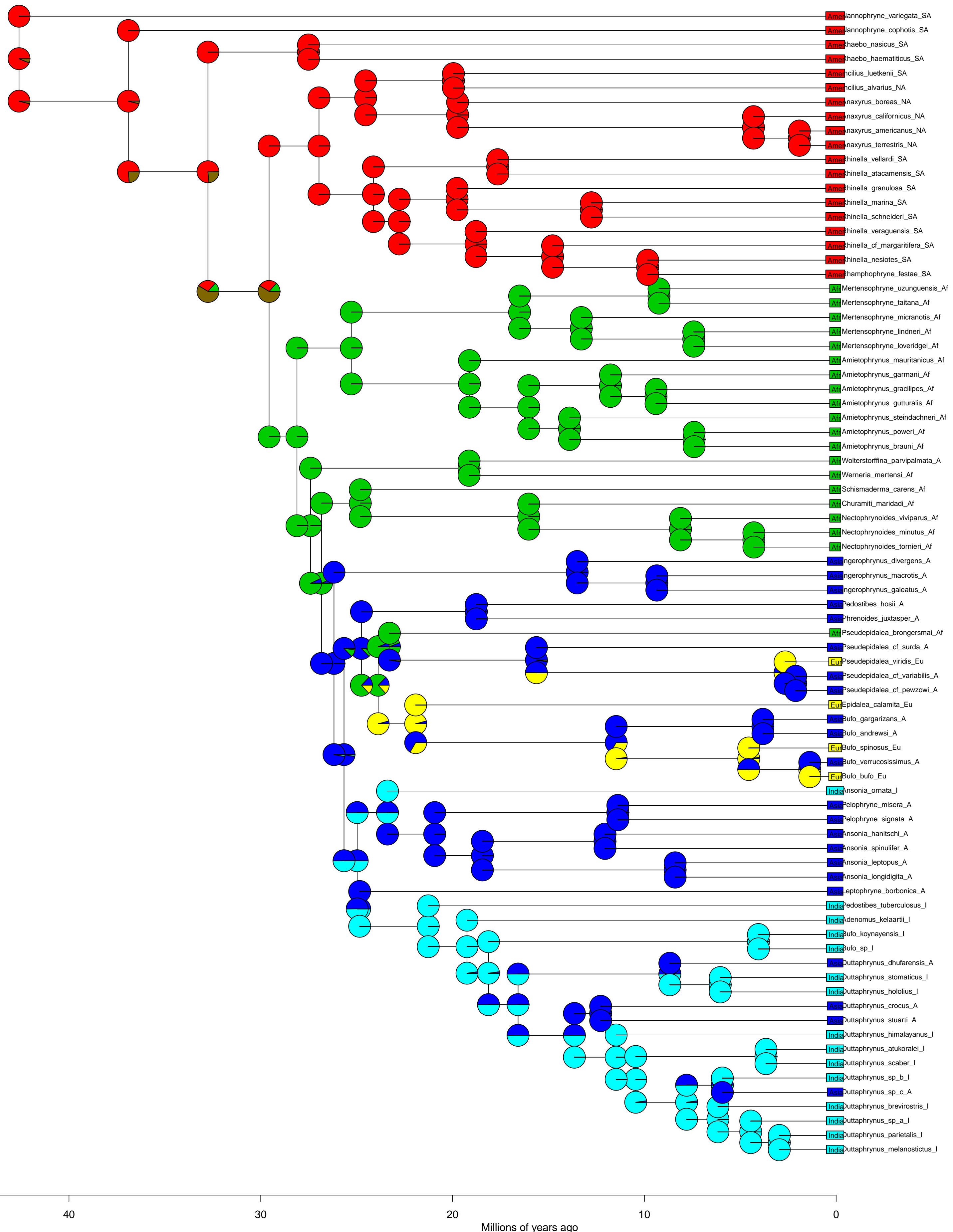


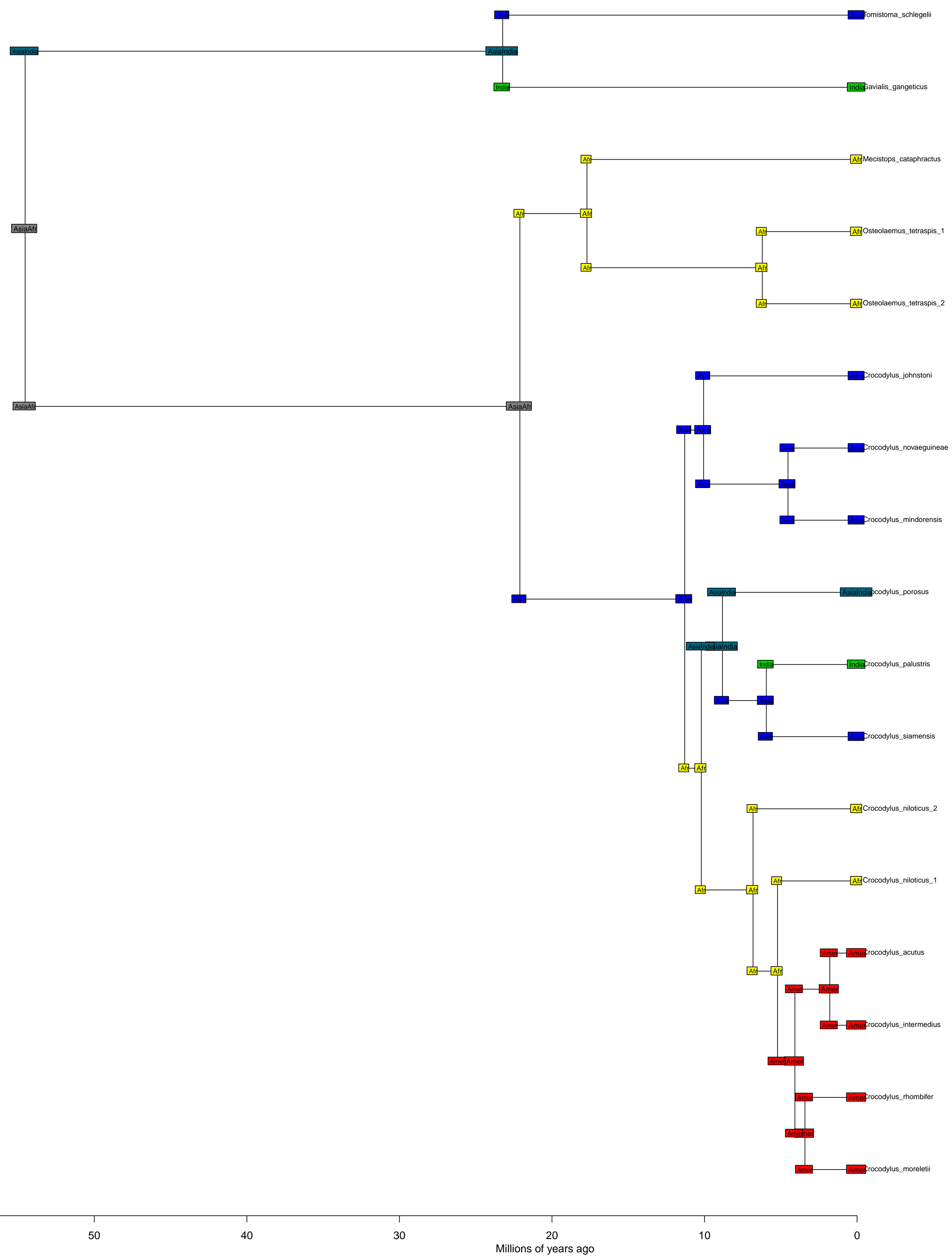
Rhacophoridae BioGeoBEARS DEC+J  
ancstates: global optim, 2 areas max. d=0.0067; e=0; j=0.0019; LnL=-307.04

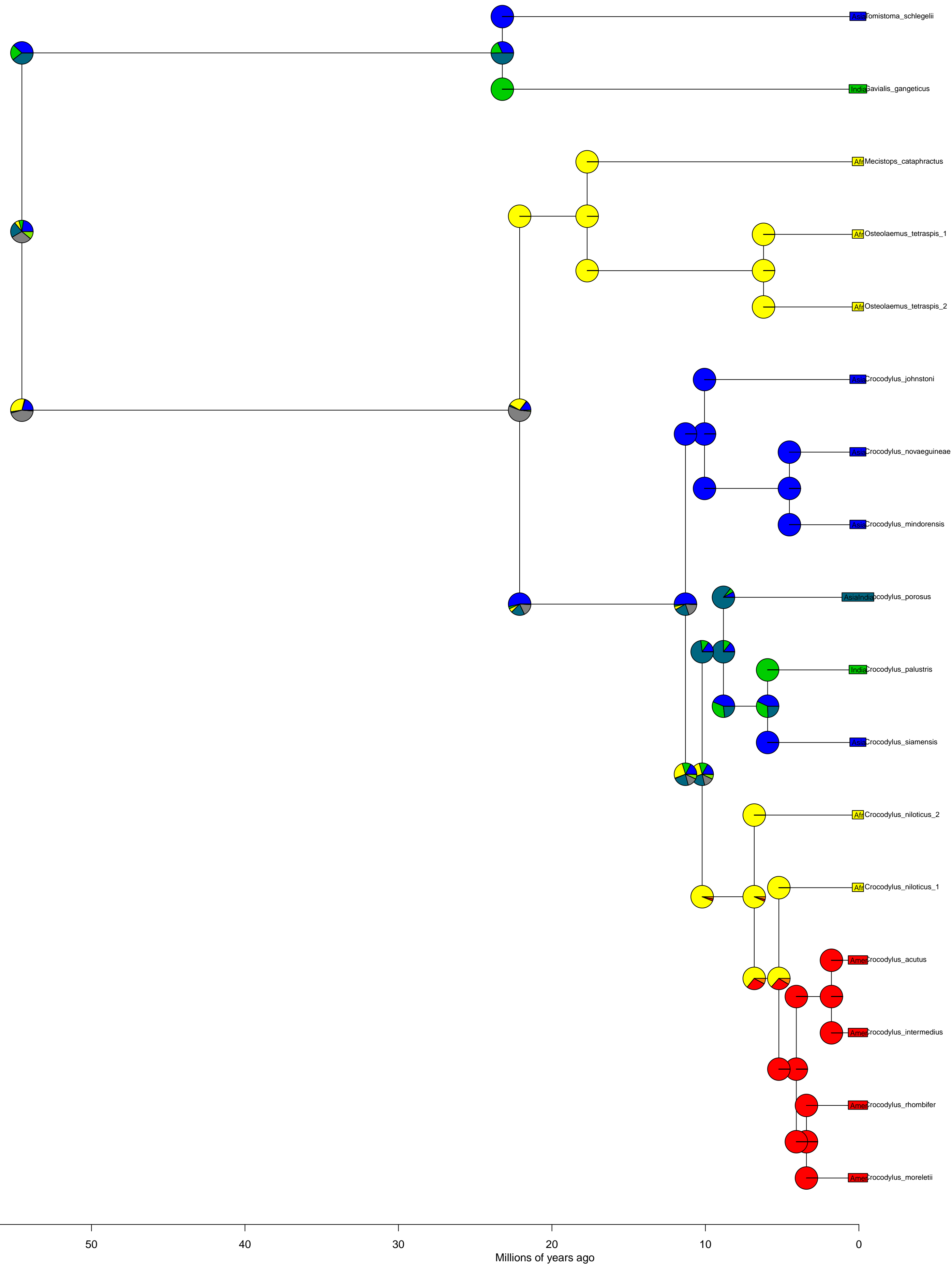


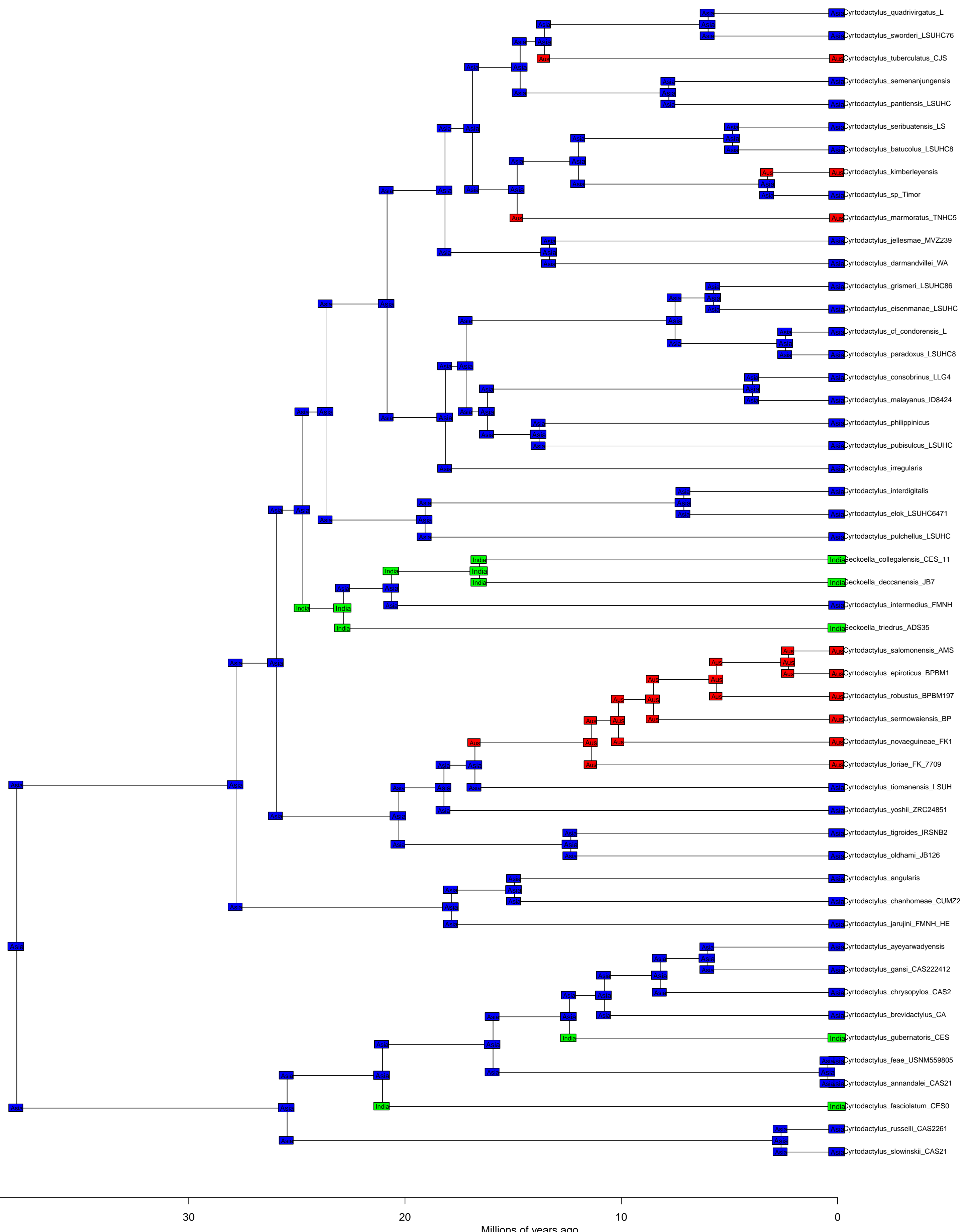


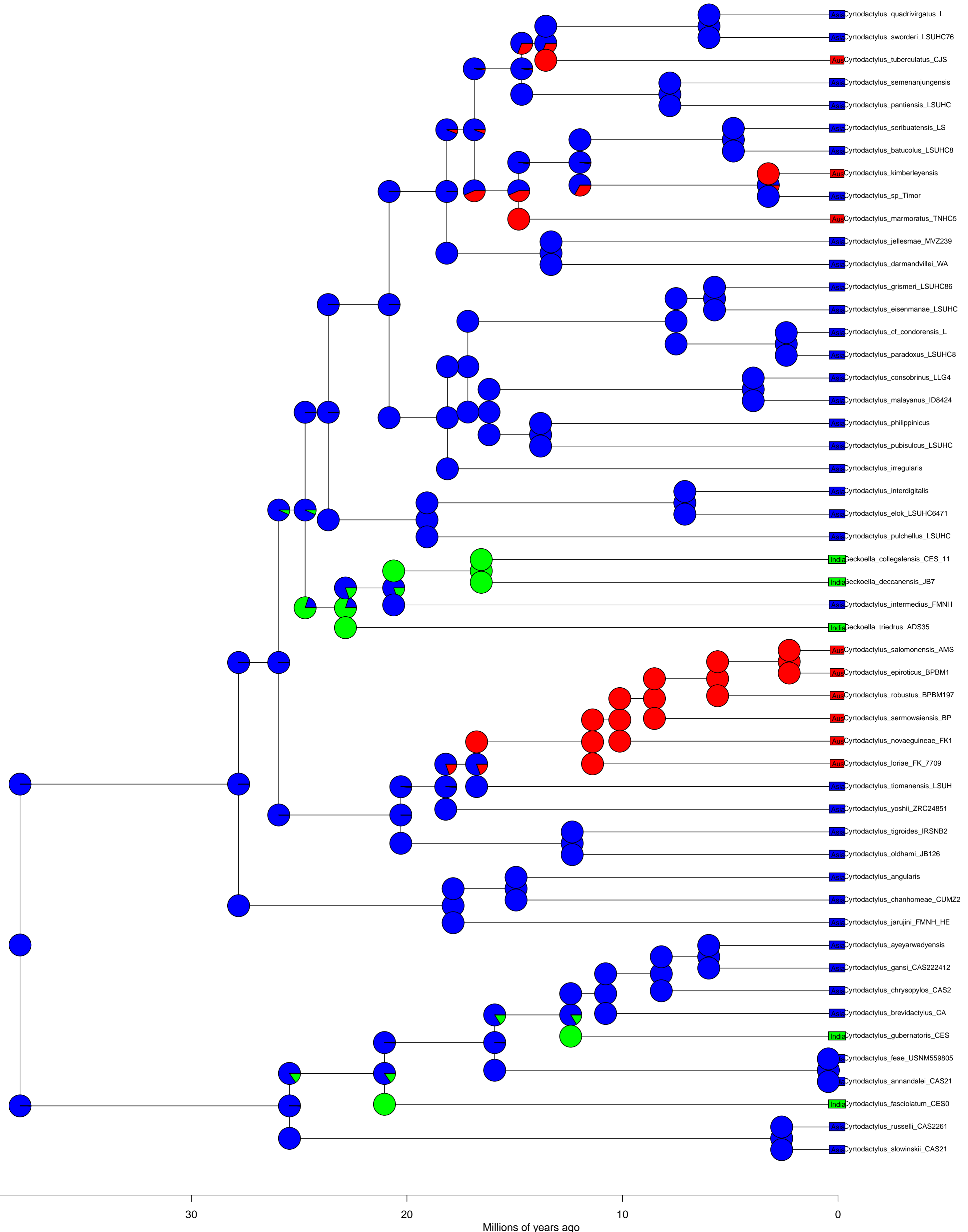


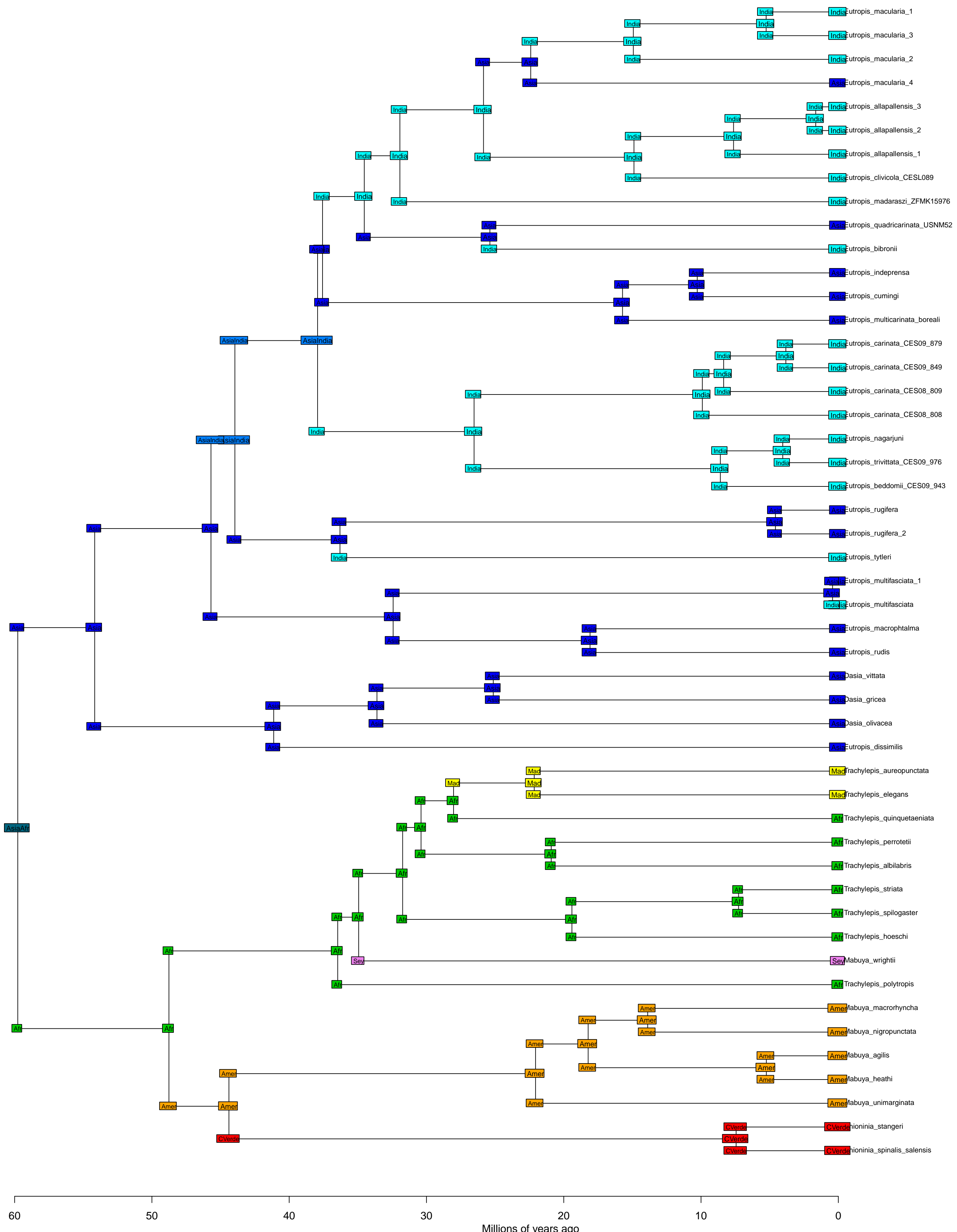


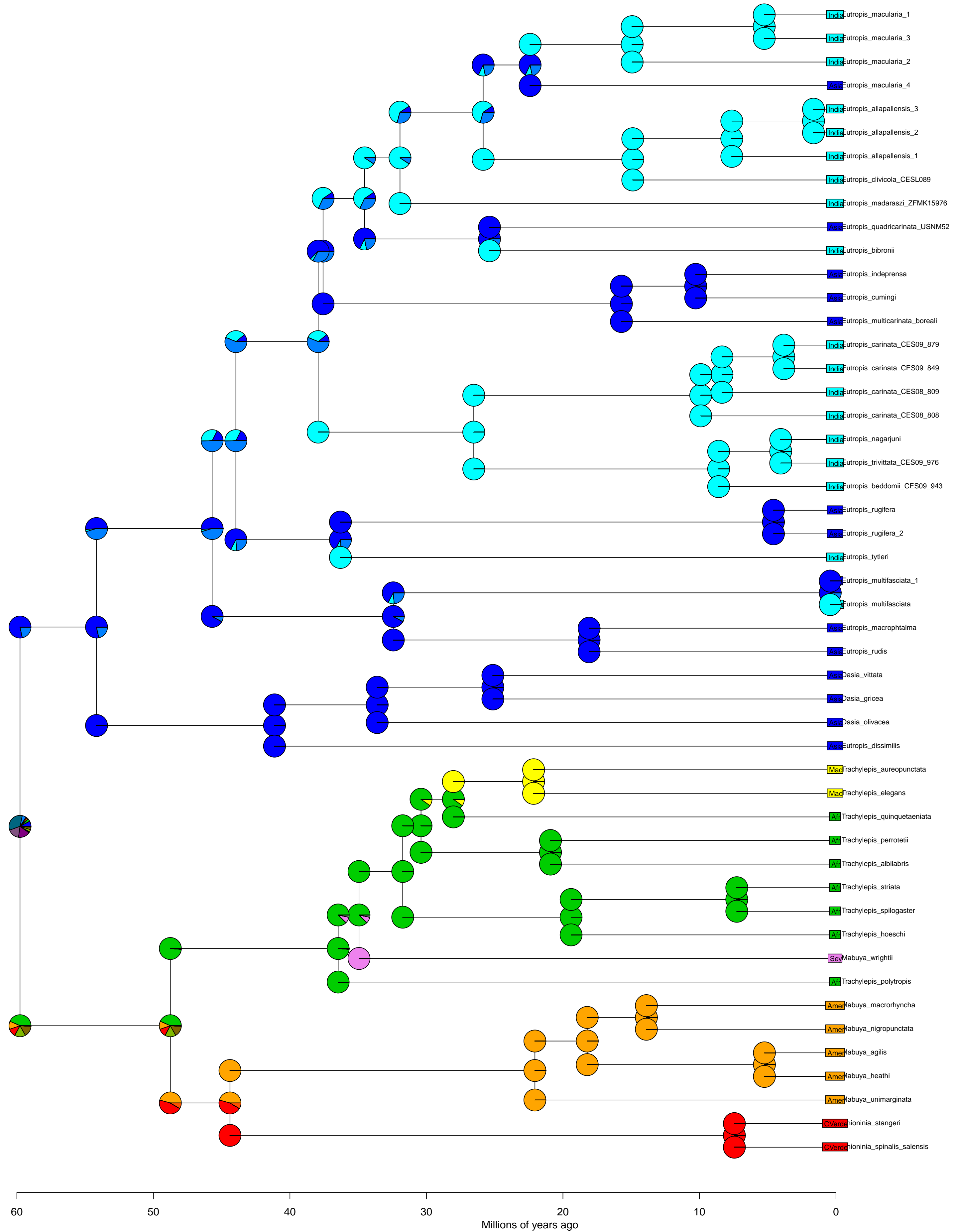


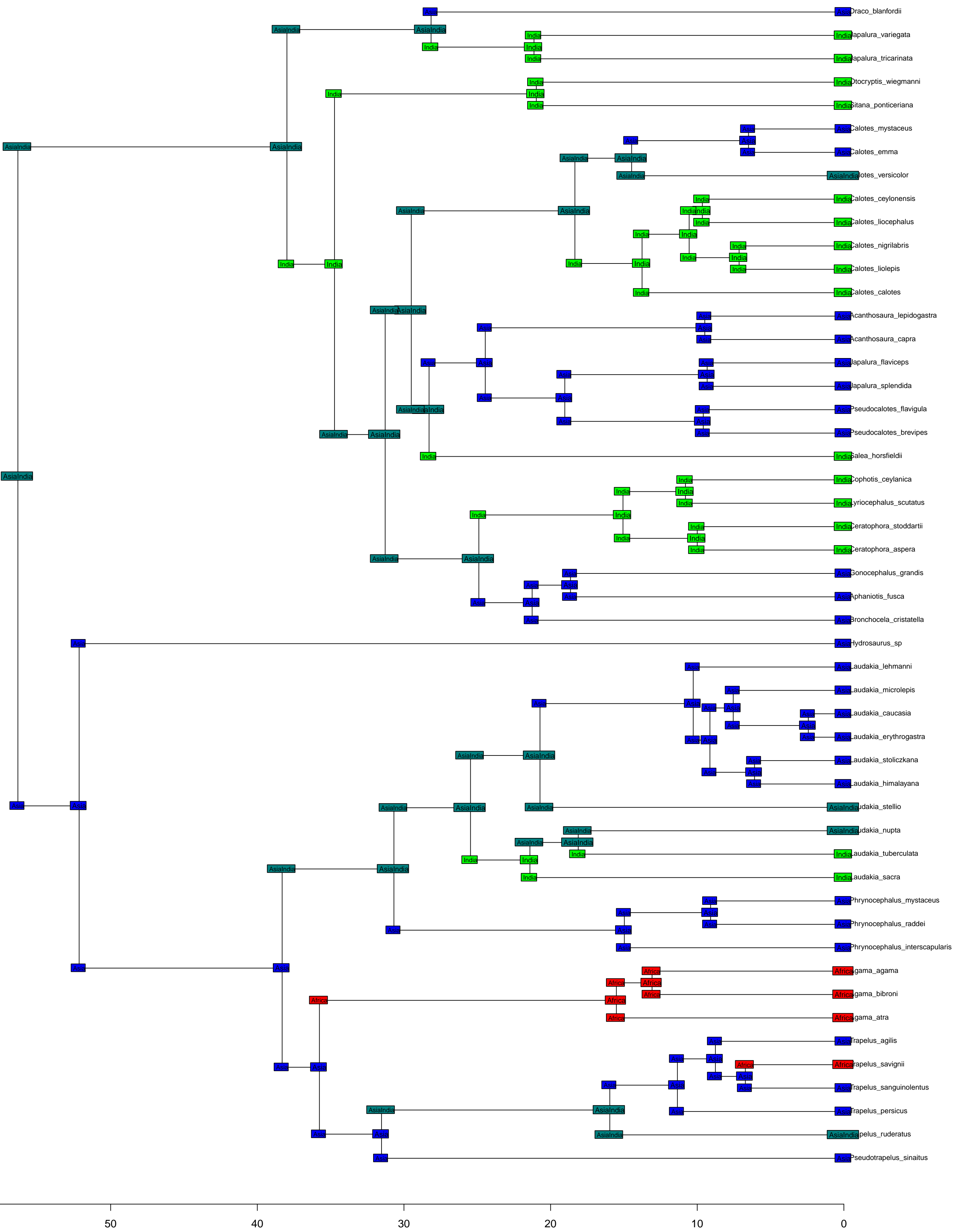




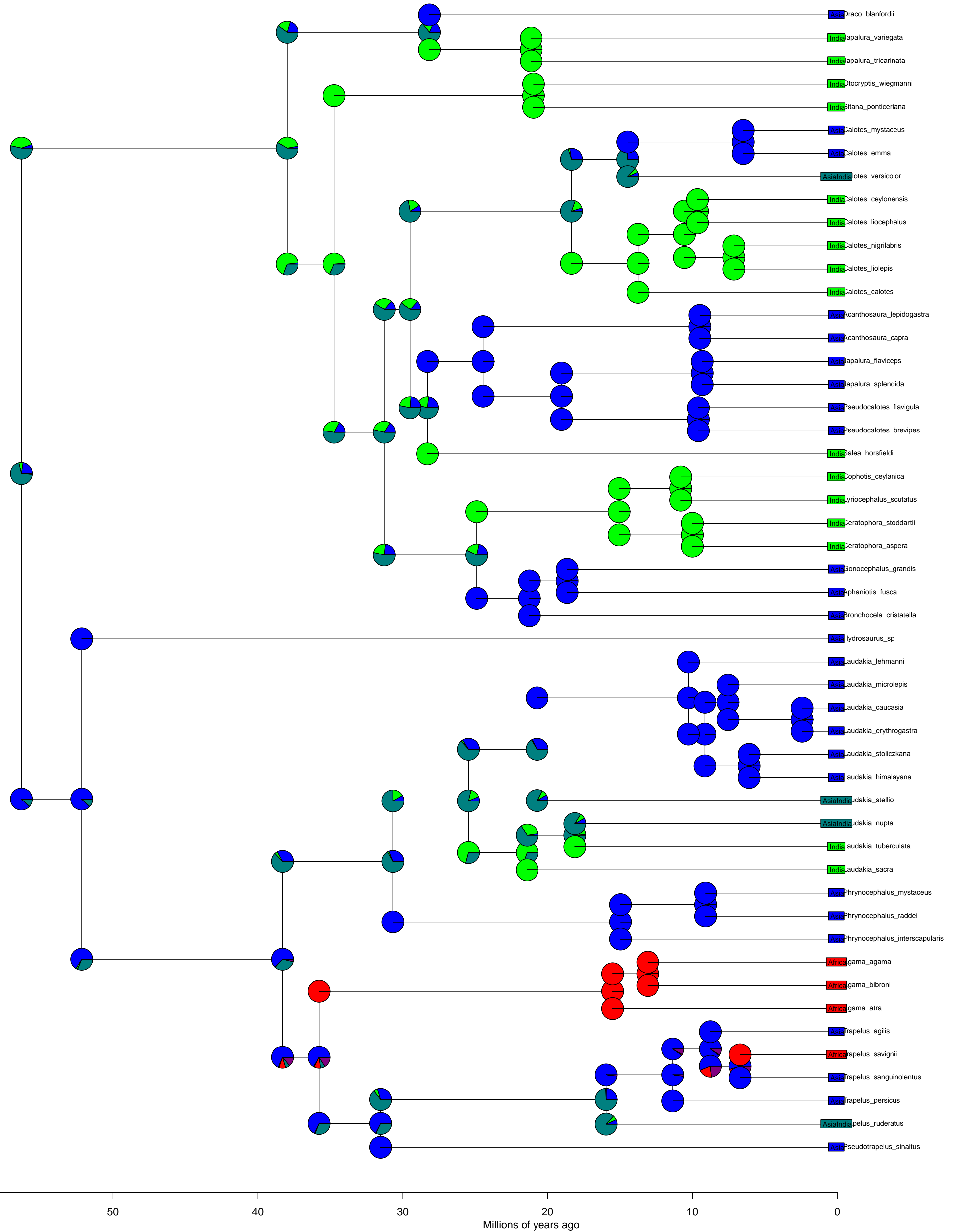


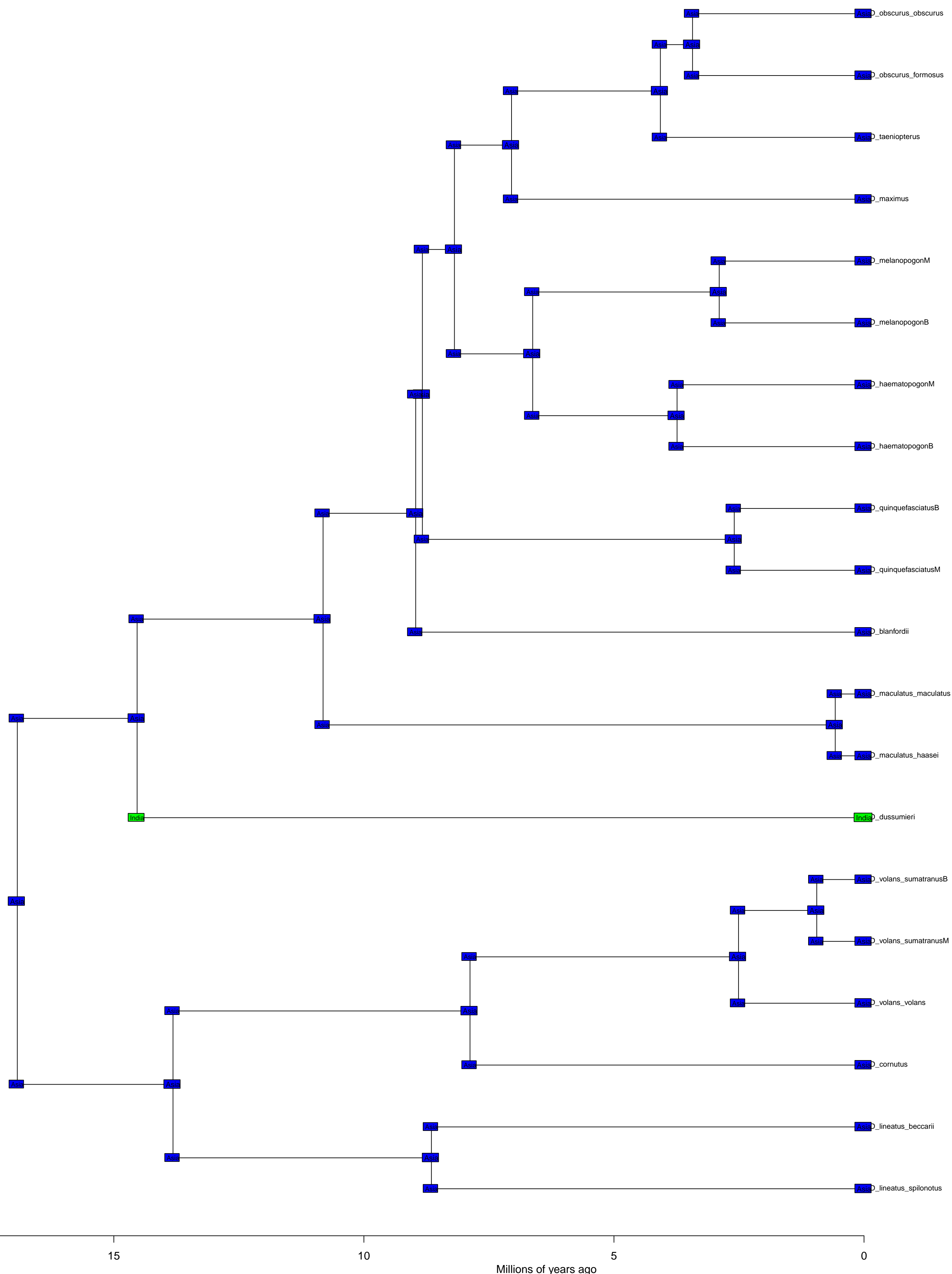


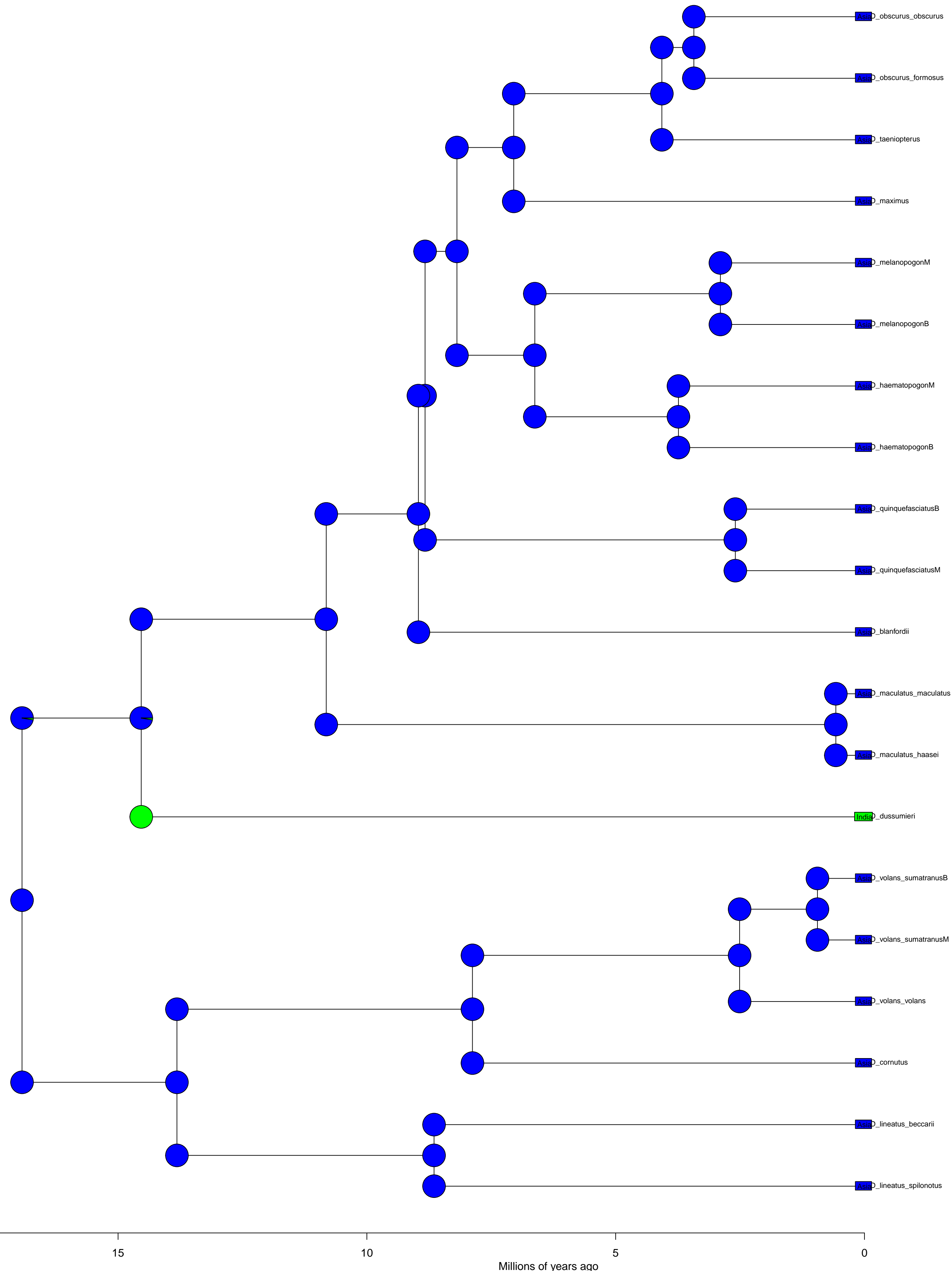


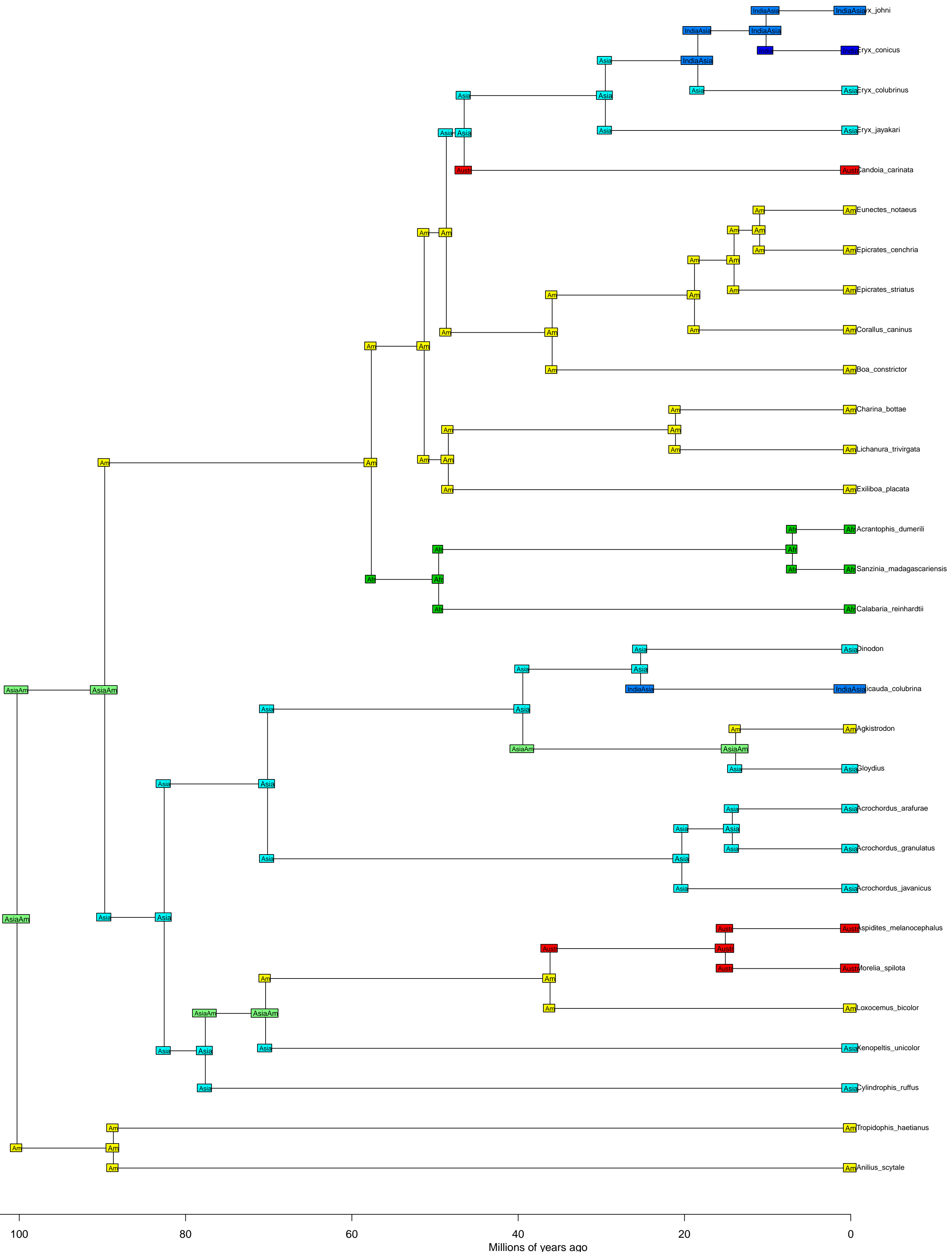


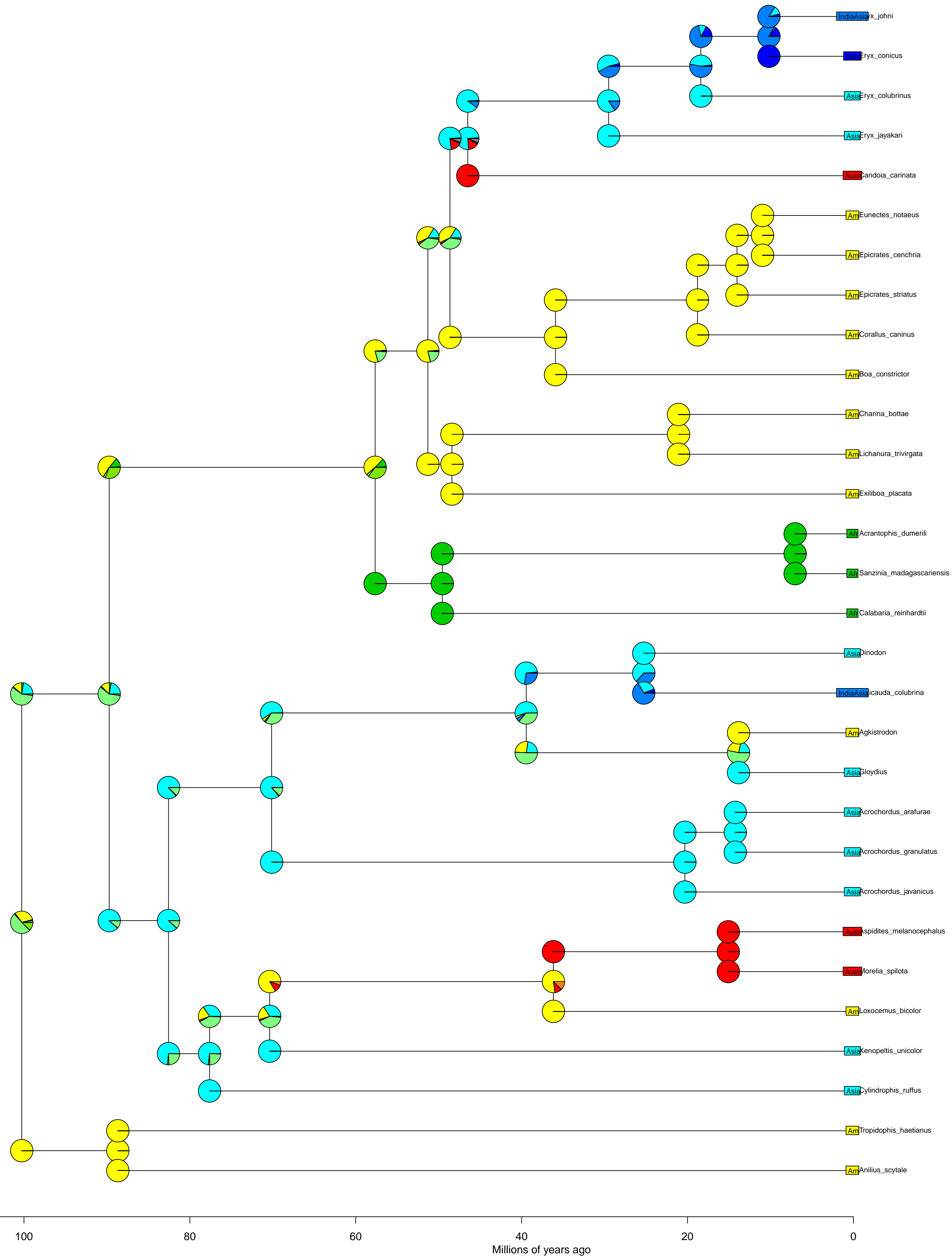
Acrodonta BioGeoBEARS DEC+J  
ancstates: global optim, 2 areas max. d=0.0024; e=0; j=0.038; LnL=-44.36

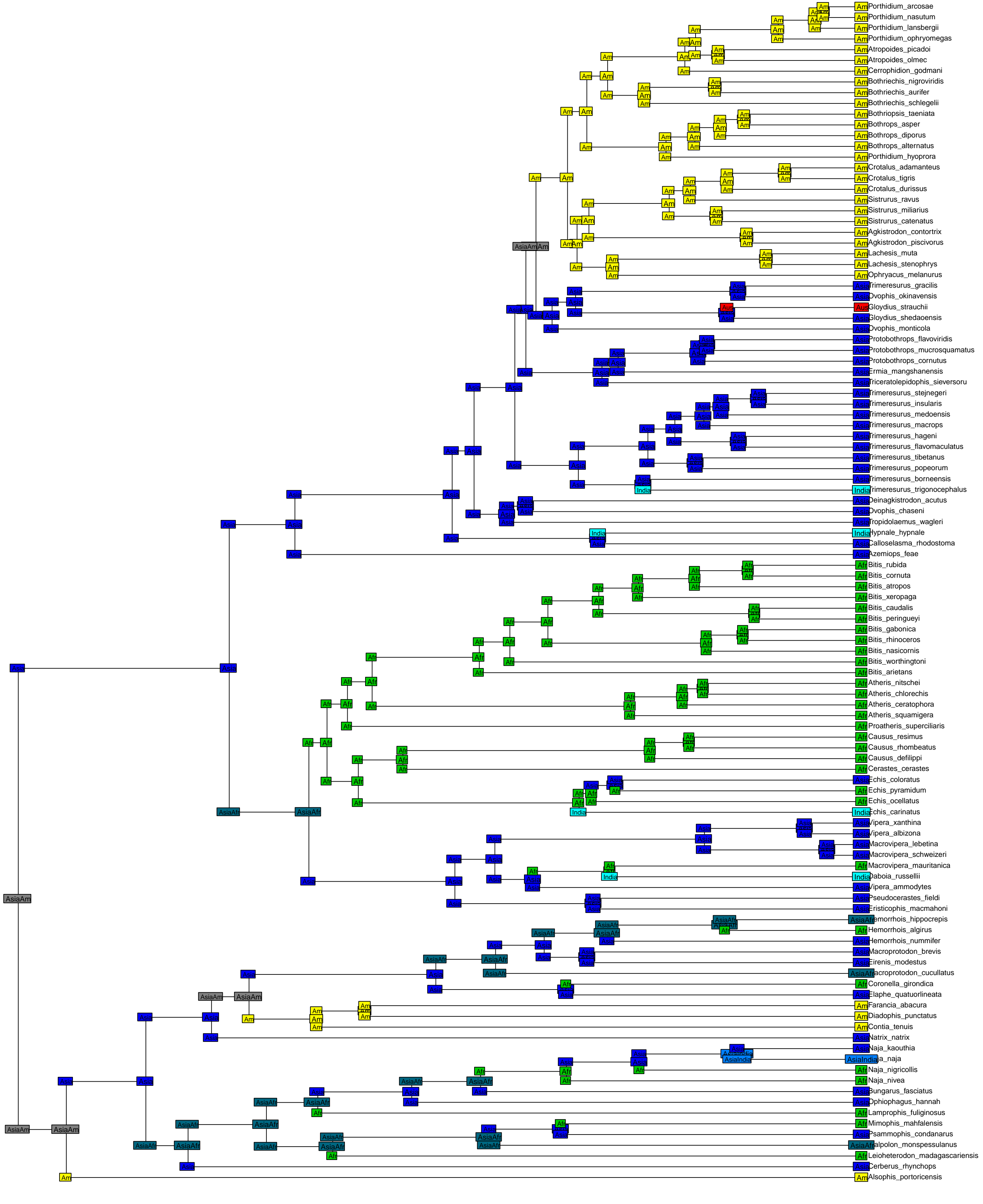


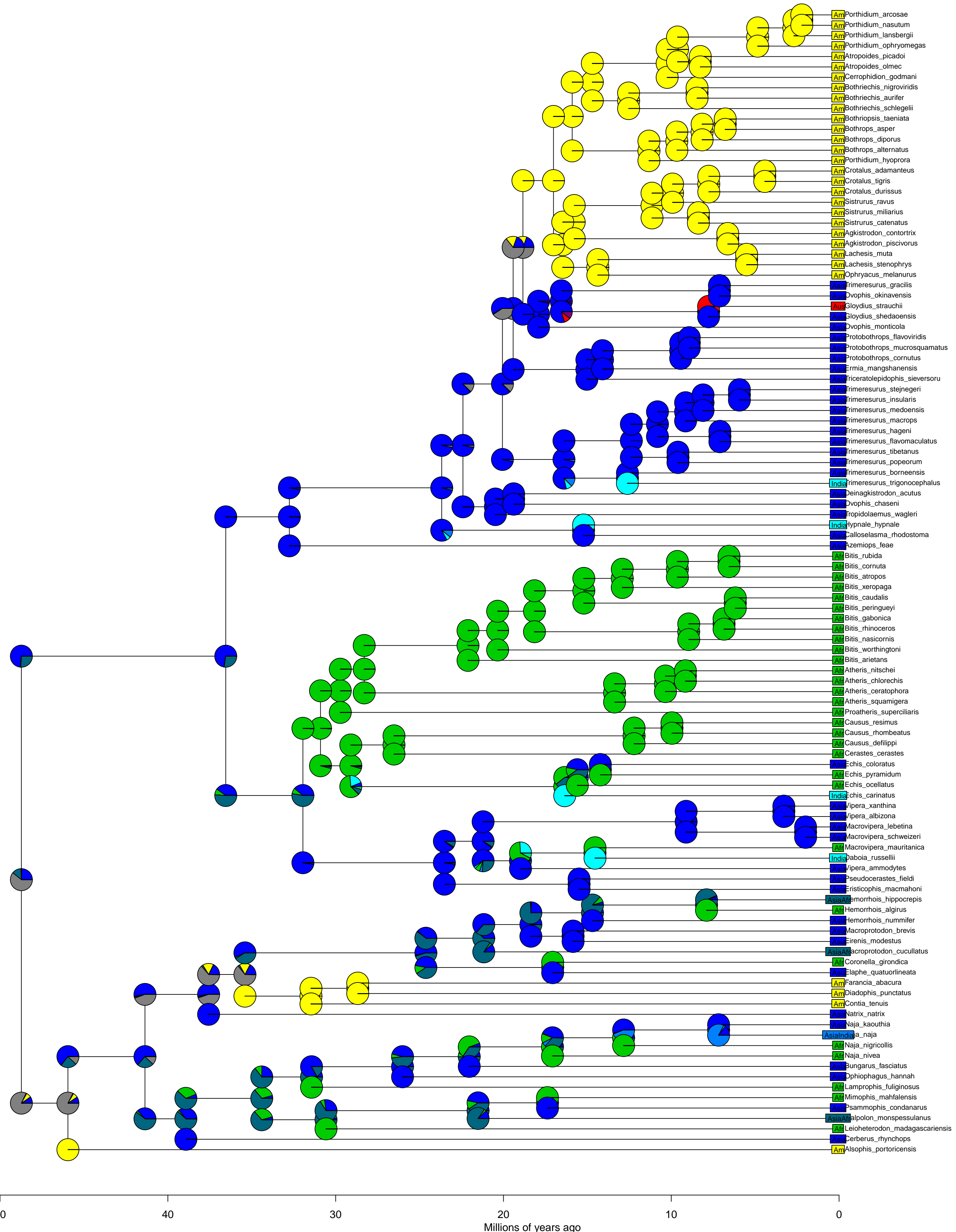


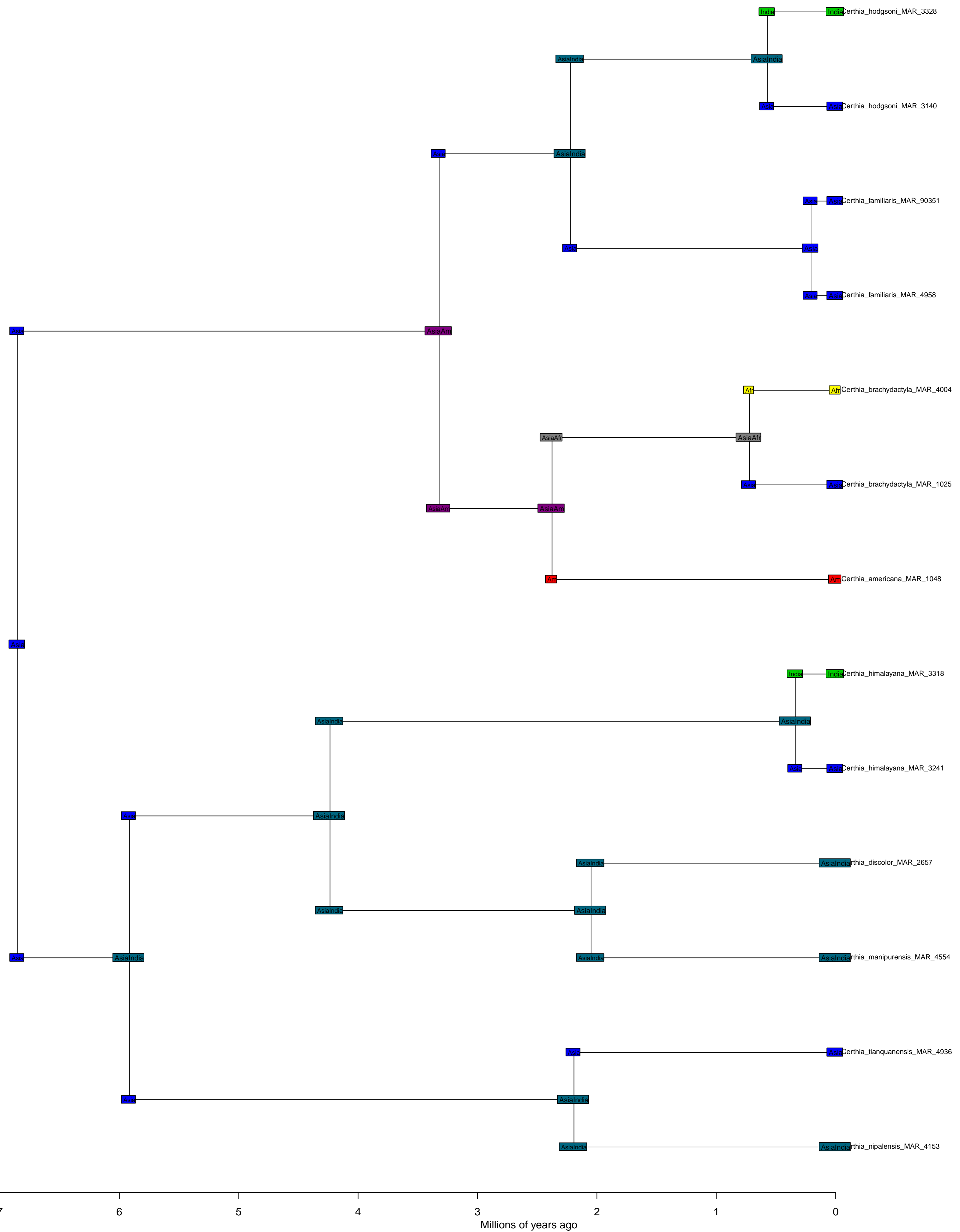


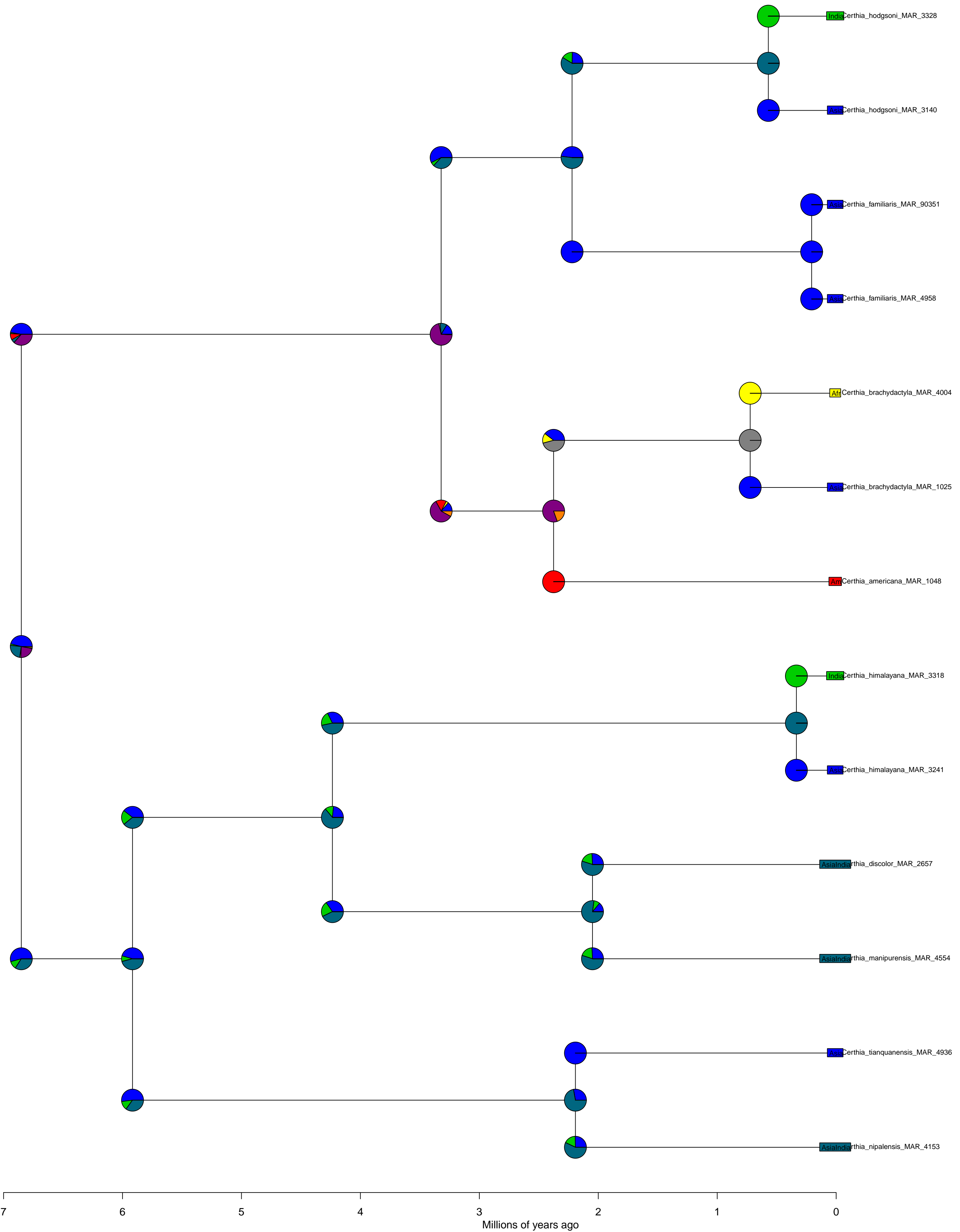


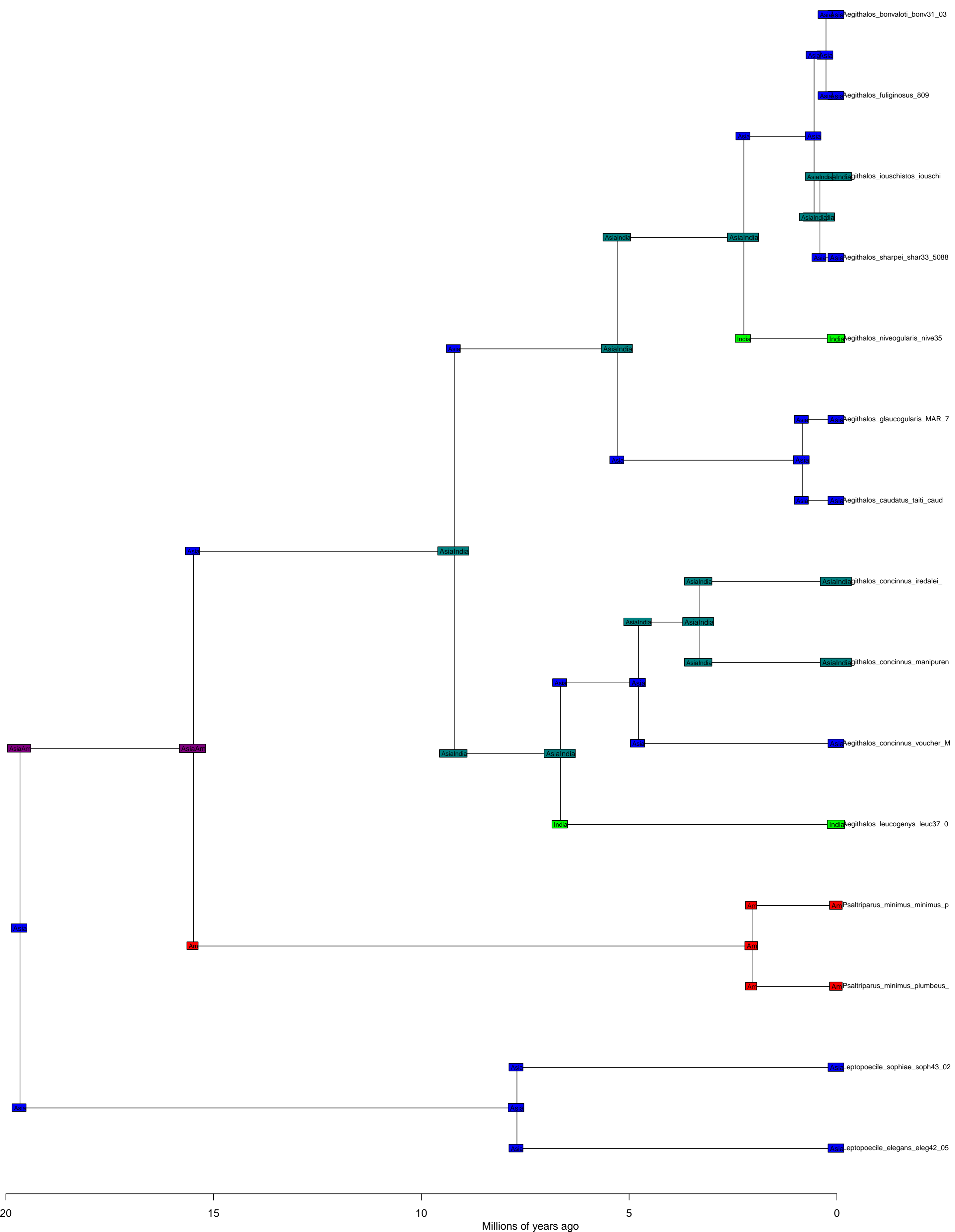


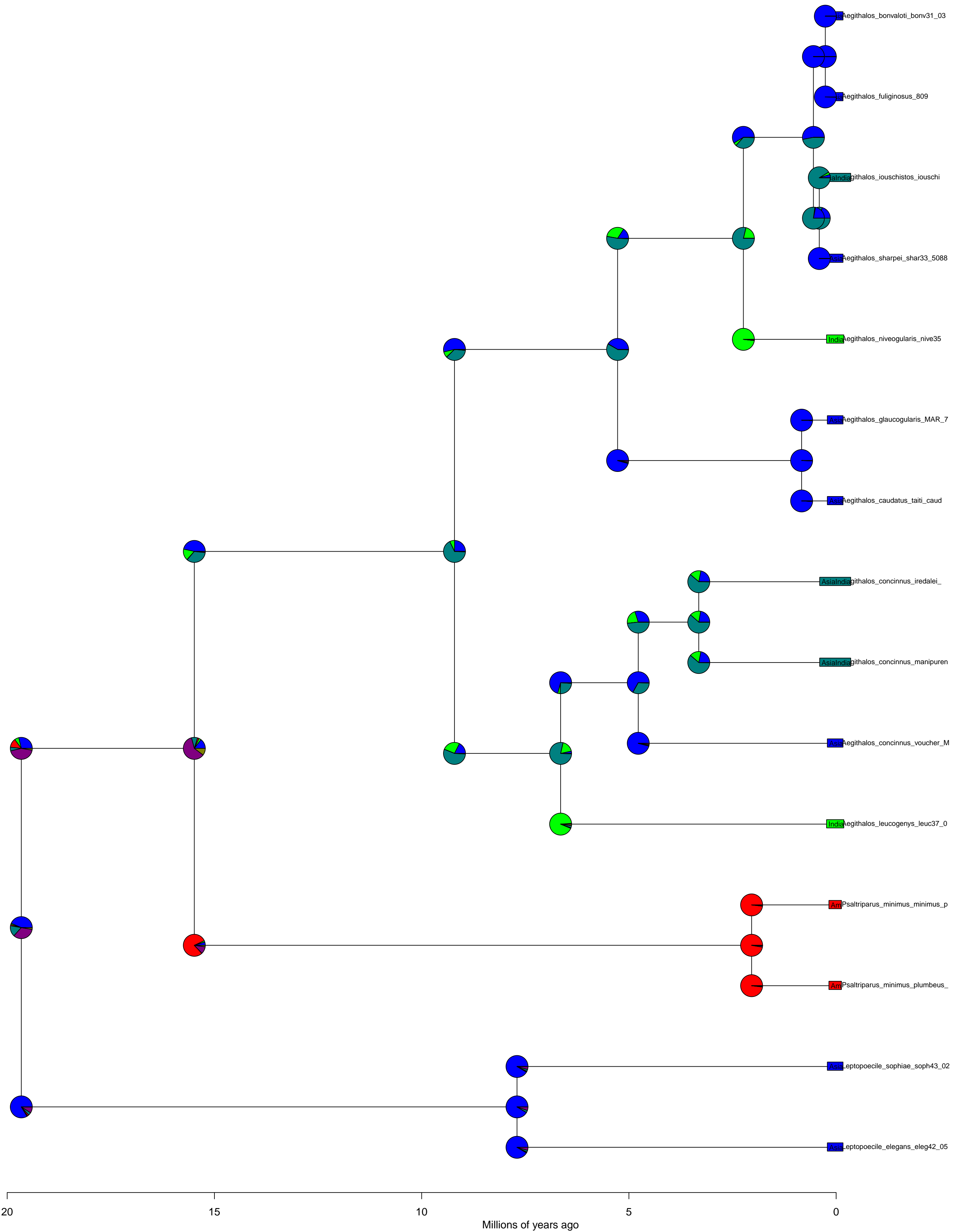


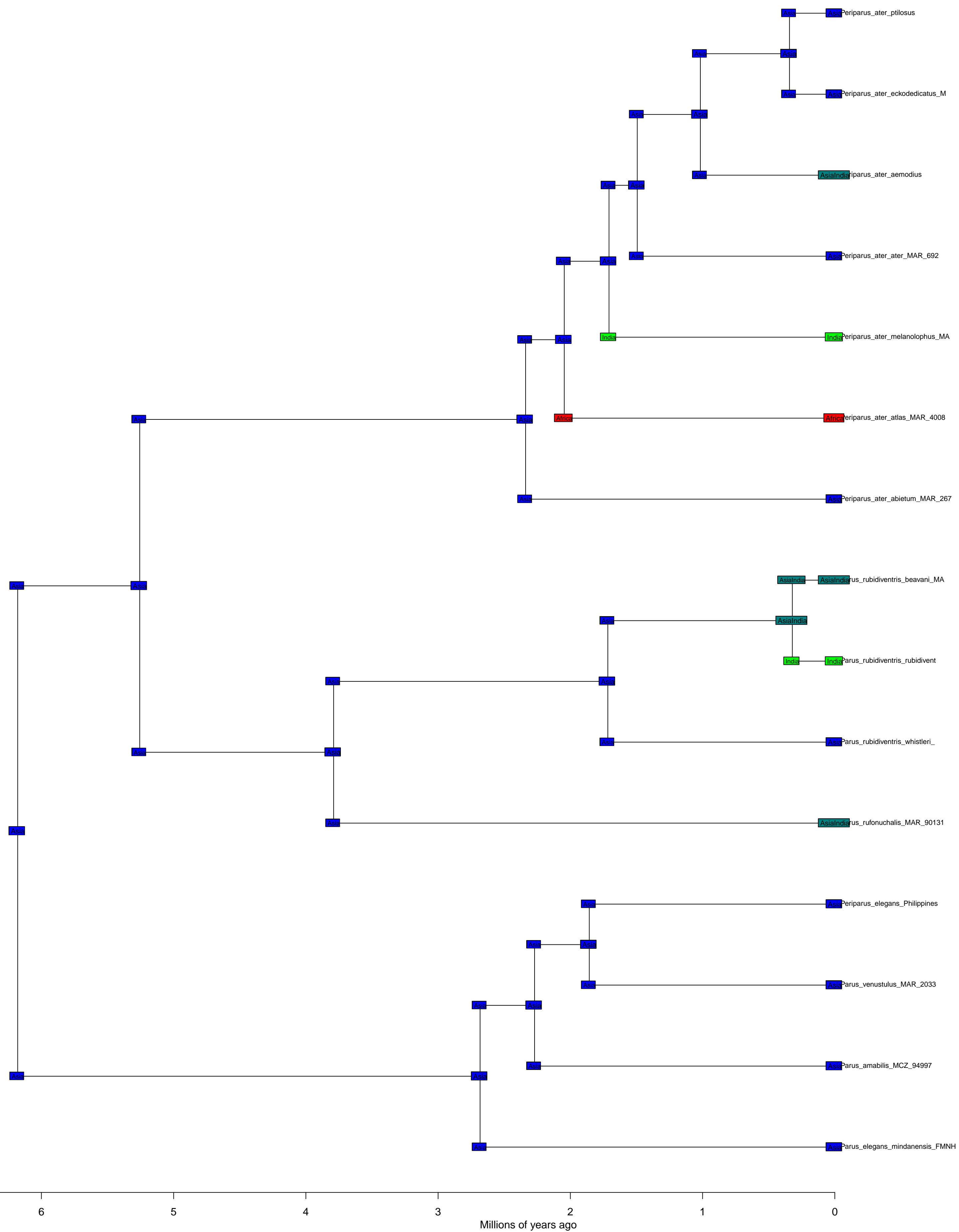


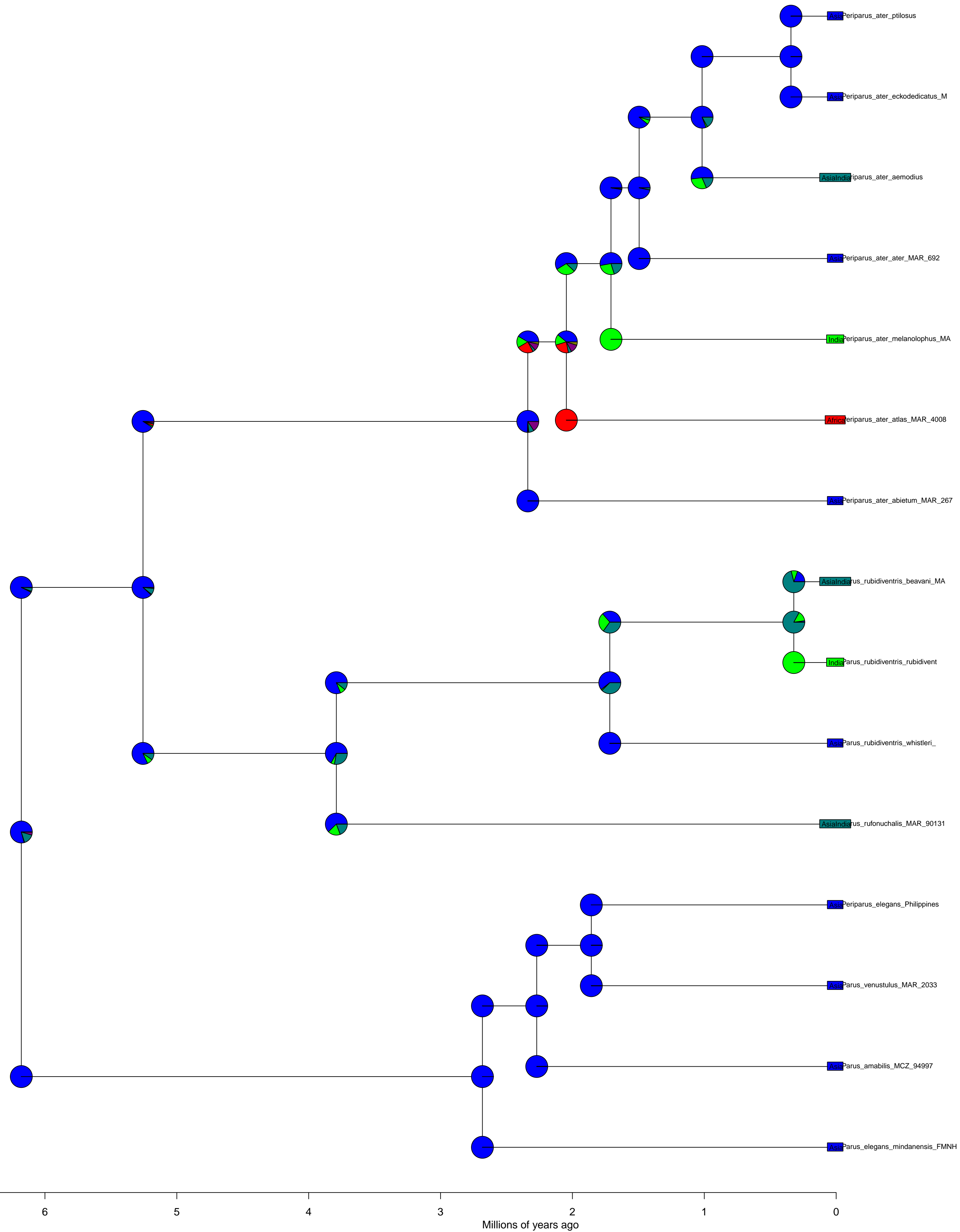




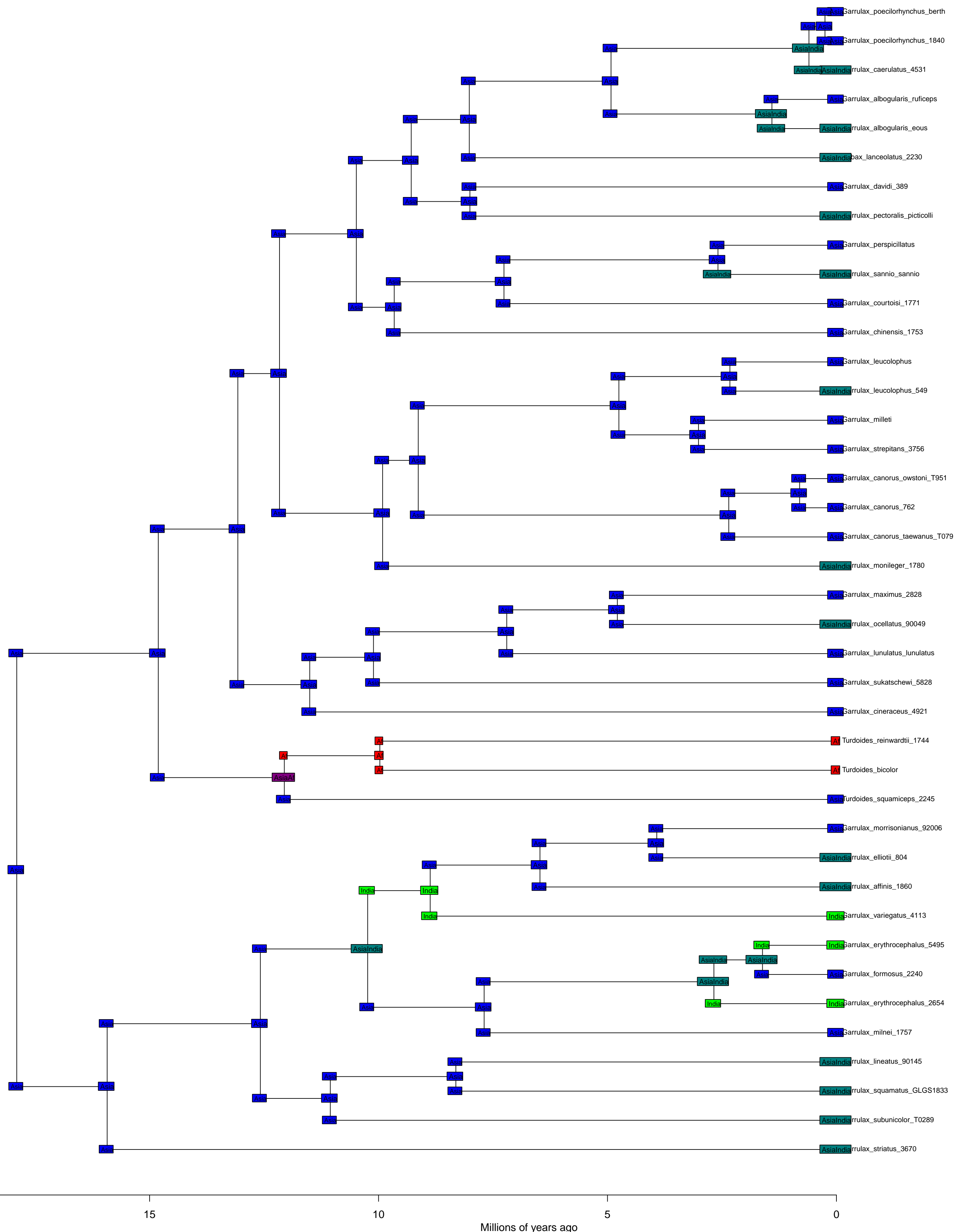


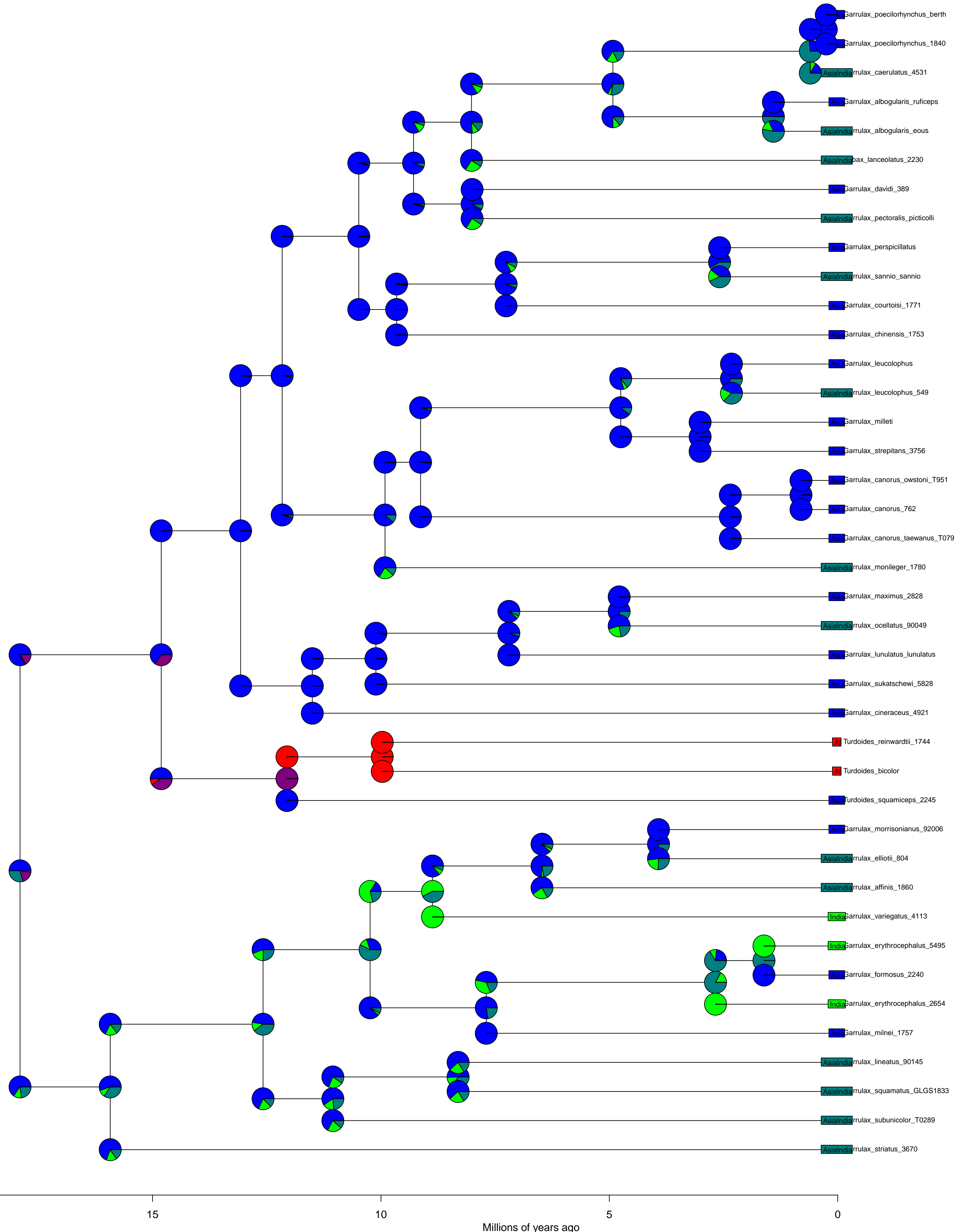


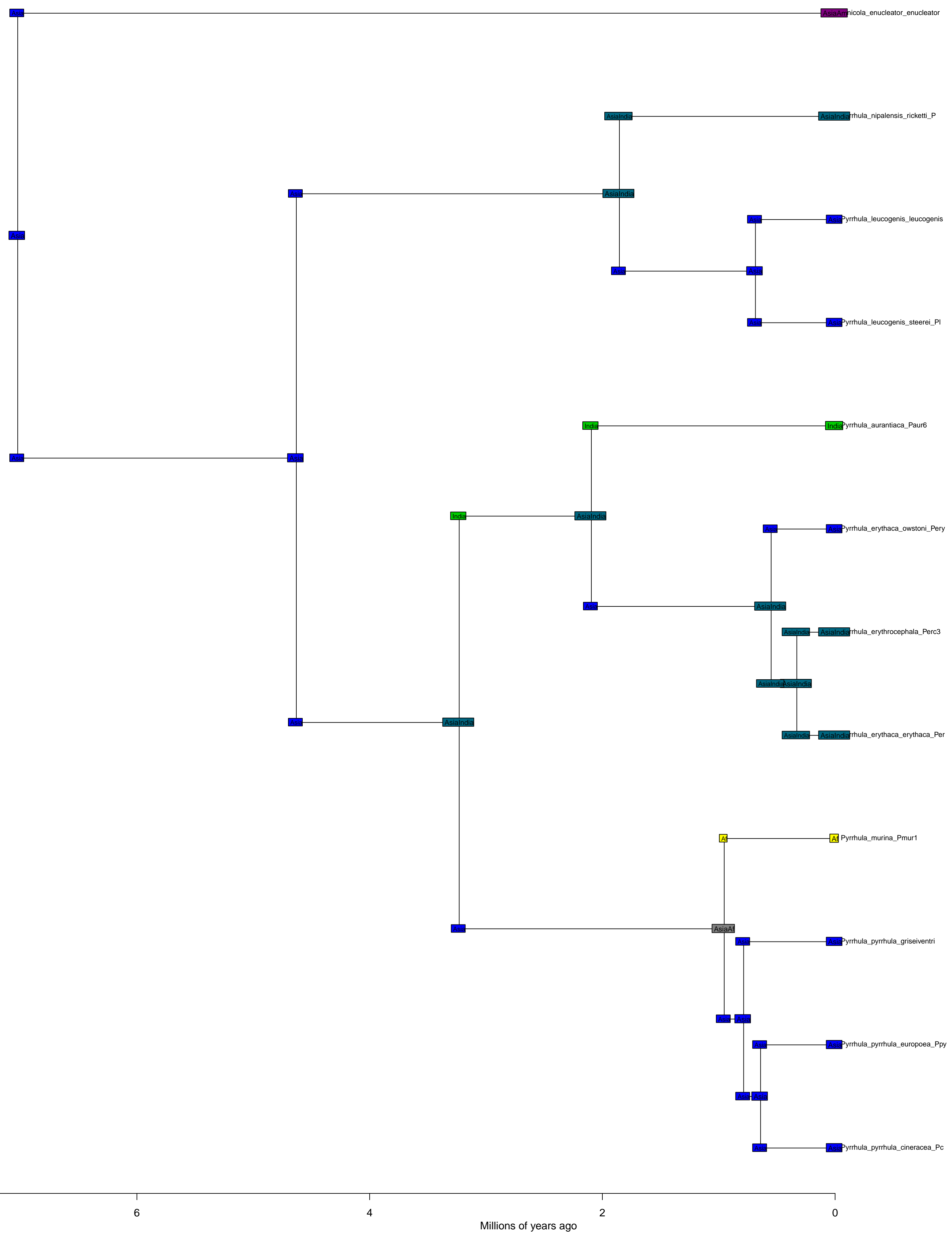


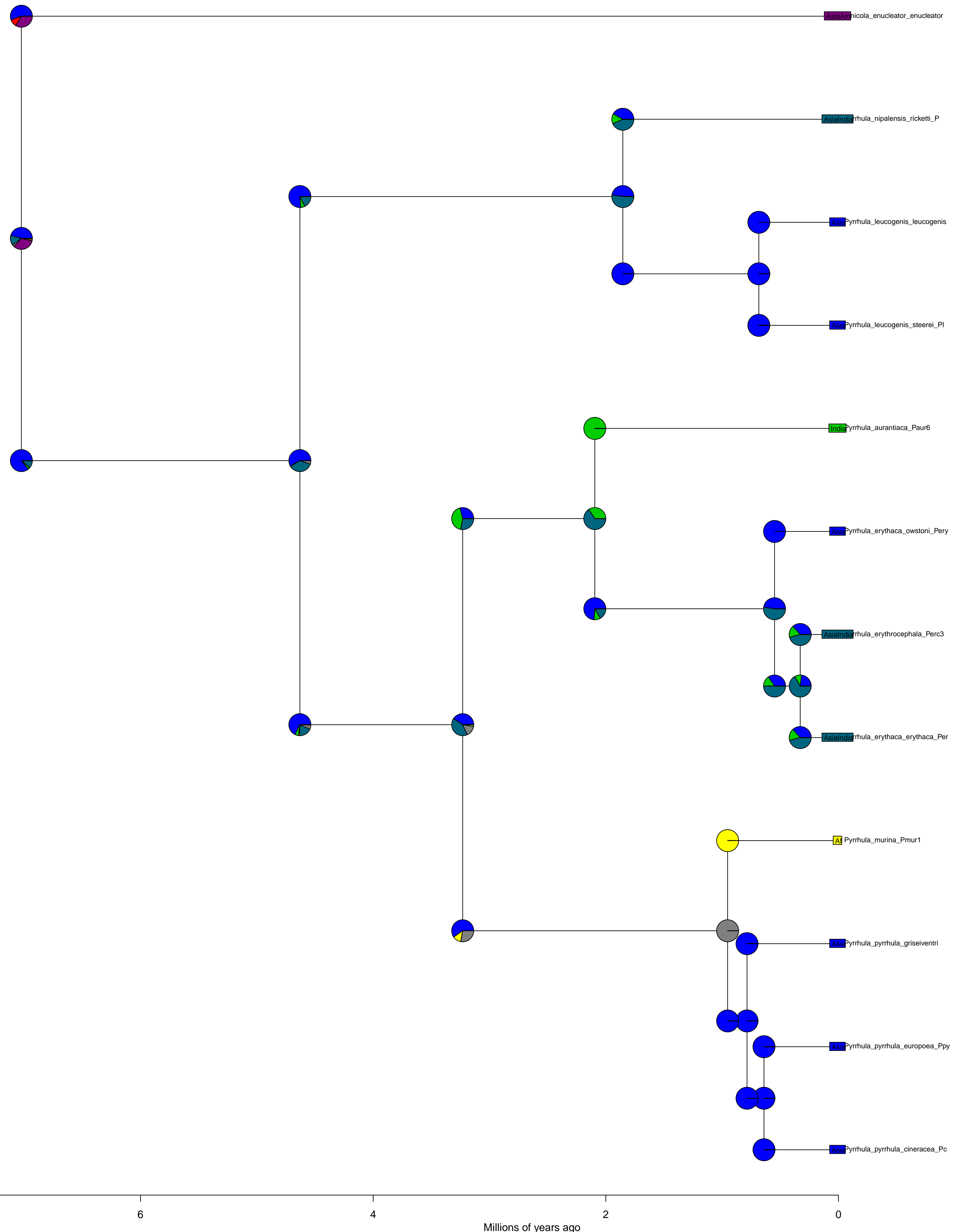


**Timaliidae BioGeoBEARS DEC**  
ancstates: global optim, 2 areas max. d=0.0345; e=0; j=0; LnL=-50.67

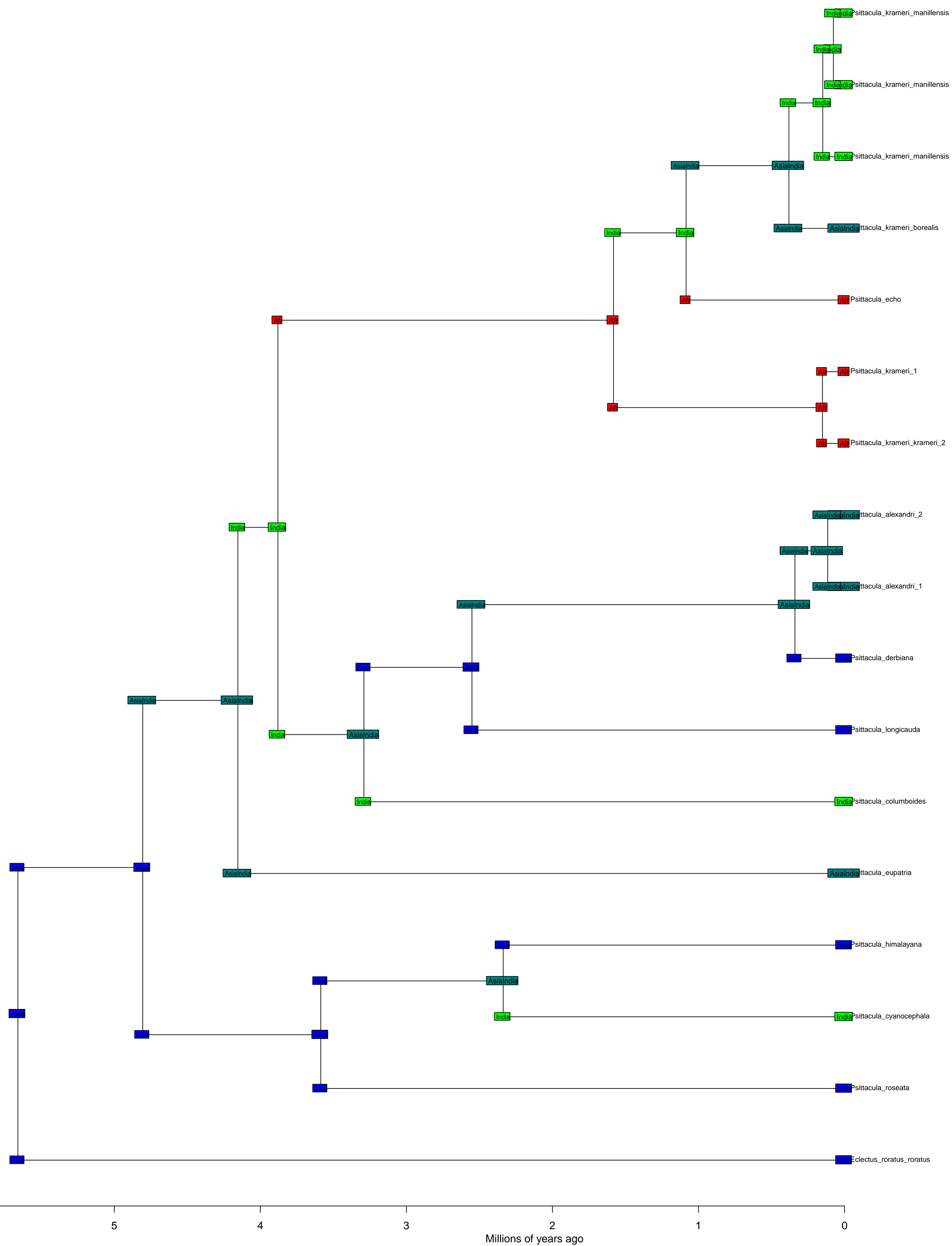


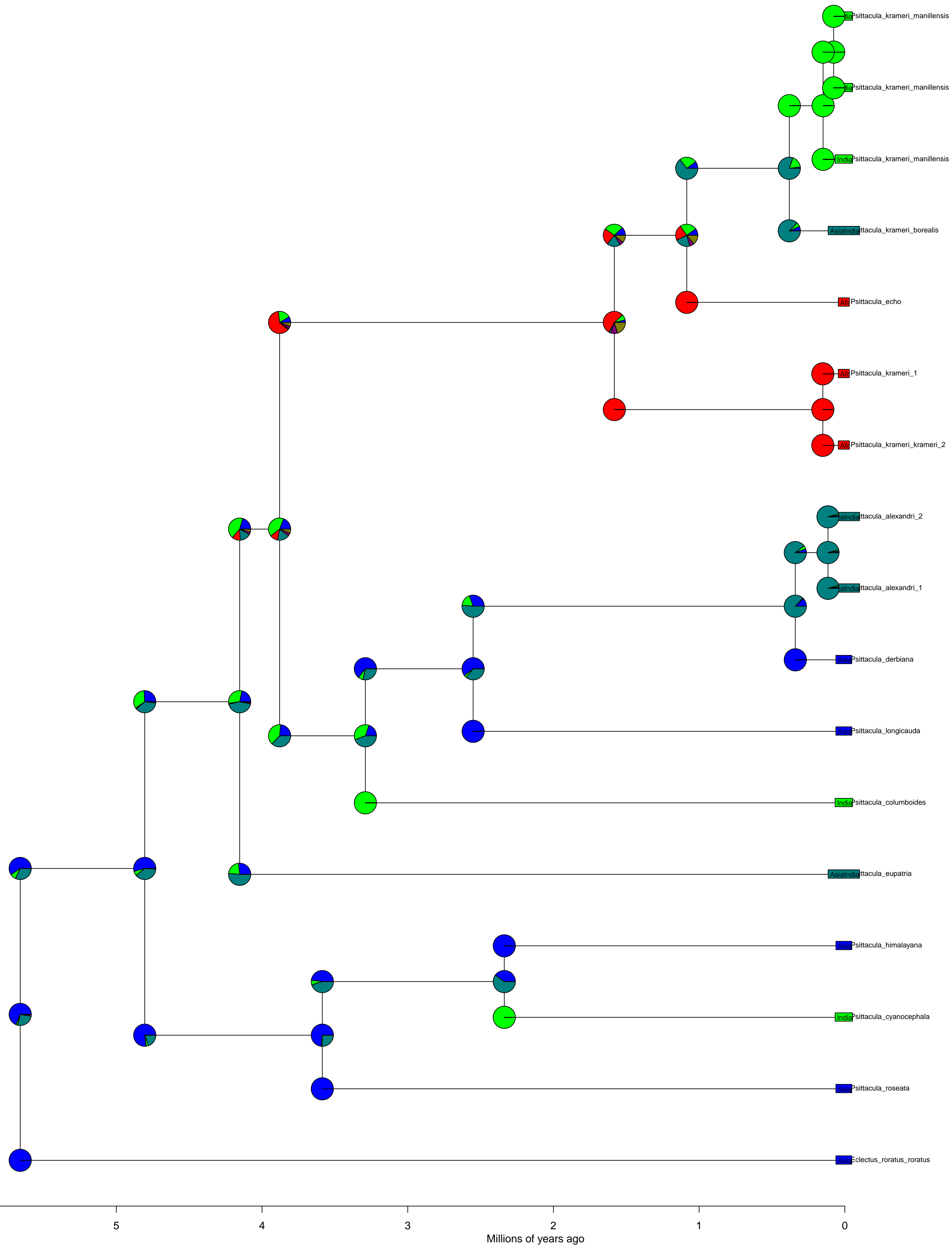


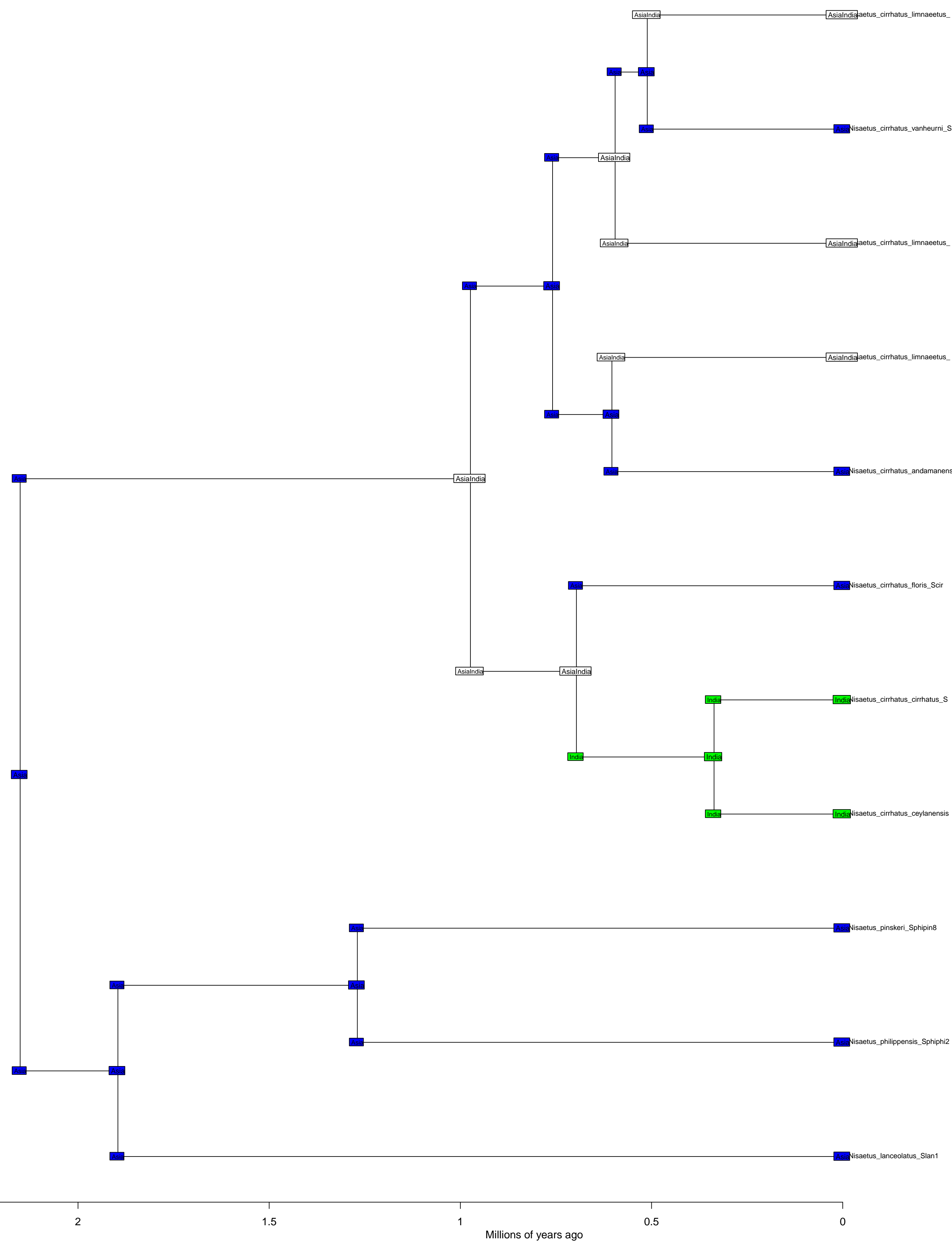


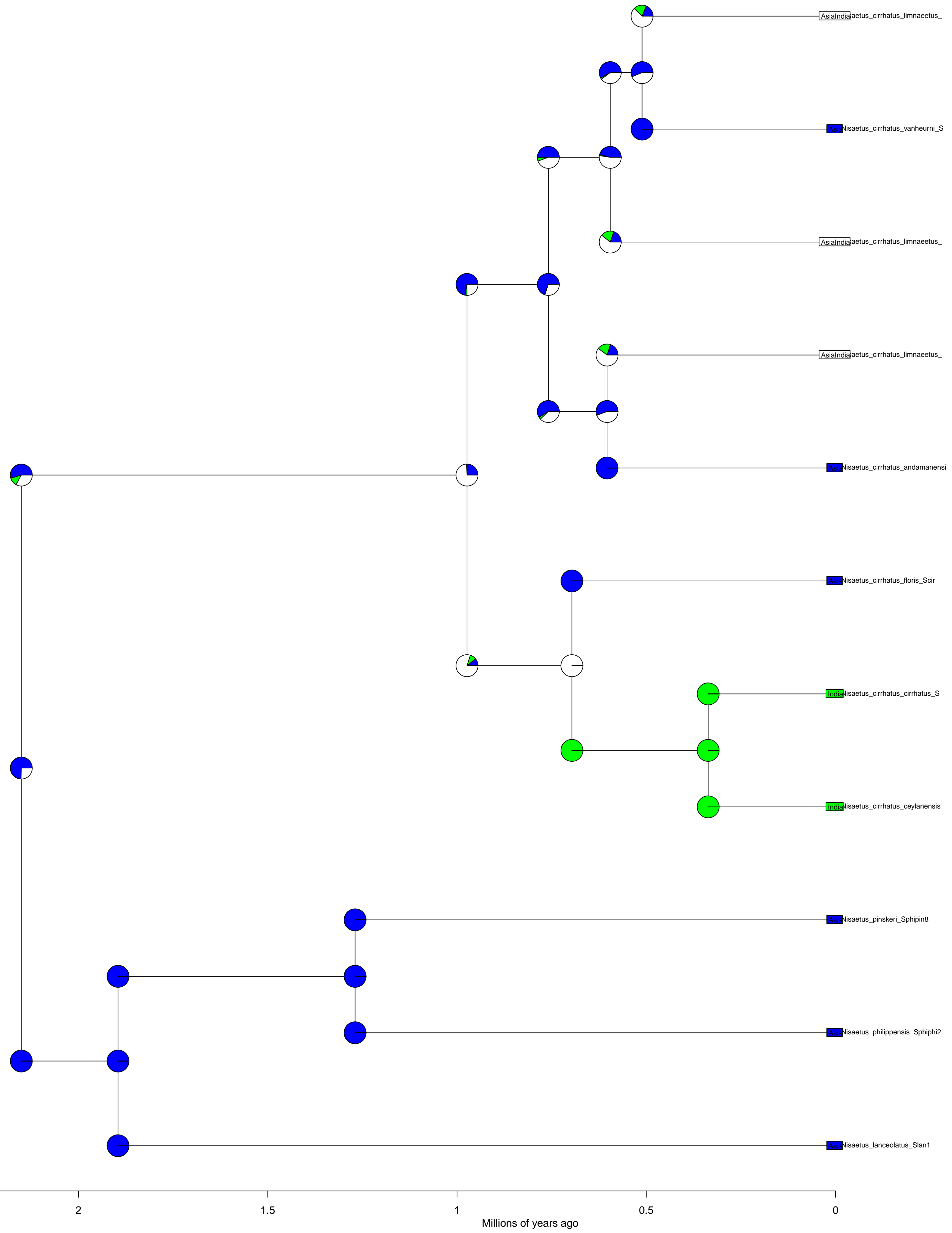


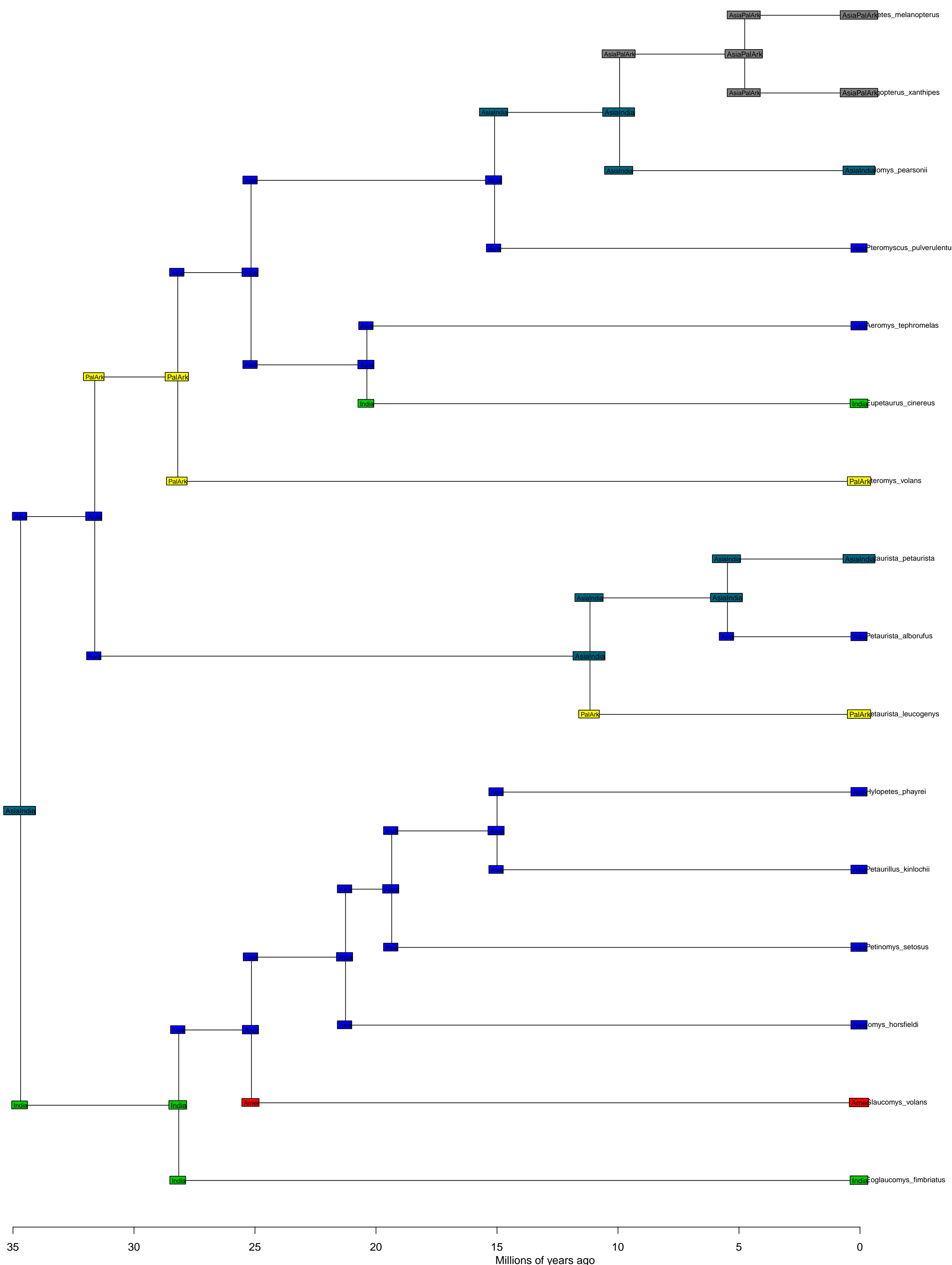
**Psittacula BioGeoBEARS DEC+J**



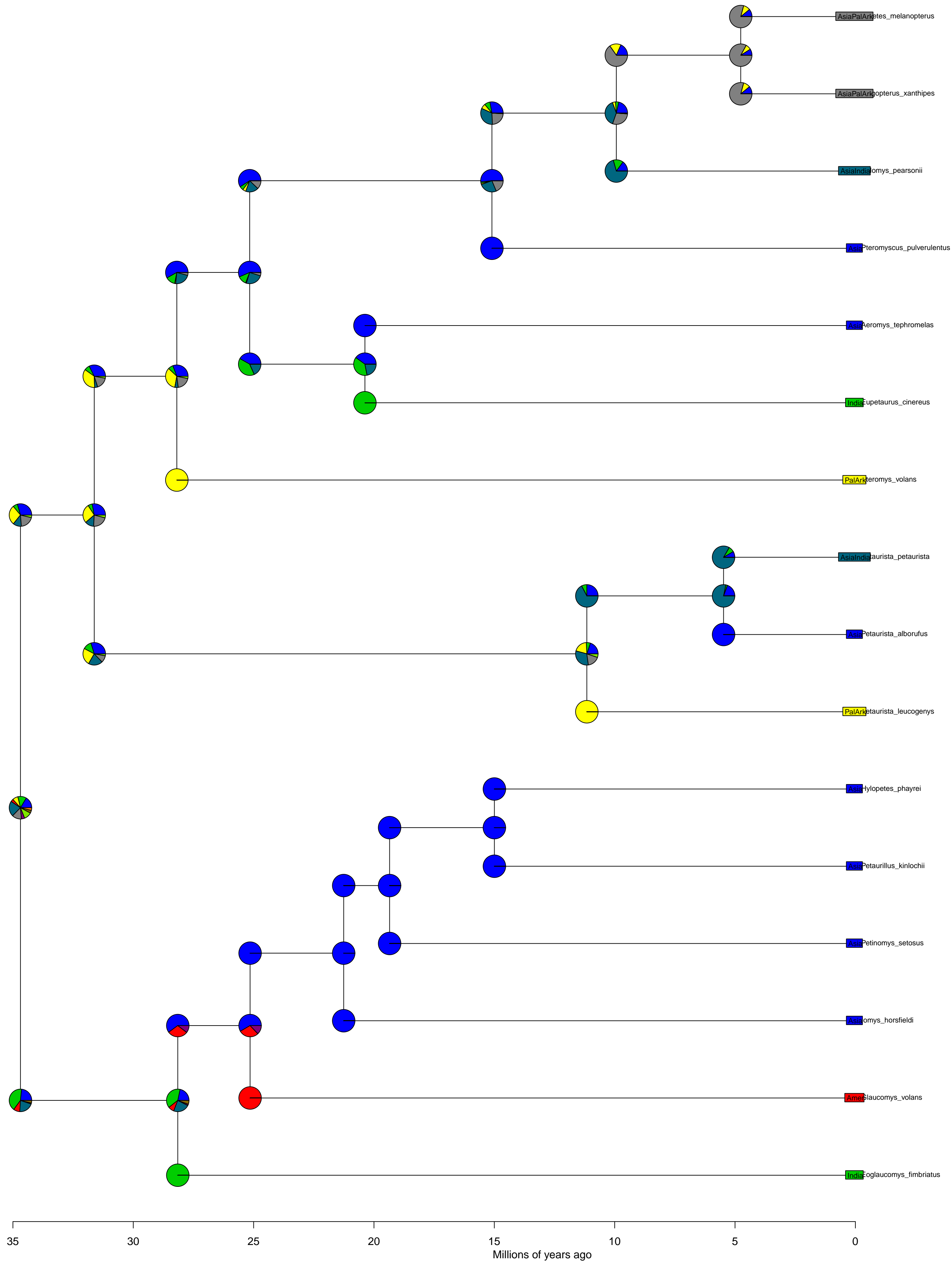




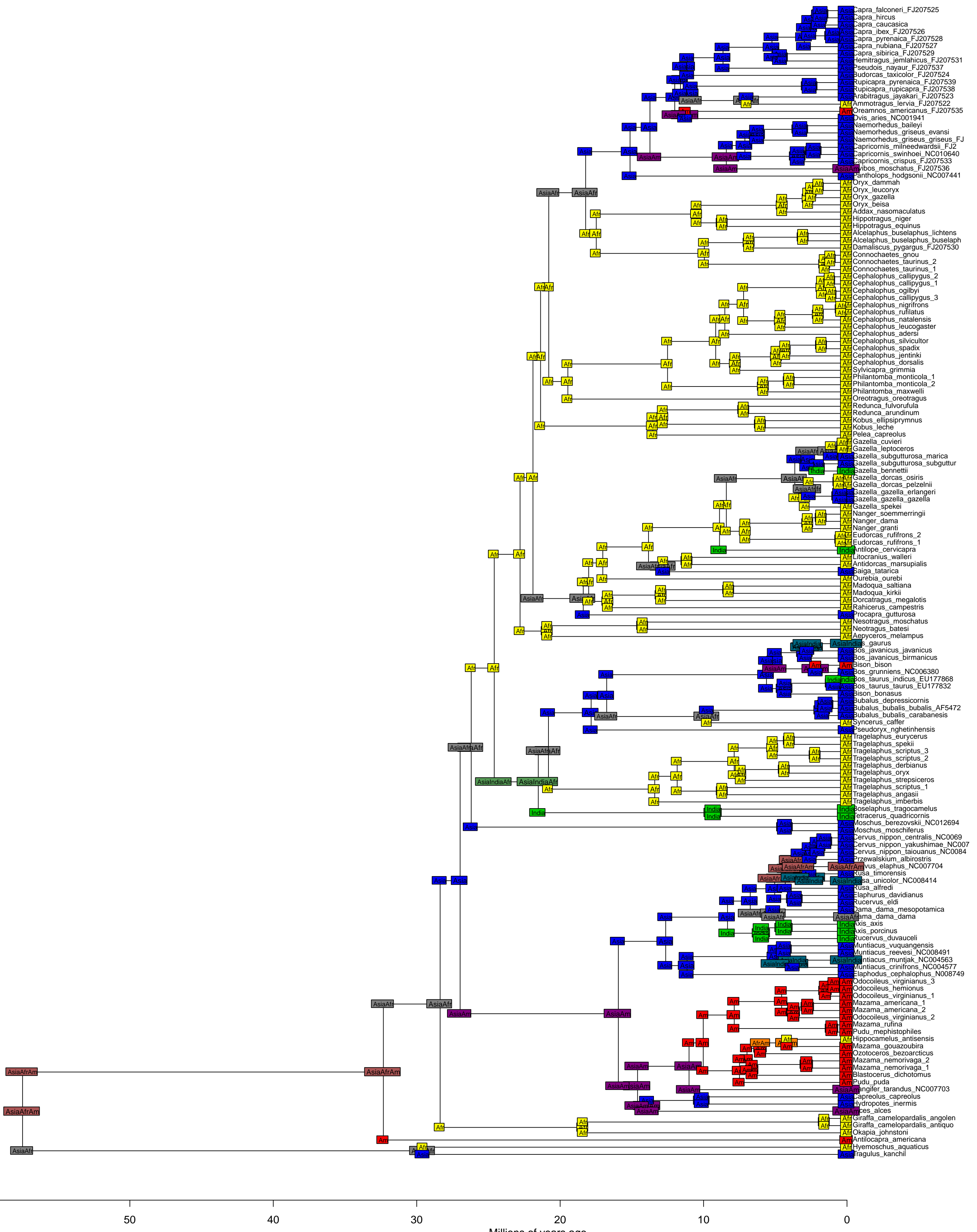




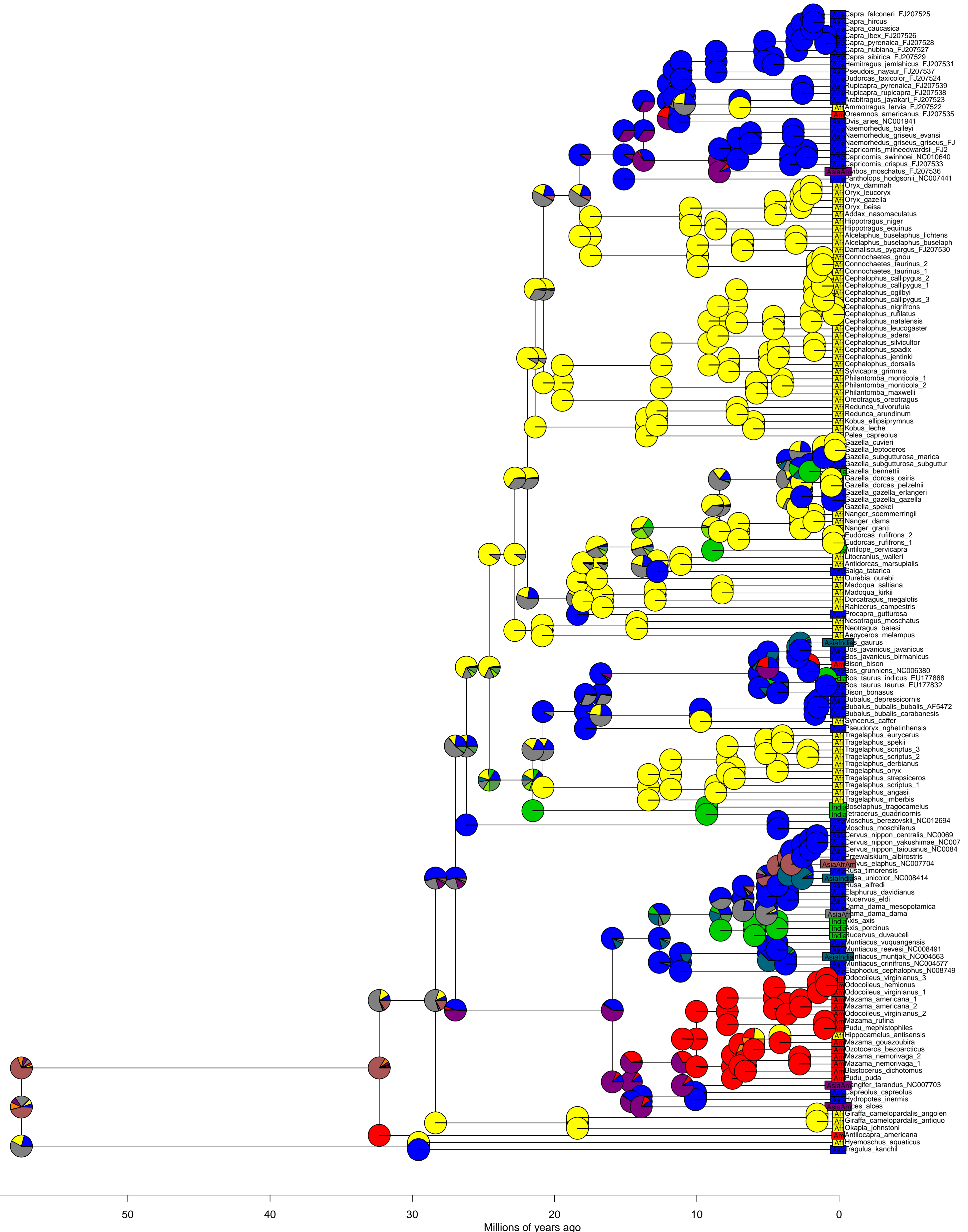
**Sciuridae, Pteromyini BioGeoBEARS DEC+J**  
ancstates: global optim, 2 areas max. d=0.0048; e=0; j=0.1439; LnL=-32.24

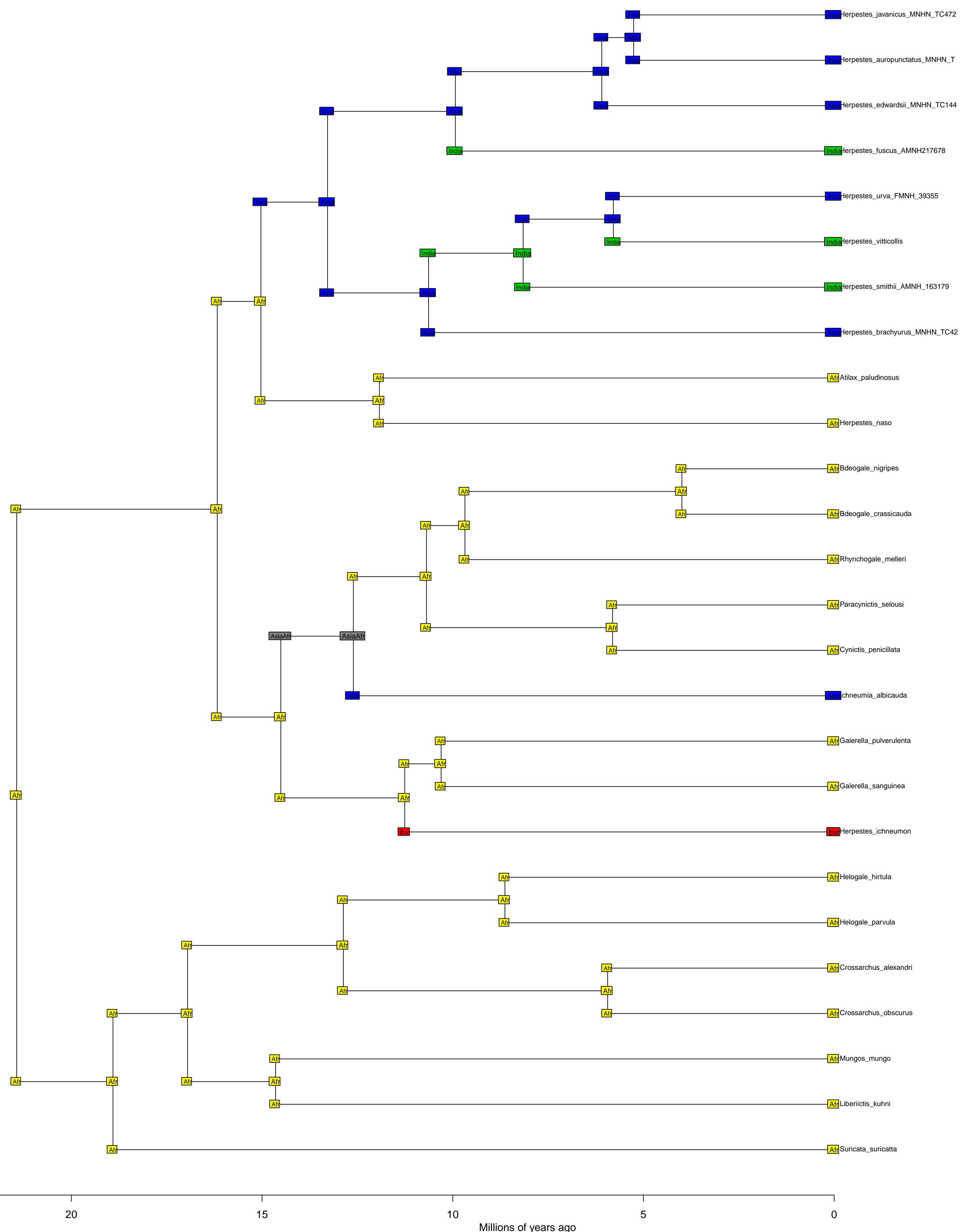


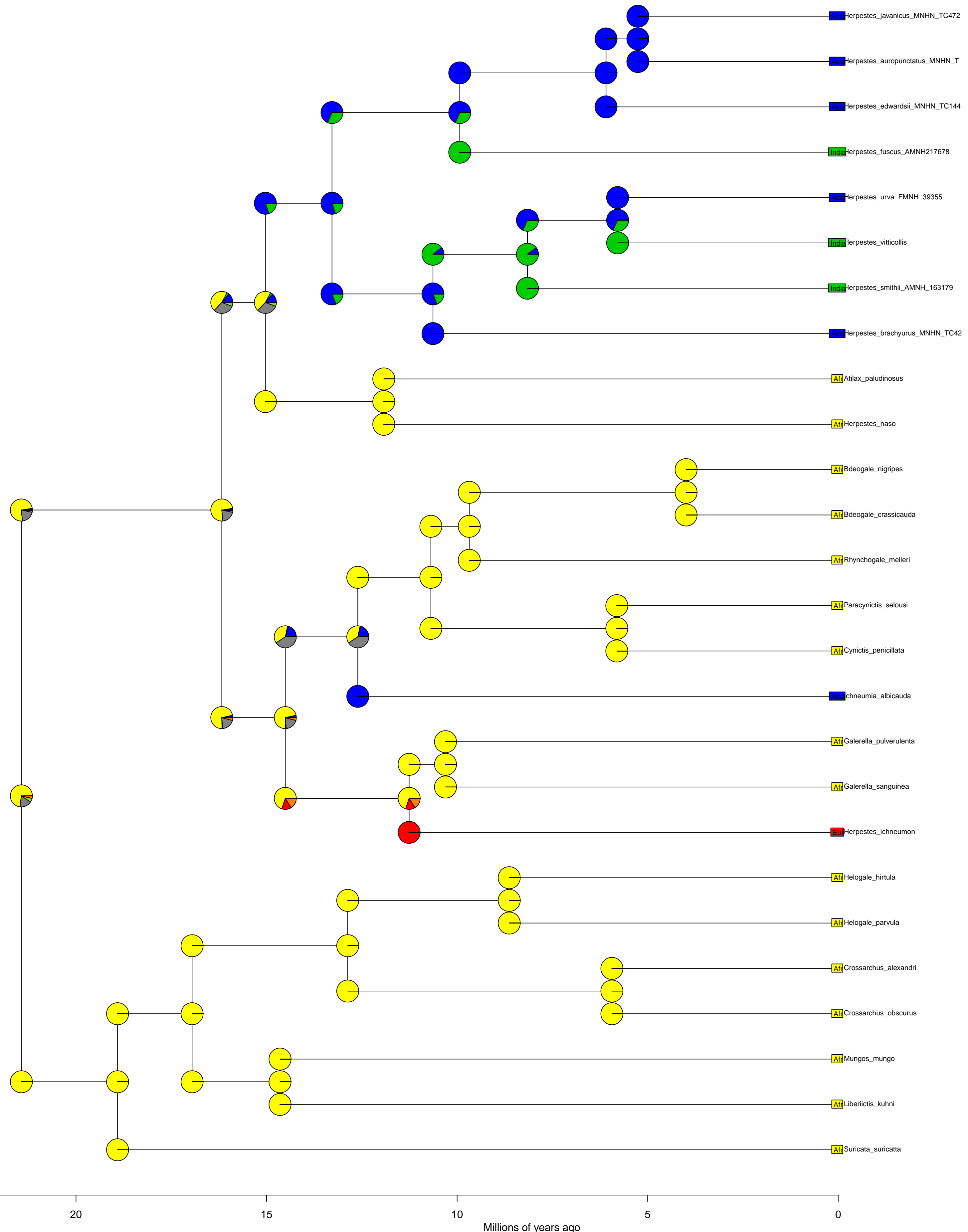
Ruminantia BioGeoBEARS DEC+J



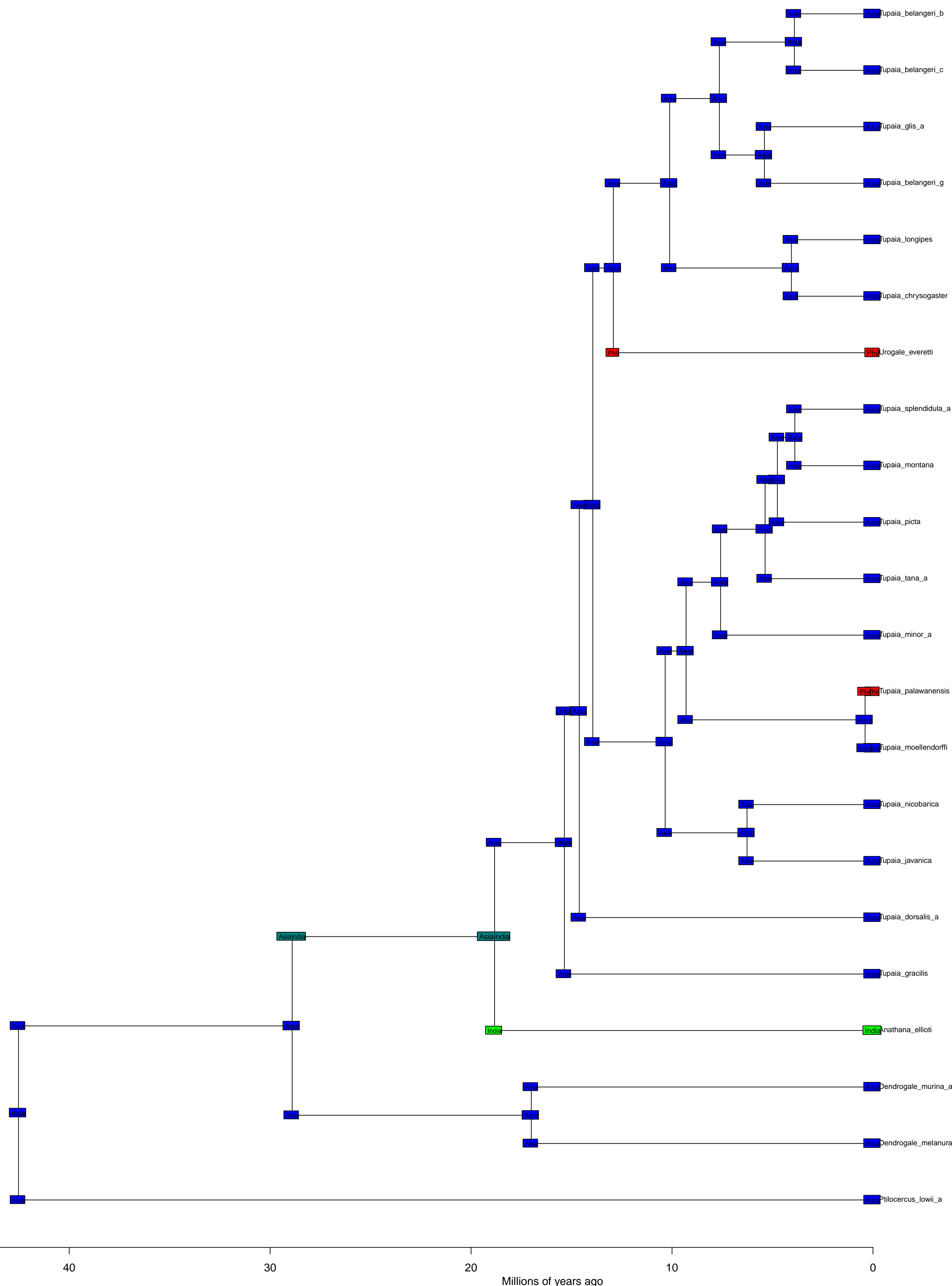
Ruminantia BioGeoBEARS DEC+J  
ancstates: global optim, 3 areas max. d=0.0027; e=0; j=0.022; LnL=-142.23

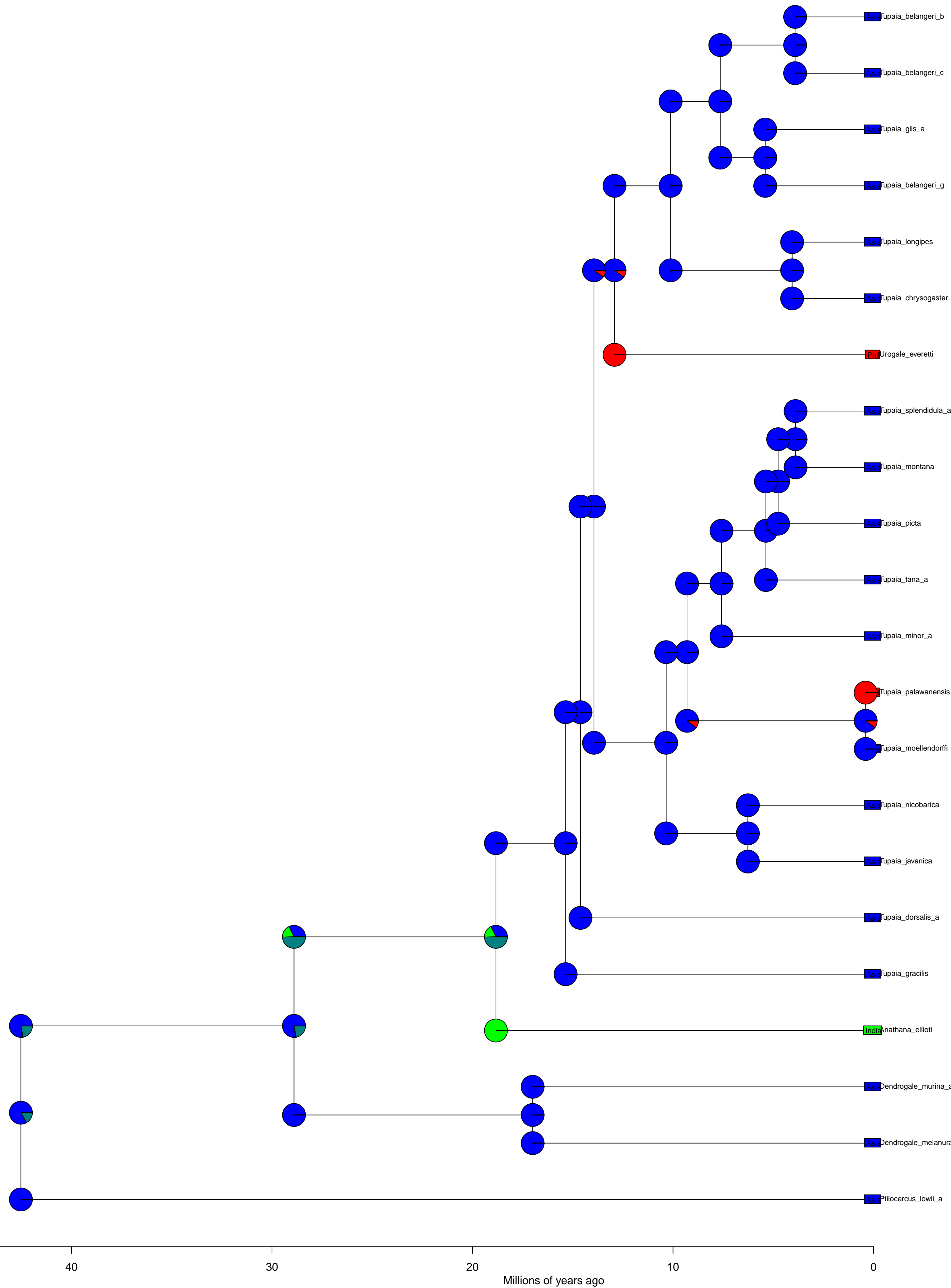


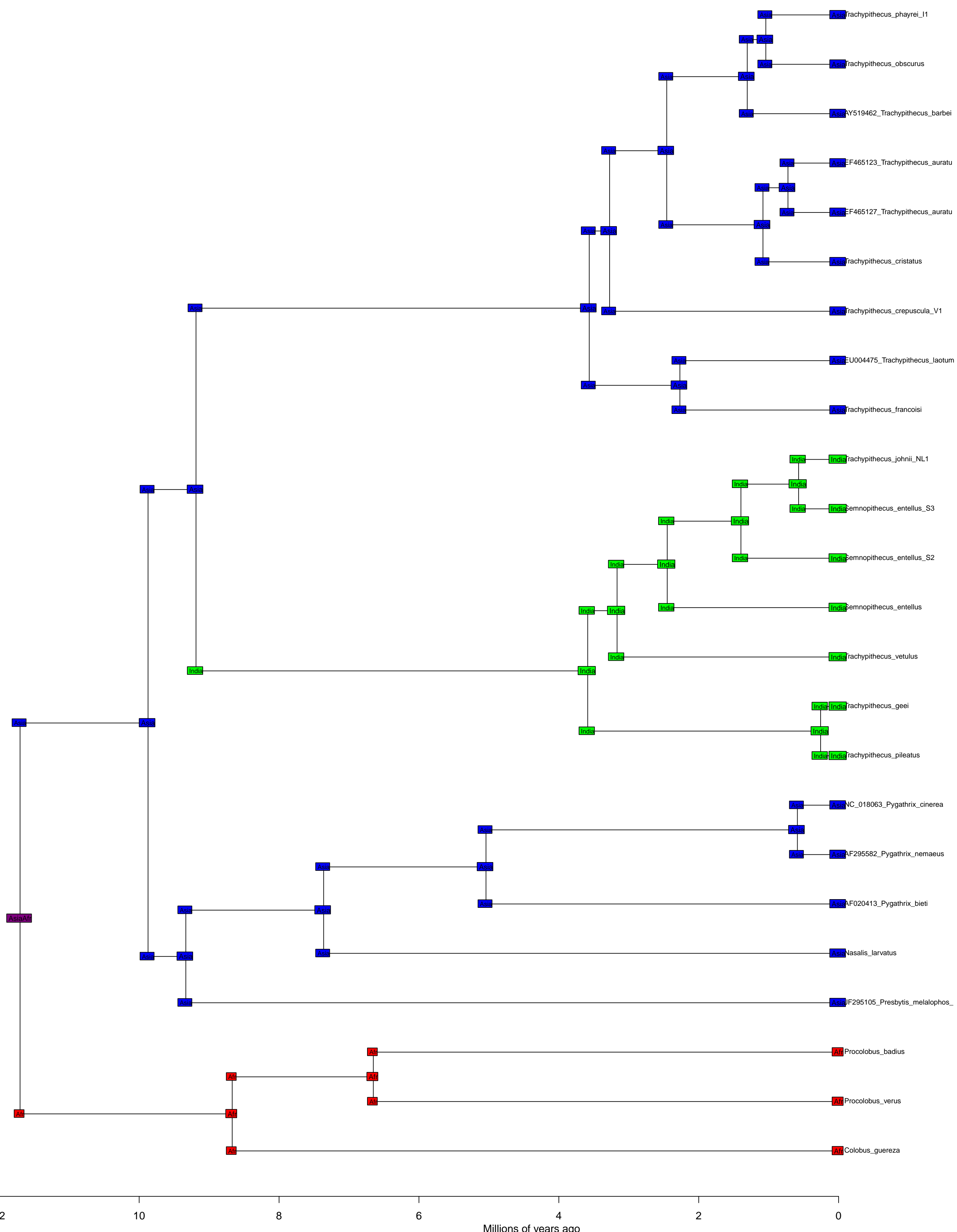


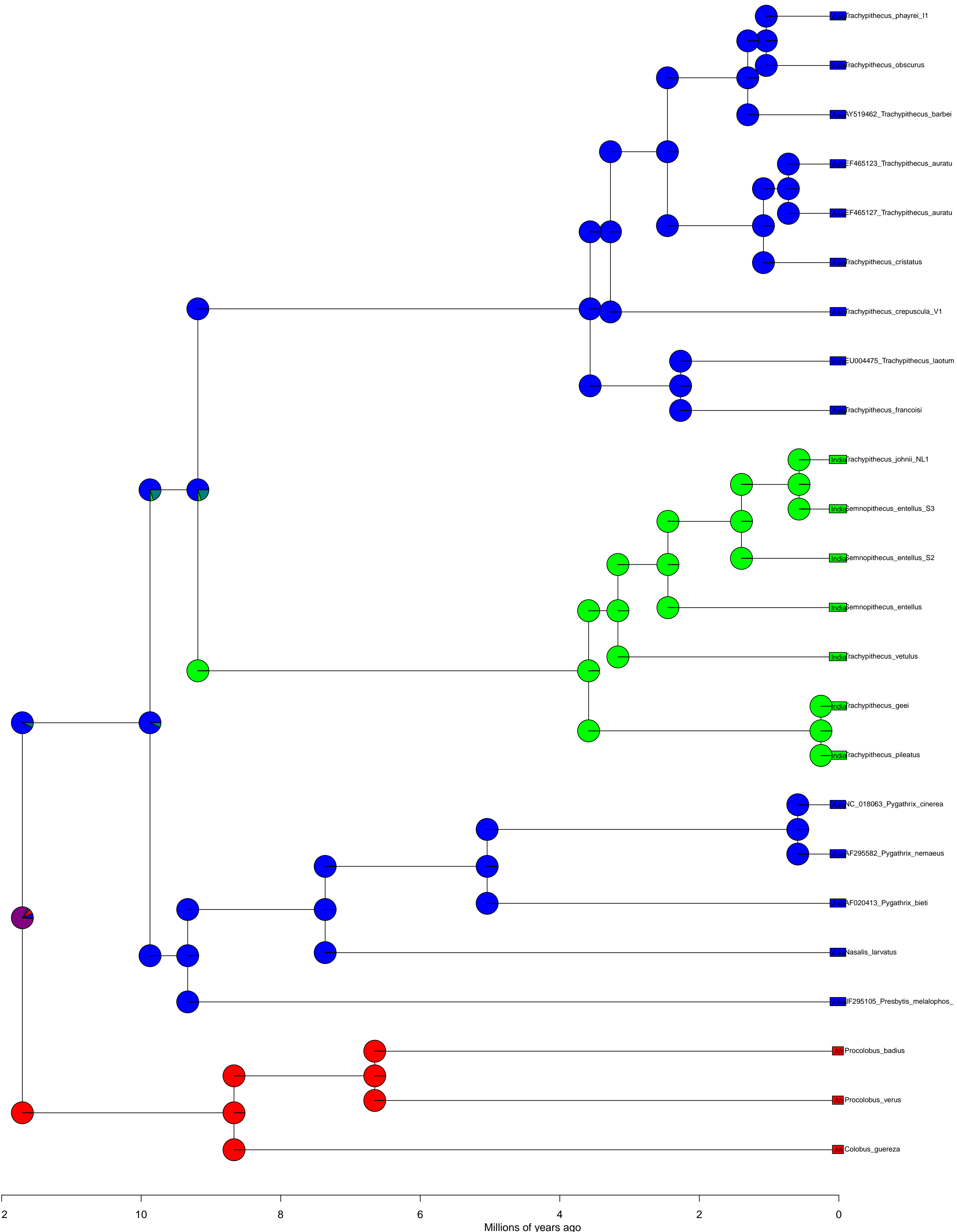


Scandentia BioGeoBEARS DEC+J  
ancstates: global optim, 2 areas max. d=0; e=0; j=0.0421; LnL=-12.45

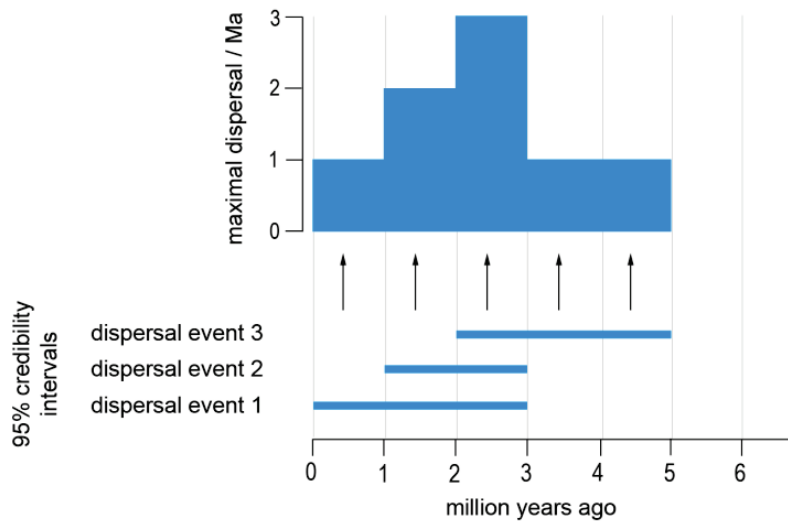






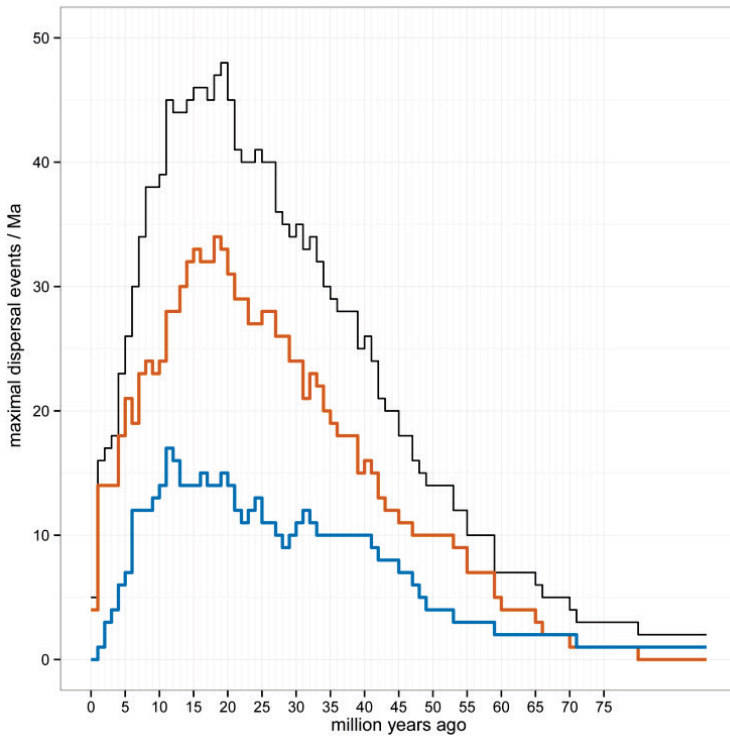


## Supplementary Figure 2



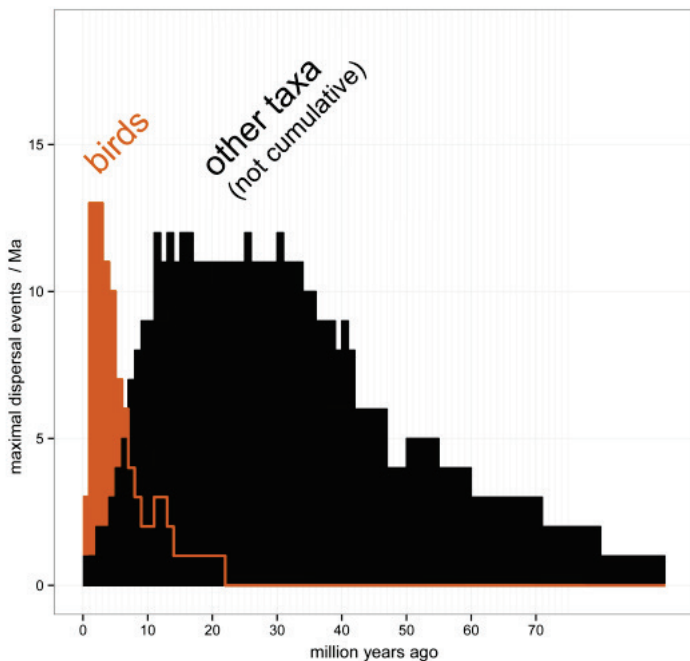
**Suppl. Fig. 2 | Example for the translation of credibility intervals of dispersal time estimation into the maximal number of observed dispersal events per Ma.** The credibility intervals for the time points of dispersal for three events overlap such that the MDE increases from one to two between 0 and 2 Ma, peaks between 2 and 3 Ma and drops down to one after 3 Ma.

### Supplementary Figure 3



**Suppl. Fig. 3 | Raw maximal dispersal events (MDE) before smoothing:** Dispersal from mainland Asia to India (orange), from India to mainland Asia (blue), and in both directions (black).

## Supplementary Figure 4



**Suppl. Fig. 4 | Influence of taxon sampling on maximal dispersal rate.** To account for a bias against more recent dispersal events due to increasing incomplete taxon sampling towards the present, we removed maximal dispersal events (MDE) with an age <7 Ma from the subsequent analyses based on the comparison of MDE between birds and other taxon groups (plants, arthropods, teleosts, amphibians, non-avian reptiles and mammals) with a less complete sampling (data not smoothed, dispersal rates for non-avian taxa not cumulative).

**Supplementary Table 1**

Taxon	95% HPD		Dispersal direction
	upper bound	lower bound	
Crypteroniaceae (Rosids, Myrtales)	5	1	A → I
Dipterocarpaceae (Rosids, Malvales)	79	36	A → I
Dipterocarpaceae (Rosids, Malvales)	59	26	A → I
Dipterocarpaceae (Rosids, Malvales)	54	18	A → I
Dipterocarpaceae (Rosids, Malvales)	28	13	A → I
Dipterocarpaceae (Rosids, Malvales)	108	50	I → A
Dipterocarpaceae (Rosids, Malvales)	70	31	I → A
Dipterocarpaceae (Rosids, Malvales)	44	18	I → A
Dipterocarpaceae (Rosids, Malvales)	29	7	I → A
Dipterocarpaceae (Rosids, Malvales)	27	5	I → A
Dipterocarpaceae (Rosids, Malvales)	24	10	I → A
Dipterocarpaceae (Rosids, Malvales)	20	6	I → A
Dipterocarpaceae (Rosids, Malvales)	16	4	I → A
Dipterocarpaceae (Rosids, Malvales)	14	2	I → A
Gentianaceae (Asterids, Gentianales)	17	8	A → I
Gentianaceae (Asterids, Gentianales)	13	6	I → A
Pachychilidae (Mollusca: Gastropoda)	65	12	A → I
Gecarcinucidae (Crustacea, Brachyura)	58	30	I → A
Gecarcinucidae (Crustacea, Brachyura)	47	24	I → A

Papilionidae (Insecta, Lepidoptera)	54	32	A → I
Papilionidae (Insecta, Lepidoptera)	30	11	A → I
Papilionidae (Insecta, Lepidoptera)	26	15	A → I
Papilionidae (Insecta, Lepidoptera)	26	15	A → I
Papilionidae (Insecta, Lepidoptera)	22	13	A → I
Papilionidae (Insecta, Lepidoptera)	22	11	A → I
Papilionidae (Insecta, Lepidoptera)	10	5	A → I
Papilionidae (Insecta, Lepidoptera)	20	12	I → A
Papilionidae (Insecta, Lepidoptera)	19	11	I → A
Papilionidae (Insecta, Lepidoptera)	16	9	I → A
Papilionidae (Insecta, Lepidoptera)	12	6	I → A
Apidae (Insecta, Hymenoptera)	27	11	A → I
Apidae (Insecta, Hymenoptera)	11	4	A → I
Apidae (Insecta, Hymenoptera)	14	4	A → I
Formicidae (Insecta, Hymenoptera, <i>Myrmica</i> spp.)	11	5	A → I
Formicidae (Insecta, Hymenoptera, <i>Tetraponera</i> spp.)	44	7	A → I
Aplocheiloidei (Teleostei, Cyprinodontiformes)	46	30	I → A
Channidae (Teleostei, Perciformes)	7	3	A → I
Channidae (Teleostei, Perciformes)	20	7	A → I
Channidae (Teleostei, Perciformes)	19	8	A → I
Channidae (Teleostei, Perciformes)	16	5	A → I
Osphronemidae (Teleostei: Perciformes)	35	23	A → I
Osphronemidae (Teleostei: Perciformes)	30	17	A → I
Osphronemidae (Teleostei: Perciformes)	33	20	A → I

Osphronemidae (Teleostei: Perciformes)	38	28	A → I
Osphronemidae (Teleostei: Perciformes)	38	22	A → I
Osphronemidae (Teleostei: Perciformes)	21	11	I → A
Cobitidae (Teleostei, Cypriniformes)	19	8	A → I
Cobitidae (Teleostei, Cypriniformes)	24	10	A → I
Cobitidae (Teleostei, Cypriniformes)	52	27	A → I
<i>Heteropneustes fossilis</i> (Teleostei, Siluriformes)	48	11	I → A
Dicroididae (Amphibia, Anura)	49	28	I → A
Dicroididae (Amphibia, Anura)	26	14	I → A
Dicroididae (Amphibia, Anura)	19	7	A → I
Dicroididae (Amphibia, Anura)	19	3	I → A
Dicroididae (Amphibia, Anura)	13	3	I → A
Microhylidae (Amphibia, Anura)	58	30	A → I
Rhacophoridae (Amphibia, Anura)	32	23	I → A
Rhacophoridae (Amphibia, Anura)	41	31	A → I
Rhacophoridae (Amphibia, Anura)	28	19	A → I
Rhacophoridae (Amphibia, Anura)	29	19	A → I
Rhacophoridae (Amphibia, Anura)	40	29	A → I
Bufoidae (Amphibia, Anura)	24	14	I → A
Bufoidae (Amphibia, Anura)	11	6	I → A
Bufoidae (Amphibia, Anura)	30	18	A → I
Bufoidae (Amphibia, Anura)	32	20	A → I
Bufoidae (Amphibia, Anura)	12	6	A → I
Bufoidae (Amphibia, Anura)	18	10	A → I

Bufonidae (Amphibia, Anura)	9	4	A → I
Geckonidae (Reptilia, Squamata, <i>Cyrtodactylus</i> spp.)	33	18	A → I
Geckonidae (Reptilia, Squamata, <i>Cyrtodactylus</i> spp.)	30	14	A → I
Geckonidae (Reptilia, Squamata, <i>Cyrtodactylus</i> spp.)	28	14	A → I
Geckonidae (Reptilia, Squamata, <i>Cyrtodactylus</i> spp.)	18	7	A → I
Geckonidae (Reptilia, Squamata, <i>Cyrtodactylus</i> spp.)	31	16	I → A
Scincidae (Reptilia: Squamata)	40	15	A → I
Scincidae (Reptilia: Squamata)	35	13	A → I
Scincidae (Reptilia: Squamata)	41	14	A → I
Scincidae (Reptilia: Squamata)	52	20	A → I
Scincidae (Reptilia: Squamata)	58	19	A → I
Scincidae (Reptilia: Squamata)	1	0	A → I
Scincidae (Reptilia: Squamata)	69	28	A → I
Agamidae 1 (Reptilia, Squamata)	46	32	A → I
Agamidae 1 (Reptilia, Squamata)	38	25	A → I
Agamidae 1 (Reptilia, Squamata)	27	17	I → A
Agamidae 1 (Reptilia, Squamata)	41	29	I → A
Agamidae 2 (Reptilia, Squamata)	10	20	A → I
Boidae (Reptilia, Squamata)	25	12	A → I
Viperidae (Reptilia, Squamata)	27	14	A → I
Viperidae (Reptilia, Squamata)	22	11	A → I
Crocodylidae (Reptilia, Crocodylia)	8	4	A → I
Crocodylidae (Reptilia, Crocodylia)	64	40	A → I
Timaliidae (Reptilia, Aves)	12	6	A → I

Timaliidae (Reptilia, Aves)	1	0	A → I
Timaliidae (Reptilia, Aves)	2	1	A → I
Timaliidae (Reptilia, Aves)	4	1	A → I
Timaliidae (Reptilia, Aves)	4	2	A → I
Timaliidae (Reptilia, Aves)	13	7	A → I
Paridae (Reptilia, Aves)	1	0	A → I
Paridae (Reptilia, Aves)	3	1	A → I
Paridae (Reptilia, Aves)	6	0	A → I
Aegithalidae (Reptilia, Aves)	1	0	A → I
Aegithalidae (Reptilia, Aves)	6	3	A → I
Aegithalidae (Reptilia, Aves)	7	4	A → I
Aegithalidae (Reptilia, Aves)	21	11	A → I
Fringillidae (Reptilia, Aves)	3	1	I → A
Fringillidae (Reptilia, Aves)	3	1	A → I
Fringillidae (Reptilia, Aves)	4	2	A → I
Certhiidae (Reptilia, Aves)	3	1	A → I
Certhiidae (Reptilia, Aves)	3	1	A → I
Certhiidae (Reptilia, Aves)	6	3	A → I
Certhiidae (Reptilia, Aves)	8	4	A → I
Psittacidae (Reptilia, Aves)	5	1	A → I
Psittacidae (Reptilia, Aves)	6	2	I → A
Psittacidae (Reptilia, Aves)	5	1	A → I
<i>Nisaetus</i> spp. (Reptilia, Aves, Accipitridae )	2	1	A → I
Bovidae (Mammalia, Ruminantia)	23	26	A → I

Cervidae (Mammalia, Ruminantia)	8	9	A → I
Bovidae (Mammalia, Ruminantia)	8	10	A → I
Bovidae (Mammalia, Ruminantia)	0	2	A → I
Herpestidae (Mammalia, Carnivora)	12	4	I → A
Herpestidae (Mammalia, Carnivora)	9	2	A → I
Herpestidae (Mammalia, Carnivora)	15	7	A → I
Herpestidae (Mammalia, Carnivora)	14	7	A → I
Sciuridae (Mammalia, Rodentia)	26	15	A → I
Sciuridae (Mammalia, Rodentia)	19	12	A → I
Sciuridae (Mammalia, Rodentia)	18	5	A → I
Tupaiidae (Mammalia, Scandentia)	34	25	A → I
Colobinae (Mammalia, Primates)	13	6	A → I

**Suppl. Table 1 | Inferred dispersal events between mainland Asia and the Indian subcontinent.** Given are the respective taxon, upper and lower bounds of the 95% highest posterior density intervals (HPD) for the age of range shifts/dispersal events in million years before present (Ma) as used for the calculation of the maximal number of dispersal events (MDE) per Ma between the Indian subcontinent (I) and mainland Asia (A).

## Supplementary Note 1

**Crypteroniaceae** (Rosids, Myrtales): We re-analysed the data set of Rutschmann *et al.*<sup>1</sup>, reduced to 44 taxa to estimate the divergence time between *Axinandra zeylanica* and SE-Asian *A. coriacea*. The data set included the *rbcL*, *ndhF*, *rpl16*-intron, *18S*, and *26S rRNA* genes (5,421 bp total alignment length). We initially applied the best calibration scheme as suggested by the authors of the original study<sup>1</sup>. However, we had severe difficulties in implementing all suggested calibration points as this dropped the initial likelihood to ‘infinity’. Therefore, we could reduce the data set, omitting the families Myrtaceae *s. lat.*, Vochysiaceae, and Onagraceae. We kept a log-normal calibration density for the MRCA of *Rhexia virginica* and *Melastoma beccarianum* (minimum age = 23 Ma; 5–95% interquartile range = 23.9–46.2 Ma), and the MRCA of *Pternandra echinata* and *M. beccarianum* (minimum age = 53 Ma; 5–95% interquartile range = 53.9–76.2 Ma). Resulting mean rates were 0.1% per Ma (95% CI = 0.08–0.13% per Ma) for *ndhF*; 0.04% per Ma (95% CI = 0.03–0.05% per Ma) for *rbcL*; 0.1% per Ma (95% CI = 0.07–0.12% per Ma) for *rpl16*; 0.02% per Ma (95% CI = 0.01–0.02% per Ma) for *18S rRNA*; and 0.05% per Ma (95% CI = 0.04–0.06% per Ma) for *26S rRNA*. We defined ranges India, mainland Asia, Africa and the New World.

**Dipterocarpaceae** (Rosids, Malvales): The phylogeny of the dipterocarp subfamily Dipterocarpoideae published by Gamage *et al.*<sup>2</sup> is based on the *trnL*-intron, *trnL-trnF* spacer region and the *matK* gene (3,926 bp total alignment length). To calibrate the phylogeny, we applied the approach described by Gunasekara<sup>3</sup> and constrained the MRCA of the genus *Hopea* to a minimum of 12 Ma (log-normal calibration density, 5–95% interquartile range = 13.4–50.3),

and that of the genus *Vatica* to 3.6 Ma (lognormal calibration density, 5–95% interquantile range = 5.0–41.9 Ma) based on the fossil record. Additionally, we included (as ‘empty sequences’) dated fossils that are closely related to the genera *Dipterocarpus* (estimated age: 65 Ma<sup>4</sup>), *Dryobalanops* (estimated age: 20 Ma<sup>5</sup>) and *Anisoptera* (estimated age: 20 Ma<sup>5</sup>). We applied a broad exponential distribution as prior for the uncorrelated relaxed clock rate, with a mean of 0.2% per Ma (5–95% interquantile range = 0.01–0.60% per Ma). The resulting mean substitution rates were 0.03 % per Ma (95% CI = 0.02–0.05% per Ma) for *matK*; 0.1% per Ma (95% CI = 0.05–0.15% per Ma) for the *trnL*-intron; and 0.06 % per Ma (95% CI = 0.04–0.08% per Ma) for the *trnL-trnF* spacer region. We defined ranges India, mainland Asia, Africa and the Seychelles. The subfamily Dipteropoideae is an example *par excellence* of a taxonomic group which—based on the biogeographical distribution of extant taxa and the fossil record—was formerly widespread in Africa, on the Indian Plate and associated continental fragments (such as the Seychelles). It subsequently diversified explosively in SE-Asia, but later became extinct in Africa and severely retracted its range in India. African fossils, including the genus *Dipterocarpus*<sup>4</sup>, and pre-collision (i.e., Early Eocene) Indian macrofossils and geochemical biomarkers have been reported by Dutta *et al.*<sup>5</sup>. To reflect this prior knowledge, we constrained the range of the MRCA of Dipteropaceae to Africa for our biogeographical estimation and adjusted the dispersal multiplier (dm) for dispersal into Africa (dm = 0.0001; thus setting Africa as origin), from mainland Asia to the Seychelles (dm = 0.01), and from Africa and the Seychelles to mainland Asia (dm = 0.01), while we kept dm = 1.00 for all other dispersal directions.

**Gentianaceae** (Asterids, Gentianales): Yuan *et al.*<sup>6</sup> based their study on the genus *Exacum* on the nuclear encoded ribosomal *ITS-1* and *ITS-2* regions, the 5.8S rRNA

gene, and the chloroplast *trnL*(UAA) intron sequence. Four independent fossil-based calibration points (minimum ages) were introduced in a phylogeny of the family Gentianaceae; resulting time estimates for the divergence between the outgroup (*Gentianothamnus*–*Tachiadenus* clade) and the ingroup (*Exacum*–*Ornichia* clade) were then used to calibrate the *Exacum* tree: tMRCA of Gentianales (60 Ma), tMRCA of *Lisianthus* (40 Ma), tMRCA of the subtribe Swertiinae (15 Ma), and tMRCA of *Gentiana* (5 Ma). We re-analysed the data set using an *ITS* rate of 0.452% per Ma (SD = 0.1)<sup>7,8</sup>, and an exponential prior distribution for *5.8S rRNA* and *trnL* with a mean of 1% per Ma (5–95% interquartile range = 0.05–3.00% per Ma). We applied a normally distributed calibration density for the tMRCA of *Exacum* (mean = 22 Ma, SD = 8.3 Ma, 5–95% interquartile range = 8.3–35.7 Ma) following the study published by Yuan *et al.*<sup>6</sup>. The resulting mean rates for the unconstrained gene partitions were 0.05% per Ma (95% CI = 0.02–0.08% per Ma) for *5.8S rRNA* and 0.07% per Ma (95% CI = 0.04–0.10% per Ma) for *trnL*. We defined ranges India, mainland Asia, the Himalayas, Africa, Madagascar and the island of Socotra.

**Pachychilidae** (Mollusca, Caenogastropoda): Unfortunately, fossil Pachychilidae have not been described that could be used for calibration, nor are reliable external rates for freshwater snails available. Therefore, we applied a broad external rate based on the data set presented by Köhler and Glaubrecht<sup>9</sup> (*16S rRNA*, and the *COI* gene; 1,511 bp total alignment length) for dating the split between the genera *Brotia* and *Paracrostoma*. After an initial series of test runs, we used a fixed strict rate with a normal prior of 1% per Ma (SD = 1.25), truncated at 5% per Ma for both partitions (5–95% interquartile range = 0.0–20.7% per Ma). This broadly covers mitochondrial substitution rates of marine gastropods that have been calibrated using the closure of the Isthmus of Panama

as a geological calibration point<sup>10,11</sup>. We defined as ranges India, mainland Asia, Australia, Africa and the Americas.

**Gecarcinucidae** (Crustacea, Brachyura): Klaus *et al.*<sup>12,13</sup> based their phylogeny of Asian freshwater crabs on the nuclear-encoded histone *H3* (318 bp) gene and the mitochondrial *16S rRNA* gene (558 bp; 876 bp total alignment length. The phylogeny was calibrated using three fossil calibration points that were translated into a gamma-distributed calibration density: fossil *Potamonautes niloticus* (node *P. niloticus*–*Platythelphusa armata*: 6 Ma), fossil *Potamon quenstedti* (node *P. fluviatile*–*P. persicum*: 16.5 Ma), and fossil *Sartoriana* sp. (node *S. spinigera*–*S. blanfordi*: 2.5 Ma). According to a recent phylogeny of the family Potamonautidae<sup>14</sup>, we corrected the first calibration point to comprise the MRCA of *Potamonautes niloticus* and *P. stanleyensis*. The analysis was run for 80 M iterations, and the first 30 M were discarded as burn-in. We applied a uniform distribution as prior for the substitution rates (0.1–10.0% per Ma for *16S rRNA* and 0.01–1.00% per Ma for histone *H3*). The resulting mean rates were 0.28% per Ma (95% CI = 0.18–0.37% per Ma) for *H3* and 0.41% per Ma (95% CI = 0.28–0.53% per Ma) for the *16S rRNA* gene. Especially the *16S rRNA* rate differs from previous studies (16S rRNA 0.64–1.42% per Ma; mean 1.02%; histone *H3* 0.12–0.26% per Ma, mean 0.19%)<sup>12</sup>. We used the same area coding as given in Klaus *et al.*<sup>12</sup> (India, East-/Southwest Asia, Philippines and Wallacea).

**Papilionidae** (Insecta, Lepidoptera): Condamine *et al.*<sup>15</sup> based their phylogeny of papilionid butterflies on ~2.3 kb of mitochondrial *CO1* and *CO2* genes and ~1.0 kb of the nuclear *EF-1a* gene. We followed their calibration scheme and translated the following age estimates into log-normally distributed calibration densities: the MRCA of the family Papilionidae was set to a minimum age of 48 Ma (fossil *Praepapilio*; mean = 2.945 Ma, SD = 1.0, offset = 15 Ma, 5–95%

interquantile range = 51.7–146.5 Ma); 30 Ma was assumed as the minimum age for the subfamily Parnassiinae (mean = 3.0708 Ma, SD = 1.0, offset = 30 Ma, 5–95% interquantile range = 34.2–141.7 Ma); and the MRCA of the tribe Luehdorfiini was set to a minimum age of 15 Ma (mean = 3.164 Ma, SD = 1.0, offset = 15 Ma, 5–95% interquantile range = 19.6–137.6 Ma). The MRCA of family Pieridae was confined to a minimum age of 34 Ma (fossil *Stolopsyche libytheoides*), as was the MRCA of the family Nymphalidae (both mean = 3.044 Ma, SD = 1.0, offset = 34 Ma, 5–95% interquantile range = 38.1–142.7 Ma). We applied a broad exponential prior for the substitution rates of the partitions (*CO1* and *CO2*: mean = 3.0% per Ma, 5–95% interquantile range = 0.15–9.00% per Ma; *EF-1a*: mean = 1.0% per Ma, 5–95% interquantile range = 0.05–3.00% per Ma). We did not constrain the root age of the phylogeny as done in the original study (183 Ma, origin of angiosperms), as this resulted in an ‘infinite negative’ initial likelihood and abortion of the analysis. 8 M iterations were discarded as burn-in. The resulting mean rates were 0.71% per Ma (95% CI = 0.55–0.86% per Ma) for the combined *CO1/CO2* partition and 0.15% per Ma (95% CI = 0.12–0.18% per Ma) for *EF-1a*. The area coding was the following: India, SE Asia, Australia, the Palearctic, the Americas, Africa, and Madagascar

**Apidae** (Insecta, Hymenoptera): To retrieve credibility intervals we re-analysed a subset of data from the study by Rehan *et al.*<sup>16</sup> on the phylogeny of carpenter bees (subfamily Xylocopinae, tribe Ceratinini; 74 taxa) using the mitochondrial-encoded *CO1* and *Cytb*, and the nuclear *EF-1a* (2,807 bp total alignment length) that includes three dispersal events from mainland Asia to the Indian subcontinent (at the divergence nodes of *Ceratina propinqua* and *C. binghami*, and at the MRCA of *C. japonica*, *C. okinawana*, *C. bowringi*, *C. hieroglyphica* and *C. moderata*). We used the three calibration points as suggested by the authors with a

log-normal calibration density: a minimum divergence between the tribes Ceratinini and Allodapini of 45 Ma (5–95% interquartile range = 45.2–50.2 Ma); a minimum divergence between *Apis mellifera* from the genus *Liotrigona* of 65 Ma (5–95% interquartile range = 65.3–73.5 Ma); and 90 Ma (5–95% interquartile range = 91.4–128.3 Ma) for the MRCA of the Xylocopinae and Apinae. The resulting mean rates were 3.14% per Ma (95% CI = 1.32–7.07% per Ma) for *Cytb*, 0.28% per Ma (95% CI = 0.21–0.34% per Ma) for *EF-1a*, and 2.08% per Ma (95% CI = 1.66–2.54% per Ma) for *COI*. We defined as ranges India, mainland Asia, Australia, Africa and the Americas.

**Formicidae** (Insecta, Hymenoptera): We combined partial sequence information of the *28S rRNA* and *LWRh* genes (1,388 bp total) obtained from the studies of Ward and Downie<sup>17</sup> on the subfamily Pseudomyrmecinae and Jansen *et al.*<sup>18</sup> on the genus *Myrmica*. Thereby, we could employ the calibration points provided by Jansen *et al.*<sup>18</sup>, i.e., the split between the subfamilies Formicinae and Myrmicinae, calibrated with fossil *Kyromyrma* (92 Ma, 5–95% interquartile range = 92.2–124.0 Ma) and the MRCA of the genus *Myrmica*, calibrated based on baltic amber fossils (44.1 Ma; 5–95% interquartile range = 41.3–73.2 Ma). We inferred dispersal times to the Indian subcontinent for *Myrmica indica* and *T. rufonigra*, with separate biogeographical analyses for the subfamily Pseudomyrmecinae and the genus *Myrmica*. The resulting mean rates were 0.08% per Ma (95% CI = 0.07–0.10% per Ma) for *28S rRNA*; and 0.34% per Ma (95% CI = 0.26–0.42% per Ma) for *LWRh*. For the biogeographical analysis we split the resulting phylogeny and used different area coding for *Pseudomyrmex*–*Tetraponera* (India, mainland Asia, Africa and the Americas) and for *Myrmica* (India, East/Southeast Asia, western Eurasia/Europe and the Americas).

**Aplocheiloidei** (Teleostei, Cyprinodontiformes): We used the mitochondrial data set of Murphy and Collier<sup>19</sup> to calibrate the split between SE-Asian *Aplocheilus panchax* and Indian *A. lineatus*, consisting of partial sequences of *12S rRNA* (333 bp), *16S rRNA* (520 bp), and *Cytb* (360 bp) genes. We applied a normally distributed divergence density for the calibrations of the following splits: the split between American and African taxa (tectonic break up of western Gondwana, 5–95% interquartile range = 81.7–88.3 Ma); the split between Asian and Madagascan species (tectonic separation of Madagascar and India, 5–95% interquartile range = 85.4–88.6 Ma); and the age of the separation of Afrotropical/Neotropical and Asian/Madagascan taxa (break up of Western and Eastern Gondwana, 5–95% interquartile range = 166.7–173.3 Ma). The resulting mean rates were 0.30% per Ma (95% CI = 0.23–0.38% per Ma) for *16S rRNA*; 0.21% per Ma (95% CI = 0.17–0.26% per Ma) for *12S rRNA*; and 1.45% per Ma (95% CI = 1.07–1.89% per Ma) for *Cytb*. For the biogeographical inference, we used mainland Asia, India, Africa, Madagascar, the Seychelles and the Americas as area coding.

**Channidae** (Teleostei, Perciformes): We re-calculated the phylogeny published by Adamson *et al.*<sup>20</sup> that was based on the mitochondrially encoded *Cytb* (809 bp) and nuclear *RAG-1* (1,484 bp) genes. We followed their calibration scheme and constrained the MRCA of the genera *Channa* and *Parachanna* with the first occurrence date of *Channa* (5–95% interquartile range = 40.9–63.2 Ma); and the divergence of the family Channidae from other members of the order Perciformes (5–95% interquartile range = 48.6–103.3 Ma). We applied broad normally distributed rate priors for *Cytb* (2.0% per Ma, SD = 1.0, 5–95% interquartile range = 0.54–3.66% per Ma) and *RAG-1* (0.1% per Ma, SD = 0.1, 5–95% interquartile range = 0.02–0.27% per Ma). Resulting mean rates were 0.51% per

Ma (95% CI = 0.43–0.61% per Ma) for *Cytb* and 0.15% per Ma (95% CI = 0.12–0.20% per Ma) for the *RAG-1* gene. For the biogeographical inference, we used mainland Asia and India as area coding. The distribution range at the root node was constrained to Asia<sup>20</sup>.

**Heteropneustidae** (Teleostei: Siluriformes): We re-analysed data from the phylogenetic study by Ratmuangkhwang *et al.*<sup>21</sup> on heteropneustid catfishes which are currently described as one species (*Heteropneustes fossilis*), based on *RAG-1* sequence information of 1,494 bp length. We followed the calibration scheme of the original study by incorporating six calibration points as normally distributed calibration densities within the outgroup taxa. These were derived as secondary calibration points from the study of Nakatani *et al.*<sup>22</sup> (phylogeny of the teleost group Otophysi; the calibration was based on 23 fossil and three biogeographical constraints), such that the 5–95% interquartile ranges correspond to the node age credibility intervals of the latter study. The resulting mean substitution rate was 0.96% per Ma (95% CI = 0.59–1.34% per Ma). The mutation rate under the calibration scheme of Ratmuangkhwang *et al.*<sup>21</sup> is thus extremely fast compared to the mutation rates of *RAG-1* inferred for the Channidae (see above) and Osphronemidae (see below), and might point to an underestimation of divergence dates. However, the resulting credibility intervals for the estimates of node ages were large (spanning >30 Ma) and thus, most likely still captured the actual divergence times. For the biogeographical inference, we used mainland Asia and India as area coding.

**Osphronemidae** (Teleostei: Perciformes): We re-analysed the data from the study of Rüber *et al.*<sup>23</sup> on the phylogeny of fishes in the family Osphronemidae. We used the complete data set comprising 60 taxa (*RAG-1* gene, complete *Cytb*, partial *12S rRNA*, *Val-tRNA* and partial *16S rRNA* genes; 4,258 bp total alignment

length). We followed the authors' calibration scheme by calibrating with fossil *Osphronemus* from Sumatra of Late Eocene/Early Oligocene age, applying the suggested crown group calibration. We translated this information into a log-normally distributed calibration density with an offset at 28 Ma (5–95% interquartile range = 29–54 Ma). Resulting rates were 0.34% per Ma for *RAG-1* (95% CI = 0.26–0.40% per Ma), 3.01% per Ma for *Cytb* (95% CI = 2.31–3.65% per Ma), and 0.47% per Ma (95% CI = 0.36–0.57% per Ma) for the combined non-protein coding mitochondrial tRNA and rRNA genes. For the biogeographical inference, we used mainland Asia, India and Africa as area coding.

**Cobitidae** (Teleostei, Cypriniformes): We re-analysed the data set on which the phylogenetic study by Šlechtová *et al.*<sup>24</sup> builds (mitochondrial *Cytb* and nuclear *RAG-1* sequences; 2,016 bp total alignment length) using an external rate for *Cytb* (normally distributed, with a mean rate of 0.68% per Ma; 5–95% interquartile range = 0.52–0.84% per Ma). A calibration for the genus *Cobitis* was available using the opening of the Strait of Gibraltar, as cobitids are primary freshwater fish and thus, incapable of dispersing through marine habitats<sup>25</sup>. We assumed three dispersal events from Southeast Asia to the Indian subcontinent (Bangladesh and N-Bengal) at the divergence of *Pangio pangia* and *P. doriae*; *Lepidocephalichthys guntea* and *L. hasselti*; and *Neoeucirrichthys maydelli* and *Somileptus gongota*. The resulting mean mutation rate of the *RAG-1* gene was 0.17% per Ma (95% CI = 0.12–0.23% per Ma). For the biogeographical inference, we used mainland Asia and India as area coding.

**Dic平glossidae** (Amphibia, Anura): In case of the anuran family Dic平glossidae we re-analysed the respective subset of data from the amphibian phylogeny published by Pyron and Wiens<sup>26</sup>, including the genera *Indiranana* (outgroup),

*Occidozyga*, *Nannophrys*, *Hoplobatrachus*, *Euphlyctis*, *Sphaerotheca*, *Fejervarya*, *Paa*, and *Limnonectes*), while we included three additional specimens of the genus *Fejervarya*<sup>27</sup>. The data consist of seven partitions, three mitochondrial (*12S* and *16S rRNA* genes, *Cytb*) and four nuclear genes (*CXCR4*, *NCXI*, *RHOD*, *TYR*). We assigned a GTR+G model of sequence evolution to all partitions except for the *12S rRNA* and *CXCR4* partitions, in which case a HKY+G model was applied. We ran the analysis for 50 M generations, sampling every 2,000<sup>th</sup> generation, discarding 10% of the samples as burn-in. We constrained the tMRCA of dicoglossids with a normally distributed calibration density with a mean of 63 Ma (SD = 9.7 Ma; 5–95% interquartile range = 47–79 Ma). This secondary calibration point is based on the study of Van Bocxlaer *et al.*<sup>28</sup>, as the different calibration schemes employed by the authors cover a range of 47–79 Ma for this split. For the biogeographical inference, we used mainland Asia, Africa and India as area coding. Although not unequivocal in our analysis, we assumed an Indian origin of the family Dicoglossidae, and thus initial dispersal from the Indian subcontinent to East-/SE-Asia at the deepest split within the subfamily Dicoglossinae<sup>28</sup>. The resulting mean rates were 0.74% per Ma (95% CI = 0.56–0.95% per Ma) for *12 rRNA*; 0.87% per Ma (95% CI = 0.64–1.10% per Ma) for *16S rRNA*; 3.70% per Ma (95% CI = 2.27–5.48% per Ma) for *Cytb*; 0.07% per Ma (95% CI = 0.04–0.12% per Ma) for *CXCR4*; 0.06% per Ma (95% CI = 0.04–0.08% per Ma) for *NCXI*; 0.08% per Ma (95% CI = 0.05–0.12% per Ma) for *RHOD*; and 0.12% per Ma (95% CI = 0.09–0.16% per Ma) for *TYR*.

**Microhylidae (Amphibia, Anura):** For the family Microhylidae we re-analysed a part of the data set published by de Sá *et al.*<sup>29</sup>, in which three nuclear (*TYR*, *BDNF*, and the *28S rRNA* gene) and one mitochondrial marker (*16S rRNA* gene) were employed. We ran the analysis for 100 M iterations, sampling every 10,000<sup>th</sup>

iteration, discarding 10% as burn-in. We applied a HKY+G model of sequence evolution for all partitions. According to the original study<sup>29</sup> we constrained (using a normally distributed calibration density) the tMRCA of the subfamily Otophryninae to 60.4 Ma (SD = 5); the tMRCA of subfamily Gastrothryninae to 79.1 Ma (SD = 5); and the tMRCA of the genus *Gastrophryne* to 1.7 Ma (SD = 0.5). The resulting mean rates were 0.06% per Ma (95% CI = 0.05–0.07% per Ma) for *BDNF*; 0.19% per Ma (95% CI = 0.15–0.25% per Ma) for *TYR*; 0.017% per Ma (95% CI = 0.01–0.02% per Ma) for *28S rRNA*; and 0.89% per Ma (95% CI = 0.69–1.11% per Ma) for *16S rRNA*. For the biogeographical inference, we used mainland Asia and India as area coding.

**Rhacophoridae** (Amphibia, Anura): The study on rhacophorid tree frogs<sup>30</sup> was based on five nuclear gene fragments (*BDNF*, 614 bp; *POMC*, 601 bp; *RAG-1*, 1,164 bp; *RHOD*, 315 bp; *TYR*, 531 bp) and 2,041 bp of mitochondrial DNA covering the *12S* and *16S rRNA* genes as well as the complete *tRNA Val* (5,266 bp total alignment length). The authors calibrated the age of the most recent common ancestor of the Rhacophoridae with fossil *Indorana prasadi* from Early Eocene sediments of India, and constrained the split between *Boophis tephraeomystax* from the Comoro island of Mayotte and its sister species *Boophis doulioti* to a maximum age of 15 Ma. We did not re-analyse this data set but used the original chronogram to calculate the biogeographic estimates. For the biogeographical inference, we used mainland Asia, India, insular SE Asia and Africa as area coding.

**Bufoidae** (Amphibia, Anura): We re-analysed the data set of Van Bocxlaer *et al.*<sup>31</sup>, which included nuclear (1,970 bp; *NCX1*, *CXCR4*) and mitochondrial genes (4,339 bp; *12S rRNA*, *tRNA Val*, *16S rRNA*, *tRNA Leu*, *ND1*, *tRNA Ile*, *tRNA Gln*, *tRNA Met*, *ND2*; 6,309 bp total alignment length), to infer the phylogeny and

divergence time estimates of toads, with the focus on the Asian subfamily Adenominae. We translated the following calibration points based on minimum ages of fossils into log-normally distributed calibration densities (SD = 1.0 in all cases): 18 Ma for the MRCA of the *Bufo viridis* group (mean = 1.7 Ma, offset = 18.0 Ma, 5–95% interquartile range = 19.1–46.7 Ma), 11 Ma for the origin of the genus *Rhinellamarina* (mean = 1.88 Ma, offset = 11.0 Ma, 5–95% interquartile range = 12.3–44.8 Ma), 9.6 Ma for the MRCA of the *Bufo bufo* group (mean = 1.905 Ma, offset = 9.6 Ma, 5–95% interquartile range = 10.9–44.4 Ma), and a minimum age of 15 Ma for the MRCA of the subgenus *Eleutherodactylus* (mean = 2.17 Ma, offset = 15.0 Ma, 5–95% interquartile range = 16.7–60.3 Ma). Divergence time analysis was run as described under “Phylogenetic methods and divergence time estimations” with the exception that we discarded 2,500 samples as burn-in. The resulting mean rates were 0.09% per Ma (95% CI = 0.07–0.11% per Ma) for the nuclear and 0.88% per Ma (95% CI = 0.65–1.10% per Ma) for the mitochondrial partition. For the biogeographical inference, we used East/SE Asia, India, Africa, and western Eurasia as area coding.

**Crocodylidae** (Reptilia, Crocodylia): Oaks<sup>32</sup> presents a phylogeny of the family Crocodylidae based on two partitions: 7,282 bp of mitochondrial *Cytb*, *tRNA Glu*, *tRNA Thr*, *ND2*, *tRNA Met*, *tRNA Trp*, *ND3*, *tRNA Gly*, *tRNA Arg*), the D-loop of the control region and *tRNAPhe*, and nuclear encoded *c-mos*, *EPIC*, *ACTC* Exon 4–5, *aTROP* Exon 5–6, *ACTB* Exon 3–4, *AChR* Exon 7–8, *GAPDH* Exon 11–12, *LDH-B* Exon 6–7, *LDH-A* Exon 7–8, and *RHO* Exon 2–3. This phylogeny was calibrated with the tMRCA of the subfamilies Alligatorinae and Caimaninae (5–95% interquartile range of a lognormal calibration density = 71–64 Ma; upper bound of the tMRCA of the order Crocodylia = 90 Ma). The \*BEAST<sup>33</sup> minimum credibility tree was kindly provided by the first author of this study and used for

our biogeographical inference. For the biogeographical inference, we used mainland Asia, India, Africa and the Americas as area coding. We assumed dispersal from SE-Asia to the Indian subcontinent at the divergence of *Crocodylus siamensis* and *C. palustris*, and – more arbitrary in light of the fossil record<sup>34</sup> – at the MRCA of the genera *Tomistoma* and *Crocodylus*.

**Geckonidae** (Reptilia, Squamata): Based on the study of Wood *et al.*<sup>35</sup>, including additional outgroup taxa from Bansal and Karanth<sup>36</sup>, we calculated a phylogeny of the gekkonid genus *Cyrtodactylus* based on the partial nuclear *RAG-1* and *PDC* genes (1,454 bp total alignment length). Substitution schemes were not partitioned between both genes. We calibrated the divergence between *Sphaerodactylus roosevelti* and *S. torrei* based on fossil *Sphaerodactylus* from Hispaniola, dated 15–20 Ma (exponential calibration density, mean = 3.0 Ma, offset = 15 Ma, 5–95% interquartile range = 15–24 Ma), the divergence between the genera *Oedura* and *Woodworthia* with fossil “*Hoplodactylus* sp.” from New Zealand, dated to 16–19 Ma (exponential calibration density, mean = 17 Ma, offset = 16 Ma, 5–95% interquartile range = 17–67 Ma). Fossil *Primaderma nessovi* served to constrain the MRCA of the split between the families Helodermatidae and Anguidae (exponential calibration density, mean = 3.0, offset = 99 Ma, 5–95% interquartile range = 99–108 Ma), and the split between *Teratoscincus scincus* and *T. robورowski* was constrained biogeographically to 10 Ma (mean = 10 Ma, SD = 0.5, 5–95% interquartile range = 9–11 Ma). The resulting mean substitution rates were 0.08% per Ma for both partitions (95% CI = 0.06–0.09% per Ma for *RAG-1* and 0.06–0.1% per Ma for *PDC*). For the biogeographical inference, we used mainland Asia, India and Australia as area coding.

**Scincidae** (Reptilia: Squamata): We re-analysed the data used for the phylogenetic analyses published by Datta-Roy *et al.*<sup>37</sup> based on partial

mitochondrial *12S* and *16S rRNA* genes and the nuclear *c-mos* gene (1,641 bp total alignment length). We added the species *Coprucia zebra*, *Tiliqua adelaidensis* and *Egernia whitii* from the study of Honda *et al.*<sup>38</sup> and calibrated the split between the latter two based on fossil *Proegernia palankarinnensis* from the Late Oligocene<sup>39</sup>. We used a lognormal calibration density with 25 Ma as a hard younger bound, resulting in a 5–95% interquartile range of 25.52–39.08 Ma for that split. The resulting rates were 0.33% per Ma (95% CI 0.19–0.47% per Ma) for *16S rRNA*, 0.30% per Ma (95% CI 0.18–0.43% per Ma) for *12S rRNA*, and 0.04% per Ma (95% CI 0.02–0.06% per Ma) for *c-mos*. For the biogeographical inference, we used mainland Asia, India, Africa, Madagascar, the Seychelles, teh Cape Verde silands and the Americas as area coding.

**Agamidae 1** (Reptilia, Squamata): We re-analysed the data set of Macey *et al.*<sup>40</sup>, based on the mitochondrial *ND1*, *tRNA Gln*, *tRNA Ile*, *tRNA Met*, *ND2*, *tRNA Trp*, *tRNA Ala*, *tRNA Asn*, *tRNA Cys*, *tRNA Tyr*, and *COI* genes (1,551 bp total alignment length). We used three fossil calibration points with a lognormal distributed calibration density<sup>41</sup> and calibrated the MRCA of crown Acrodonta (families Chamaeleonidae and Agamidae; 5–95% interquartile range = 46.4–134.0 Ma), the MRCA of crown Agamidae (5–95% interquartile range = 32.3–124.4 Ma), and the MRCA of *Istiurus lesuseurii* and *Pogona vitticeps* (5–95% interquartile range = 20.4–56.7 Ma). The resulting rates were 2.20% per Ma (95% CI 1.20–3.20% per Ma) for *CXI*, 1.90% per Ma (95% CI 1.10–2.51 per Ma) for *ND1*, 1.32% per Ma (95% CI 1.08–1.56 per Ma) for *ND2*, 0.95% per Ma (95% CI 0.68–1.23 per Ma) for *tRNA Ala*, 0.87% per Ma (95% CI 0.49–1.24 per Ma) for *tRNA Asn*, 1.50% per Ma (95% CI 1.09–1.95 per Ma) for *tRNA Cys*, 0.61% per Ma (95% CI 0.42–0.82 per Ma) for *tRNA Gln*, 0.66% per Ma (95% CI 0.37–0.97 per Ma) for *tRNA Ile*, 1.50% per Ma (95% CI 0.94–2.15 per Ma) for *tRNA Met*,

1.53% per Ma (95% CI 1.14–1.94 per Ma) for *tRNA Trp*, and 1.46% per Ma (95% CI 1.08–1.86 per Ma) for *tRNA Tyr*. For the biogeographical inference, we used mainland Asia, India, and Africa as area coding.

**Agamidae 2** (Reptilia, Squamata): The aforementioned data set on agamids included only one Asian specimen of *Draco*; however, there are also Indian representatives this genus. Therefore, we re-analysed the data set of Honda *et al.*<sup>42</sup> based on mitochondrial *12S* and *16S rRNA* gene fragments (780 bp total alignment length). To estimate the divergence of Indian *D. dussumieri*, we calibrated the root of the tree (tMRCA [*Draco* + *Aphaniotis fusca*]) with a secondary calibration point based on the previous analysis ('Agamidae 1'; normal calibration density with 5–95% interquartile range of 32–45 Ma). The resulting rates were 1.30% per Ma (95% CI = 0.91–1.74 per Ma) for *12S*; and 0.71% per Ma (95% CI = 0.48–0.96 per Ma) for the *16S rRNA* gene. For the biogeographical inference, we used mainland Asia and India as area coding.

**Boidae** (Reptilia, Squamata): We reanalysed the phylogeny of the family Boidae by Noonan and Chippindale<sup>43</sup> based on the nuclear *RAG-1*, *c-mos*, *NT3*, *ODC*, and *BDNF* genes and the mitochondrial *Cyt-b* gene (~4.3 kb total alignment length). We followed the suggestions for calibrating snake phylogenies provided by Sanders *et al.*<sup>44</sup>: the MRCA of *Acrochordus javanicus* and the clade including *A. granulatus* and *A. arafurae* (5–95% interquartile range = 18.7–25.0 Ma), the split between the genus *Acrochordus* and the superfamily Colubroidea (5–95% interquartile range = 51.0–69.9 Ma), the MRCA of Boidae (5–95% interquartile range = 57.3–83.7 Ma), the split between the families Colubridae and Elapidae (5–95% interquartile range = 21.7–35.1 Ma), and the most basal split in extant snakes (uniform calibration density = 85.0–140.0 Ma). We assumed dispersal from SE Asia to India to have occurred between the MRCA of *Eryx colubrinus*

and the clade comprising *E. johni* and *E. conicus*, and the MRCA of *E. johni* and *E. conicus*, resulting in a time range of the combined 95% credibility intervals of 25–5 Ma. The resulting rates were 0.07% per Ma (95% CI = 0.05–0.09% per Ma) for *ODC*, 0.03% per Ma (95% CI = 0.02–0.04% per Ma) for *BDNF*, 0.05% per Ma (95% CI = 0.03–0.06% per Ma) for *RAG-1*, 0.05% per Ma (95% CI = 0.04–0.06% per Ma) for *c-mos*, and 0.07% per Ma (95% CI = 0.05–0.1% per Ma) for *NT3*. For the biogeographical inference, we used mainland Asia, India, Australia, Africa and the Americas as area coding.

**Viperidae** (Reptilia, Squamata): We re-analysed the mitochondrial data set used in the study of Wüster *et al.*<sup>45</sup> on the phylogeny of viperid snakes (based on *Cytb*, *ND4*, *12S* and *16S rRNA* genes; 2,962 bp total alignment length) that—following biogeographical inference—includes two dispersal events from SE-Asia to India, namely, at the split nodes between *Hypnale hypnale* and *Calloselasma rhodostoma*, and between *Trimeresurus borneensis* and *T. trigonocephalus*. We incorporated five calibrations points: the divergence of South American populations of the Neotropical pitviper genus *Porthidium* with the uplift of the Isthmus of Panama (mean = 3.5 Ma, SD = 0.51, 5–95% interquartile range = 2.7–4.4 Ma), minimum divergence of the Eurasian viper clade (excluding *Pseudocerastes* and *Eristicophis*) at 20 Ma (lognormal calibration density, mean = 1.0 Ma, SD = 1.0, offset = 20.0 Ma, 5–95% interquartile range = 20.5–34.1 Ma), a minimum age of 16 Ma for the divergence between the Asian clade of the genus *Naja* and its African sister clade (lognormal calibration density, mean = 1.0 Ma, SD = 1.0, offset = 16.0 Ma, 5–95% interquartile range = 16.5–30.1 Ma), the divergence between *Crotalus* and *Sistrurus* before 9 Ma (lognormal calibration density, mean = 0.0 Ma, SD = 1.0, offset = 9.0 Ma, 5–95% interquartile range = 9.2–14.2 Ma), and the tMRCA of the genus *Hemorrhois* (normal calibration

density, mean = 18.0 Ma, SD = 2.04, offset = 9.0 Ma, 5–95% interquartile range = 14.6–21.4 Ma). The resulting mean substitution rates were 1.64% per Ma (95% CI = 1.41–1.87% per Ma) for *ND4*, 2.12% per Ma (95% CI = 1.82–2.42% per Ma) for *Cytb*, 0.75% per Ma (95% CI = 0.60–0.92% per Ma) for *16S*, and 1.39% per Ma (95% CI = 0.95–1.89% per Ma) for *12S rRNA*. For the biogeographical inference, we used mainland Asia, India, Australia, Africa and the Americas as area coding.

**Passeriform birds** (Reptilia, Aves): Päckert *et al.*<sup>46</sup> presented a study on the biogeography of Himalayan and SE Asian songbirds (order Passeriformes) that included time-calibrated phylogenies (Bayesian approach in BEAST 1.4.8) and biogeographical reconstructions (parsimony approach) of several genera belonging to the families Phylloscopidae (*Cytb*, *12S rRNA* gene, *myoglobin* intron 2; 1,899 bp total alignment length), Timaliidae (*Cytb*; 861 bp; external rate 2.1% per Ma), Paridae (*Cytb*, *16S rRNA* gene, control region, and *fib7*; 2,527 bp total alignment length), Aegithalidae (*Cytb*, *16S rRNA* gene, *ND2*, *fib7*, *GAPDH11*, *ODC6*, and *TGFB2*; 3,995 bp total alignment length), Fringillidae (genus *Pyrrhula*; *Cytb*, *16S rRNA* gene, *fib7*, and *GAPDH11*; 2,357 bp total alignment length) and Certhiidae (*Cytb*, *16S rRNA* gene, *myo2*, and *GAPDH11*; 2,019 bp total alignment length) that we re-analysed for the present study. They calibrated these trees with various biogeographic events, i.e., the opening of the Bering Strait (uniform calibration density = 10.0–4.8 Ma and 14.0–4.8 Ma, respectively), the Messinian salinity Crisis (5.96 Ma), Pleistocene glaciations (2.4–0.18 Ma), the age of lava flows to calibrate splits between Africa and the Canary Islands (5.96–1.22 Ma), within the Canary Islands (1.77–0.00 Ma, 1.22–0.00 Ma), between Africa and the Azores (0.88–0.00 Ma), and within the Azores (0.2–0.0 Ma). However, we were not able to run the analyses under these calibration schemes, as

these priors resulted in extremely low initial model likelihoods. Therefore, we applied an external substitution rate for the *Cytb* partition of 1.35 % per Ma (SD = 0.4; 5–95% interquartile range = 0.7–2.3% per Ma). This broadly covers previously suggested avian *Cytb* substitution rates<sup>47,48</sup>. The resulting divergence times are considerably younger than in the original study (except for the Timaliidae), indicating that Päckert *et al.*<sup>46</sup> used pairwise divergence instead of substitution rates. We included those splits that separated west-Himalayan endemics (the authors' 'bioregion F04a') from their eastern relatives.

**Psittacidae** (Reptilia, Aves): We re-analysed the phylogeny by Groombridge *et al.*<sup>49</sup> of the genus *Psittacula* (*Cytb*, 800 bp), applying the above-mentioned external rate of 1.35 % per Ma (SD = 0.4; 5–95% interquartile range = 0.7–2.3% per Ma). We inferred a shift from SE-Asia to India at the divergence of *P. cyanocephala* and *P. longicauda*, and for the other dispersal direction at the divergence of *P. columboides*. For the biogeographical inference, we used mainland Asia, India, and Africa as area coding.

**Accipitridae** (Reptilia, Aves): We re-analysed the phylogeny of Asian hawk-eagles of the genus *Nisaetus* published by Gamauf *et al.*<sup>50</sup> that used mitochondrial *Cytb* and control region sequences (502 bp total alignment length). We applied an external rate of 1.35 % per Ma (SD = 0.4; 5–95% interquartile range = 0.7–2.3% per Ma) under an uncorrelated relaxed lognormal clock prior. For the biogeographical inference, we used mainland Asia and India as area coding. We inferred dispersal from Asia to India along the branch leading to the MRCA of the subspecies of *Nissaetus cirrhatus*.

**Bovidae** (Mammalia, Ruminantia): We re-analysed parts of the data set from the study by Hassanin *et al.*<sup>51</sup>, who presented a phylogeny of the Cetartiodactyla

based on partial mitochondrial genome sequences (14,904 bp total alignment length). We followed their approach and calibrated (with normally distributed prior densities) the tMRCA of whales (Cetaceae) to 35 Ma (SD = 1), the tMRCA of the Cetaceae and *Hippopotamus* to 55 Ma (SD = 5), the tMRCA of Hippopotamus to 8 Ma (SD = 1), the divergence between the tribes Muntiacini and Cervini to 9 Ma (SD = 1), the tMRCA of the tribe Odocoileini to 5 Ma (SD = 1), and the tMRCA of the family Bovidae to 20 Ma (SD = 2). We removed 1,300 samples of the Bayesian analysis as burn-in. The resulting rates were 0.38% per Ma (95% CI = 0.35–0.42% per Ma) for the tRNAs, 0.35% per Ma (95% CI = 0.32–0.31% per Ma) for *12S rRNA*, 0.4% per Ma (95% CI = 0.37–0.44% per Ma) for *16S rRNA*, 0.80% per Ma (95% CI = 0.74–0.85% per Ma) for *ND1*, 0.96% per Ma (95% CI = 0.90–1.02% per Ma) for *ND2*, 0.75% per Ma (95% CI = 0.70–0.80% per Ma) for *CO1*, 0.69% per Ma (95% CI = 0.64–0.73% per Ma) for *CO2*, 0.75% per Ma (95% CI = 0.70–0.80% per Ma) for A8A6, 0.82% per Ma (95% CI = 0.76–0.88% per Ma) for *CO3*, 0.81% per Ma (95% CI = 0.75–0.89% per Ma) for *ND3*, 0.85% per Ma (95% CI = 0.79–0.90% per Ma) for *ND4*, 0.85% per Ma (95% CI = 0.79–0.90% per Ma) for *ND5*, 1.10% per Ma (95% CI = 1.00–1.20% per Ma) for *ND6*, and 0.90% per Ma (95% CI = 0.84–0.96% per Ma) for *CBP*. For the biogeographical inference, we used mainland Asia, India, Australia, Africa and the Americas as area coding.

**Herpestidae** (Mammalia, Carnivora): We re-analysed the data from the phylogenetic study by Patou *et al.*<sup>52</sup> on mongooses (family Herpestidae) based on the mitochondrial *Cytb* and *ND2* genes, and nuclear *FGBi7* sequences (2,770 bp total alignment length). We followed the authors' approach and calibrated the minimum age of the MRCA of the Herpestidae with fossil *Leptolesictis* (uniform calibration density = 18–66 Ma), and of the MRCA of the genus *Galerella* based

on fossil evidence (7–66 Ma). The resulting mean substitution rates were 0.69% per Ma (95% CI = 0.50–0.87% per Ma) for *Cytb*, 0.56% per Ma (95% CI = 0.41–0.70% per Ma) for *ND2*, and 0.12% per Ma (95% CI = 0.08–0.16% per Ma) for *FGBi7*. For the biogeographical inference, we used SE Asia, India, Africa, Europe and the Americas as area coding.

**Sciuridae** (Mammalia, Rodentia): We re-analysed the data set of Lu *et al.*<sup>53</sup> on flying squirrels (subfamily Pteromyinae), including the *IRBP* gene, and partial *12S* and *16S rRNA* gene sequences; 2,584 bp total alignment length). We calibrated the MRCA of the tribe Pteromyini with the first appearance date of the pteromyine fossil *Oligopetes* spp. from southern Germany in the Early Oligocene (MP21, 33.9–32.6 Ma)<sup>54</sup>. We translated this date into a lognormal calibration density with an offset of 32.6 Ma and a 5–95% interquartile range of 33.1–46.7 Ma. The resulting rates were 0.45% per Ma (95% CI = 0.34–0.56% per Ma) for the *12S rRNA*, 0.39% per Ma (95% CI = 0.29–0.50% per Ma) for the *16S rRNA*, and 0.08% per Ma (95% CI = 0.06–0.09% per Ma) for the *IRBP* gene. For the biogeographical inference, we used East/SE Asia, the Palearctic, India and the Americas as area coding.

**Tupaiidae** (Mammalia, Scandentia): We re-analysed the data set of Roberts *et al.*<sup>55</sup> using the alignment provided by the authors and also applied the fossil calibration points as suggested by the authors. However, we were unable to run the analysis using all suggested calibration points. Therefore, we reduced the number of calibration points to the two ingroup calibrations (lognormal calibration densities with mean and SD = 1.0; tMRCA [*Tupaia*, *Urogale* and *Anathana*] = 18.0 Ma, and tMRCA of the order Scandentia = 38.2 Ma as offset points), and also used a re-aligned data set without excluding the more variable parts of the sequences (*12S rRNA*, *16S rRNA*, *tRNA Leu*, *tRNA Val* and *tRNA Phe*

genes; 2,849 bp total alignment length). Credibility intervals of divergence events overlap with those given by Roberts *et al.*<sup>55</sup>, but the retrieved mean values were considerably younger. The resulting rates were 0.86% per Ma (95% CI = 0.70–1.02% per Ma) for the *12S rRNA* gene, 1.18% per Ma (95% CI = 0.99–1.38% per Ma) for the *16S rRNA* gene, 0.85% per Ma (95% CI = 0.07–3.0% per Ma) for the *tRNA Leu* gene, 1.28% per Ma (95% CI = 0.49–2.09% per Ma) for the *tRNA Phe* gene, and 1.62% per Ma (95% CI = 0.96–2.36% per Ma) for the *tRNA Val* gene. For the biogeographical inference, we used mainland Asia, India, and the Philippines as area coding. Dispersal to the Indian subcontinent was inferred at the MRCA of the genera *Dendrogale* and *Tupaia*.

**Colobinae** (Mammalia, Primates): We re-analysed the phylogeny by He *et al.*<sup>56</sup> that used 1,140 bp sequence information of *Cytb* and 376 bp of the nuclear *PRMI* gene to infer the phylogeny and divergence times for the genus *Trachypithecus* in the subfamily Colobinae. To calibrate the phylogeny, we applied a secondary calibration point based on the study of He *et al.*<sup>56</sup> for the MRCA of Colobinae using a normal calibration density (mean = 12.28 Ma, SD = 1.74, 5–95% interquartile range = 9.4–15.1 Ma). Resulting mean substitution rates were 1.74% per Ma (95% CI = 1.17–2.36% per Ma) for *Cytb*, and 0.16% per Ma (95% CI = 0.05–0.35% per Ma) for *PRMI*. For the biogeographical inference, we used mainland Asia, India, and Africa as area coding.

## Supplementary References

1. Rutschmann, F., Eriksson, T., Salim, K. A. & Conti, E. Assessing calibration uncertainty in molecular dating: the assignment of fossils to alternative calibration points. *Syst. Biol.* **56**, 591–608 (2007).
2. Gamage, D. T., Silva, M. P. de, Inomata, N., Yamazaki, T. & Szmidt, A. E. Comprehensive molecular phylogeny of the sub-family Dipterocarpoideae (Dipterocarpaceae) based on chloroplast DNA sequences. *Genes. Genet. Syst.* **81**, 1–12 (2006).
3. Gunasekara, N. Masters-thesis. Concordia University, 01.01.2004.
4. Bancroft, H. The taxonomic history and geographical distribution of the Monotoideae. *Am. J. Bot.*, 505–519 (1935).
5. Dutta, S. *et al.* Eocene out-of-India dispersal of Asian dipterocarps. *Rev. Palaeobot. Palyno.* **166**, 63–68 (2011).
6. Yuan, Y.-M. *et al.* Phylogeny and biogeography of *Exacum* (Gentianaceae): a disjunctive distribution in the Indian Ocean Basin resulted from long distance dispersal and extensive radiation. *Syst. Biol.* **54**, 21–34 (2005).
7. Hagen, K. B. von & Kadereit, J. W. The phylogeny of *Gentianella* (Gentianaceae) and its colonization of the southern hemisphere as revealed by nuclear and chloroplast DNA sequence variation. *Org. Divers. Evol.* **1**, 61–79 (2001).
8. Hagen, K. B. von & Kadereit, J. W. Phylogeny and flower evolution of the Swertiinae (Gentianaceae-Gentianeae): Homoplasy and the principle of variable proportions. *Syst. Bot.* **27**, 548–572 (2002).
9. Koehler, F. & Glaubrecht, M. Out of Asia and into India: on the molecular phylogeny and biogeography of the endemic freshwater gastropod *Paracrostoma* Cossmann, 1900 (Caenogastropoda: Pachychilidae). *Biol. J. Linn. Soc.* **91**, 627–651 (2007).
10. Hellberg, M. E. & Vacquier, V. D. Rapid evolution of fertilization selectivity and lysin cDNA sequences in teguline gastropods. *Mol. Biol. Evol.* **16**, 839–848 (1999).

11. Marko, P. B. Fossil calibration of molecular clocks and the divergence times of geminate species pairs separated by the Isthmus of Panama. *Mol. Biol. Evol.* **19**, 2005–2021 (2002).
12. Klaus, S., Schubart, C. D., Streit, B. & Pfenniger, M. When Indian crabs were not yet Asian-biogeographic evidence for Eocene proximity of India and Southeast Asia. *BMC Evol. Biol.* **10**, 287 (2010).
13. Klaus, S., Fernandez, K. & Yeo, D. C. J. Phylogeny of the freshwater crabs of the Western Ghats (Brachyura, Gecarcinucidae). *Zool. Scripta* **43**, 651–660 (2014).
14. Daniels, S. R., Phiri, E. E., Klaus, S., Albrecht, C. & Cumberlidge, N. Multilocus phylogeny of the Afrotropical freshwater crab fauna reveals historical drainage connectivity and transoceanic dispersal since the Eocene. *Syst. Biol.*, syv011 (2015).
15. Condamine, F. L., Sperling, F. A. H. & Kerfoot, G. J. Global biogeographical pattern of swallowtail diversification demonstrates alternative colonization routes in the Northern and Southern hemispheres. *J. Biogeogr.* **40**, 9–23 (2013).
16. Rehan, S. M. *et al.* Molecular phylogeny of the small carpenter bees (Hymenoptera: Apidae: Ceratinini) indicates early and rapid global dispersal. *Mol. Phylogen. Evol.* **55**, 1042–1054 (2010).
17. Ward, P. S. & Downie, D. A. The ant subfamily Pseudomyrmecinae (Hymenoptera: Formicidae): phylogeny and evolution of big-eyed arboreal ants. *Syst. Entomol.* **30**, 310–335 (2005).
18. Jansen, G., Savolainen, R. & Vepsäläinen, K. Phylogeny, divergence-time estimation, biogeography and social parasite-host relationships of the Holarctic ant genus *Myrmica* (Hymenoptera: Formicidae). *Mol. Phylogen. Evol.* **56**, 294–304 (2010).
19. Murphy, W. J. & Collier, G. E. A molecular phylogeny for aplocheiloid fishes (Atherinomorpha, Cyprinodontiformes): the role of vicariance and the origins of annualism. *Mol. Biol. Evol.* **14**, 790–799 (1997).
20. Adamson, E. A. S., Hurwood, D. A. & Mather, P. B. A reappraisal of the evolution of Asian snakehead fishes (Pisces, Channidae) using molecular data

from multiple genes and fossil calibration. *Mol. Phylogenet. Evol.* **56**, 707–717 (2010).

21. Ratmuangkhwang, S., Musikasinthorn, P. & Kumazawa, Y. Molecular phylogeny and biogeography of air sac catfishes of the *Heteropneustes fossilis* species complex (Siluriformes: Heteropneustidae). *Mol. Phylogenet. Evol.* **79**, 82–91 (2014).
22. Nakatani, M., Miya, M., Mabuchi, K., Saitoh, K. & Nishida, M. Evolutionary history of Otophysi (Teleostei), a major clade of the modern freshwater fishes: Pangaea origin and Mesozoic radiation. *BMC Evol. Biol.* **11**, 177 (2011).
23. Rüber, L., Britz, R. & Zardoya, R. Molecular phylogenetics and evolutionary diversification of labyrinth fishes (Perciformes: Anabantoidei). *Syst. Biol.* **55**, 374–397 (2006).
24. Šlechtová, V., Bohlen, J. & Perdices, A. Molecular phylogeny of the freshwater fish family Cobitidae (Cypriniformes: Teleostei): delimitation of genera, mitochondrial introgression and evolution of sexual dimorphism. *Mol. Phylogenet. Evol.* **47**, 812–831 (2008).
25. Doadrio, I. & Perdices, A. Phylogenetic relationships among the Ibero-African cobitids (*Cobitis*, Cobitidae) based on cytochrome b sequence data. *Mol. Phylogenet. Evol.* **37**, 484–493 (2005).
26. Pyron, R. A. & Wiens, J. J. A large-scale phylogeny of Amphibia including over 2800 species, and a revised classification of extant frogs, salamanders, and caecilians. *Mol. Phylogenet. Evol.* **61**, 543–583 (2011).
27. Kotaki, M. *et al.* Molecular phylogeny of the diversified frogs of genus *Fejervarya* (Anura: Dicroglossidae). *Zool. Sci.* **27**, 386–395 (2010).
28. van Bocxlaer, I., Roelants, K., Biju, S. D., Nagaraju, J. & Bossuyt, F. Late Cretaceous vicariance in Gondwanan amphibians. *PLoS ONE* **1**, e74 (2006).
29. Sá, R. O. de *et al.* Molecular phylogeny of microhylid frogs (Anura: Microhylidae) with emphasis on relationships among New World genera. *BMC Evol. Biol.* **12**, 241 (2012).

30. Li, J.-T. *et al.* Diversification of rhacophorid frogs provides evidence for accelerated faunal exchange between India and Eurasia during the Oligocene. *Proc. Natl. Acad. Sci. U.S.A.* **110**, 3441–3446 (2013).
31. van Bocxlaer, I., Biju, S. D., Loader, S. P. & Bossuyt, F. Toad radiation reveals into-India dispersal as a source of endemism in the Western Ghats-Sri Lanka biodiversity hotspot. *BMC Evol. Biol.* **9**, 131 (2009).
32. Oaks, J. R. A time-calibrated species tree of *Crocodylia* reveals a recent radiation of the true crocodiles. *Evolution* **65**, 3285–3297 (2011).
33. Heled, J. & Drummond, A. J. Bayesian inference of species trees from multilocus data. *Mol. Biol. Evol.* **27**, 570–580 (2010).
34. Brochu, C. A. Morphology, fossils, divergence timing, and the phylogenetic relationships of Gavialis. *Syst. Biol.* **46**, 479–522 (1997).
35. Wood, P. L., Heinicke, M. P., Jackman, T. R. & Bauer, A. M. Phylogeny of bent-toed geckos (*Cyrtodactylus*) reveals a west to east pattern of diversification. *Mol. Phylogenet. Evol.* **65**, 992–1003 (2012).
36. Bansal, R. & Karanth, K. P. Phylogenetic analysis and molecular dating suggest that *Hemidactylus anamallensis* is not a member of the *Hemidactylus* radiation and has an ancient Late Cretaceous origin. *PLoS ONE* **8**, e60615 (2013).
37. Datta-Roy, A., Singh, M., Srinivasulu, C. & Karanth, K. P. Phylogeny of the Asian *Eutropis* (Squamata: Scincidae) reveals an 'into India' endemic Indian radiation. *Mol. Phylogenet. Evol.* **63**, 817–824 (2012).
38. Honda, M. *et al.* Phylogenetic relationships, character evolution, and biogeography of the subfamily Lygosominae (Reptilia: Scincidae) inferred from mitochondrial DNA sequences. *Mol. Phylogenet. Evol.* **15**, 452–461 (2000).
39. Martin, J. E., Hutchinson, M. N., Meredith, R., Case, J. A. & Pledge, N. S. The oldest genus of scincid lizard (Squamata) from the tertiary Etadunna Formation of South Australia. *J. Herpetol.* **38**, 180–187 (2004).
40. Macey, J. R. *et al.* Evaluating trans-tethys migration: an example using acrodont lizard phylogenetics. *Syst. Biol.* **49**, 233–256 (2000).

41. Townsend, T. M. *et al.* Phylogeny of iguanian lizards inferred from 29 nuclear loci, and a comparison of concatenated and species-tree approaches for an ancient, rapid radiation. *Mol. Phylogen. Evol.* **61**, 363–380 (2011).
42. Honda, M. *et al.* Phylogenetic Relationships of the Flying Lizards, Genus *Draco* (Reptilia, Agamidae). *Zool. Sci.* **16**, 535–549 (1999).
43. Noonan, B. P. & Chippindale, P. T. Dispersal and vicariance: the complex evolutionary history of boid snakes. *Mol. Phylogen. Evol.* **40**, 347–358 (2006).
44. Sanders, K. L., Mumpuni, Hamidy, A., Head, J. J. & Gower, D. J. Phylogeny and divergence times of filesnakes (*Acrochordus*): inferences from morphology, fossils and three molecular loci. *Mol. Phylogen. Evol.* **56**, 857–867 (2010).
45. Wüster, W., Peppin, L., Pook, C. E. & Walker, D. E. A nesting of vipers: Phylogeny and historical biogeography of the Viperidae (Squamata: Serpentes). *Mol. Phylogen. Evol.* **49**, 445–459 (2008).
46. Päckert, M. *et al.* Horizontal and elevational phylogeographic patterns of Himalayan and Southeast Asian forest passerines (Aves: Passeriformes). *J. Biogeogr.* **39**, 556–573 (2012).
47. Päckert, M. *et al.* Calibration of a molecular clock in tits (Paridae)--do nucleotide substitution rates of mitochondrial genes deviate from the 2% rule? *Mol. Phylogen. Evol.* **44**, 1–14 (2007).
48. Weir, J. T. & Schluter, D. Calibrating the avian molecular clock. *Mol. Ecol.* **17**, 2321–2328 (2008).
49. Groombridge, J. J., Jones, C. G., Nichols, R. A., Carlton, M. & Bruford, M. W. Molecular phylogeny and morphological change in the *Psittacula* parakeets. *Mol. Phylogen. Evol.* **31**, 96–108 (2004).
50. Gamauf, A., Gjershaug, J.-O., Røev, N., Kvaløy, K. & Haring, E. Species or subspecies? The dilemma of taxonomic ranking of some South-East Asian hawk-eagles (genus *Spizaetus*). *Bird Conserv. Int.* **15**, 99–117 (2005).

51. Hassanin, A. *et al.* Pattern and timing of diversification of Cetartiodactyla (Mammalia, Laurasiatheria), as revealed by a comprehensive analysis of mitochondrial genomes. *C. R. Biol.* **335**, 32–50 (2012).
52. Patou, M.-L. *et al.* Molecular phylogeny of the Herpestidae (Mammalia, Carnivora) with a special emphasis on the Asian *Herpestes*. *Mol. Phylogenet. Evol.* **53**, 69–80 (2009).
53. Lu, X. *et al.* The Evolution and paleobiogeography of flying squirrels (Sciuridae, Pteromyini) in response to global environmental change. *Evol. Biol.* **40**, 117–132 (2013).
54. Heissig, K. Die frühesten Flughörnchen und primitive Ailuravinae (Rodentia, Mamm.) aus dem süddeutschen Oligozän. *Mitt. Bayer. Staatssamml. Palaeontol. Hist. Geol.*, 139–169 (1979).
55. Roberts, T. E., Lanier, H. C., Sargis, E. J. & Olson, L. E. Molecular phylogeny of treeshrews (Mammalia: Scandentia) and the timescale of diversification in Southeast Asia. *Mol. Phylogenet. Evol.* **60**, 358–372 (2011).
56. He, K. *et al.* Molecular phylogeny and divergence time of *Trachypithecus*: with implications for the taxonomy of *T. phayrei*. *Zool. Res.* **33**, E104-10 (2012).